HIGHER-ORDER CORRECTIONS IN QUANTUM ELECTRO-DYNAMICS AND QUANTUM CHROMODYNAMICS

By

MORTEN LAURITS LAURSEN

Candidatus Scientarum

Niels Bohr Institute

University of Copenhagen

Copenhagen, Denmark

1980

Submitted to the Faculty of the Graduate College
of the Oklahoma State University
in partial fulfillment of the requirements
for the Degree of
DOCTOR OF PHILOSOPHY
July, 1981

TO MOTHER

PREFACE

This work is devoted to a calculation of various higher-order processes in perturbative Quantum Electrodynamics (QED) and Quantum Chromodynamics (QCD).

We have analytically determined, in sixth-order, the contributions to the muon anomalous magnetic moment from second and proper fourth-order electron vacuum polarization to order $\frac{m_e}{m_\mu}$. We have also analytically calculated the mass-dependent n-bubble diagram contribution to the muon anomaly to O(1).

An extensive review of the current experimental and theoretical situation for the lepton anomalies is given.

We have evaluated in detail the three gluon final state produced in the weak decay of the heavy neutral vector boson Z^o and, also, in electron-positron annihilation. A detailed comparison with the more familiar quark-antiquark-gluon final state is given.

Finally, in order for the reader to follow these calculations, some topics in Gauge Theories are discussed.

I would like to express my deep appreciation to my adviser, Dr. Mark A. Samuel, for inviting me to work with him, for his help and guidance, and for our excellent collaboration during the course of this work. I have profited very much from this experience.

I am thankful to Dr. N. V. V. J. Swamy, Dr. Paul Westhaus and Dr. John Chandler for serving on my Committee.

I am very grateful to Dr. Karnig O. Mikaelian for his suggestion of and collaboration on the three gluon jet problem. Also thanks to Dr. Ashok Ray and Dr. Katsunori Mita for collaboration on interesting subjects.

It is a pleasure to thank my former adviser, Dr. Benny E. Lautrup, by whom I was introduced to the very fascinating subject of field theory, and Dr. Bob W. Brown and Dr. Stan Brodsky for stimulating discussions and suggestions. I also thank Dr. Robert Coquereaux for introducing me to the Borel transform technique.

Moreover, I wish to thank Janet Sallee for her excellent typing of the manuscript.

I am thankful to the United States Department of Energy for financial support, in the form of research assistantships.

Last but not least, I am deeply grateful to my mother, Ruth Martine Laursen, to whom this thesis is dedicated, for her everlasting love, patience and continuing interest in my work.

TABLE OF CONTENTS

LIST OF TABLES

LIST OF FIGURES

CHAPTER I

INTRODUCTION

The purpose of this work has been to calculate certain higher-order processes in Quantum Electrodynamics (QED) and perturbative Quantum Chromodynamics (QCD), the latter being the candidate for the theory of strong interactions.[1]

They are both renormalizable gauge field theories with gauge groups U(1) and SU(3)-color respectively.[1]

QED has existed for the last three decades and is now the well-established theory of pure electromagnetic interactions. It consists of massive spin-½ particles, called leptons, which come in three different varieties: electron, muon and tauon, denoted e, μ and τ. They interact electromagnetically via the Abelian spin-1 photon field. This theory has had tremendous success over the years, particularly in predicting the gyromagnetic ratios of the electron and muon.[2] For the electron, the experiments are now so precise,[3] (performed on a single electron in a Penning-trap), that we can actually test the anomalous magnetic moment of the electron $a_e = \frac{g_e - 2}{2}$ in sixth-order rigorously. At the present stage, theory and experiment for g_e agree to 10 significant figures. The theoretical uncertainty is due to the experimental error in the fine structure constant α and errors coming from numerical integration of certain sixth-order diagrams, which have not yet been analytically evaluated. Finally, the contribution from the eighth-order term is not yet known

although an attempt to numerically evaluate this contribution from the 891 diagrams is under way,[4] and a result is anticipated within the next year.

The situation for the muon magnetic moment is almost as impressive.[5] However, since the muon is much heavier than the electron, the situation is complicated by the fact, that strong interaction effects are significant. The hadronic contribution is calculable only as a spectral integral over the experimental cross section for e^+e^- annihilation into hadrons and the experimental error here dominates the errors. Since the weak interaction effects are calculable in the Weinberg-Salam model,[6] we would be able to isolate these (therefore serving as an independent check of W-S model), by an improvement in the measurement of $a_\mu = \frac{g_\mu - 2}{2}$ and a better knowledge of the strong interaction contribution.

In QED the only difference between the electron and muon anomalies comes from the mass-dependent diagrams, giving rise to potentially large $\log \frac{m_\mu}{m_e}$ terms. One usually calculates also the O(1) term, but neglects $O(\frac{m_e}{m_\mu})$ and lower. To remedy this, we have calculated their contribution analytically in sixth-order from 17 of the 24 mass-dependent diagrams.[7-8] To see if their effects could be large in higher order we then evaluated analytically to O(1), the muon anomaly from the mass-dependent n-bubble diagram.[9] We found that the neglected terms are non-negligible, in fact bigger than the sum of the terms included for $n \gtrsim 10$.

Although pure QED has been so successful as a theory, it is now widely believed that the electromagnetic and weak interactions can be unified into one gauge theory, with a bigger gauge group SU(2)⊗U(1), known as the Weinberg-Salam model (W-S) of electro-weak interactions.[10-11]

This model, besides the massless photon, also contains three heavy vector bosons, two charged $W^{\pm}$ and one neutral Z^{o}, which mediate the electro-weak force.[12] In addition, we have three massless neutrinos ν_e, ν_μ and ν_τ.

The W's and Z^{o} are very heavy, around 90 GeV, which is the reason that they have not yet been produced in the laboratory, but one will be able to obtain CM energies of this magnitude within the next few years at the CERN $p\bar{p}$ collider, ISABELLE at Brookhaven and the Fermilab $p\bar{p}$ project.[13]

So far, the W-S model has been successfully tested in high-energy neutrino experiments,[14] and the prediction of parity violation effects has also been experimentally verified.[15]

The theory of QCD was developed by Fritzsch, Gell-Mann, Leutwyler, Weinberg, Gross and Wilczek[16] and is based on the non-Abelian Yang-Mills (YM) theory.[17] In a sense it is very similar to QED. It consists of massive, fractionally charged spin-½ particles called quarks. They come in five flavors: up, down, strange, charm and beauty denoted u, d, s, c and b. A sixth flavor, top, denoted t is conjectured with a mass around 19 GeV but has, so far, not been seen.[18] The quarks are the building blocks for the strongly interacting particles called hadrons. These can be subdivided into two groups: baryons (like the proton and neutron) are composed of three quarks, and mesons (like the pion and kaon) are composed of a quark-antiquark pair. The quarks interact strongly via eight non-Abelian spin-1 gluon fields. Like the photon, the gluons are massless, and electrically neutral, but they carry, as do the quarks, a non-Abelian charge called color. Each quark then comes in three colors: "red," "green" and "blue".

The non-Abelian nature of the gluons has the consequence that they

can interact among themselves, in contrast with the photons of QED. A further consequence of this, is that the strong coupling constant $\alpha_s(q^2)$, in the so-called Renormalization Group improved perturbation theory, actually goes to zero for large q^2 (momentum transfer), i.e., small distances, and the theory is said to be asymptotically free.[19] This is exactly the property that makes the theory tractable and enables one to study high energy scattering processes, like deep inelastic e^-p and νN scattering (space like q^2), and, also, e^+e^- and $p\bar{p}$ annihilation into hadrons (time-like q^2).

A general term for quarks and gluons is the word parton. It was originally suggested by Bjorken, Feynman and Paschos[20] and motivated by the SLAC deep inelastic e^-p scattering experiments, in which the electron was actually being scattered by pointlike (non-interacting) objects inside the proton. The processes were described by structure functions depending only on the fraction x of the parton energy to the proton energy, and not on the momentum transfer. This leads to scale invariance. This is only approximately true, however, and QCD, in fact, predicts a logarithmic scale violation[21], best seen in the Nachtmann moment analysis, which seems to agree with experiment. However, there are indications that higher twist terms (m_q^2/q^2) can modify this analysis.[22]

At large distances (typically of the order of 1 fm, radius of the proton), α_s becomes infinite, thus, presumably, leading to confinement of quarks and gluons. This is known as infrared slavery, but whether or not QCD actually leads to confinement is still an open question.

The cleanest test of QCD is electron-positron annihilation into hadrons.[23] In lowest order perturbation theory, a quark-antiquark pair is produced, which then materializes into two jets of hadrons. The distribution of jets in the angle θ (angle between jet axis and e^+e^- beams)

is consistent with the form $1 + \cos^2\theta$ which is expected for the production of a pair of spin-$\frac{1}{2}$ pointlike quarks.

At higher CM-energies, $\sqrt{S} \gtrsim 30$ GeV, planar three jet events have been seen at PETRA.[24] They are interpreted as a quark, an antiquark and a gluon radiated off from the quarks, and they are evidence for the spin-1 nature of the gluon. Other sources for three jet events are e^+e^- annihilation into quarkonia states J/ψ and Ψ which predominantly decay into three gluons (one gluon forbidden by color and two gluons by charge conjugation). For the Ψ the experimental data is consistent with an angular distribution of the form $1-1/3\ \cos^2\theta$, which is a clear indication of the spin-1 nature of the gluon. One problem is that the energies of the gluons are rather low (around 3 GeV) and toponium is expected to give us a much cleaner three jet structure.

Three gluon jets can also be produced in Z^o decay[25] and in the continum $e^+e^- \to \gamma^* \to ggg$[26] in higher order. We were motivated to study this by the expected Z^o-factory at LEP.[27] In contrast to the $q\bar{q}g$ process, the three gluon decay is actually an infrared finite process. To see the full gauge structure of QCD, i.e., the self-coupling of the gluons, one has to study radiative corrections to $q\bar{q}g$ and, in same order, four-jet events.[28] Evidence for four-jet events has recently been reported at PETRA.

QCD is the only field theory available for strong interactions. This has motivated people to construct toy models with scalar gluons or simply Monte Carlo phase space models, in order to have alternative models to compare with QCD. But so far QCD has been successful in agreeing with the experimental data while these toy models have not.

Once we reach the thresholds for producing W's and Z^o we should be

able to study many interesting weak and strong decay processes, thus, hopefully, leading to a better understanding of the W-S model and QCD.

The thesis is organized as follows: In Chapter II, we give a status report of the anomalous magnetic moments of the electron and muon and compare the theoretical values with the experimental ones.

In Chapter III, we analytically calculate the order $\frac{m_e}{m_\mu}$ corrections to the sixth-order muon anomaly, which arise from the proper fourth-order electron vacuum polarization insertion into the lowest order muon vertex. Of the 24 mass-dependent diagrams, three diagrams contribute to this process.

Chapter IV is a continuation of this work and we calculate, also analytically, the order $\frac{m_e}{m_\mu}$ terms due to second-order electron vacuum polarization insertion into the fourth-order muon vertex. Fourteen diagrams contribute to this process.

In Chapter V, we calculate analytically the muon anomaly to O(1) from the mass-dependent n-bubble diagram using the Borel transform technique, and we show how this expansion breaks down in high order.

Chapter VI contains the basic elements of the gauge-theories of the electro-weak and strong interactions. We describe the experimental and theoretical basis for color. Gauge invariance of QED and QCD are described in detail. This is followed by a discussion of the Weinberg-Salam model and the so-called Standard Model. We then set up the propagators and vertices using a method due to t'Hooft-Veltman. Finally, we discuss the so-called running coupling constant in QED and QCD, and what is meant by Renormalization-Group-improved perturbation theory.

In Chapter VII, we study the three gluon decay of the Z^o. The process proceeds mainly through the six box diagrams with one heavy external leg.

This process is quite similar to photon splitting in QED, and, along with photon-photon scattering, which so far has been tested only in the electron and muon magnetic moments, are examples of non-linear effects in QED and QCD.

We calculate the differential and the total decay rates, using the standard W-S model and QCD.

In Chapter VIII, we present the differential and the total cross sections for the process $e^+e^- \to ggg$ mediated by a virtual photon in the continuum. A detailed comparison with $e^+e^- \to q\bar{q}g$ is given.

Finally, Chapter IX contains a summary of the obtained results and conclusions.

REFERENCES

1. Reviews of Quantum Chromodynamics can be found in W. Marciano and H. Pagels, Phys. Rep. 36C, 137 (1978); H. D. Politzer, Phys. Rep. 14C, 129 (1974); E. Reya, "Perturbative Quantum Chromodynamics", DESY Preprint 79/88, December 1979; R. D. Field, "Perturbative Quantum Chromodynamics and applications to large momentum transfer processes", NATO Advanced Study Institutes Series, Vol. 54B (Plenum Press, N.Y., 1980); S. J. Brodsky and G. P. Lepage, "Perturbative Quantum Chromodynamics", SLAC Summer Institute on Particle Physics, (1979).

2. Status of the electron and muon anomalous magnetic moments can be found in G.P. Lepage, "Theoretical Advances in Quantum Electrodynamics", CLNS 80/474, November 1980 (unpublished); S. D. Drell, "Experimental Status of Quantum Electrodynamics", SLAC-PUB-2222, October 1978, (unpublished); T. Kinoshita, "Recent Developments of Quantum Electrodynamics", CLNS-410, September 1978, (unpublished); C. D. Chlouber, Ph.D. Thesis, Oklahoma State University, 1977; Extensive reviews are given in J. Calmet, S. Narison, M. Perottet and E. de Rafael, Reviews of Modern Physics, Vol. 49, 21 (1977); B. E. Lautrup, A Peterman and E. de Rafael, Phys. Rep. C3, 193, (1972).

3. H. Dehmelt, R. S. Van Dyck, Bull. Am. Phys. Soc., 24, 758 (1979).

4. T. Kinoshita and W. B. Lindquist, "Eight-Order Magnetic Moment of the Electron, CLNS-426, June 1979, CLNS-424, April 1979 and CLNS-423, April 1979.

5. F. Combley and F. J. M. Farley, Phys. Rep. 68C, 93 (1981).

6. W. A. Bardeen, A. R. Gastmans and B. E. Lautrup, Nucl. Phys. B46, 319 (1972).

7. M. L. Laursen and M. A. Samuel, Phys. Rev. D19, 1281 (1979).

8. M. L. Laursen, M. A. Samuel, and A. K. Ray, Zeit. für. Physik 6C, 3 (1980).

9. M. L. Laursen and M. A. Samuel, To be published in Phys. Rev. D23, (May, 1981).

10. The original work on W-S model can be found in S. Weinberg, Phys. Rev. Lett. 19, 1264 (1967); A. Salam, Elementary Particle Theory P. 367 (Stockholm: Almquist and Wiksell).

11. S. L. Glashow, Nucl. Phys. 22, 579 (1961).

12. Reviews of gauge theories can be found in I. J. R. Aitchison, "An Informal Introduction to Gauge Theories", Oxford Univ. preprint, September 1980 (unpublished); H. Fritzsch and P. Minkowski, Flavor dynamics of Quarks and Leptons", MPI preprint 1981, (unpublished); J. J. Sakurai, "Introduction to Electro-Weak gauge theory", UCLA/79/TEP/18 October 1979 (unpublished); J. Ellis, "Status of Gauge Theories", CERN-TH-2701, July 1979 (unpublished); E. A. Paschos, "Some current issues in Gauge Theories", Dortmund preprint July 1979, (unpublished); L. Maiani, "Lepton Physics", Rome preprint 134, February 1979, (unpublished); E. S. Abers and B. W. Lee, Phys. Rep. 9C, 1 (1973); J. C. Taylor, "Gauge Theories of Weak Interactions (Cambridge Univ. Press, London 1972).

13. J. D. Bjorken, SLAC-PUB-2281 (1979) (unpublished); B. Richter, SLAC-PUB-2290 (1979) (unpublished).

14. G. Alterelli, "Phenomenology of Flavordynamics", NATO Advanced Study Institutes Series Vol. 54B (Plenum Press, New York, 1980).

15. C. Y. Prescott, et al., Phys. Lett. 84B, 524 (1979); Ibid., 77B, 347 (1978); Conti et al., Phys. Rev. Lett. 42, 343 (1979); L. M. Barkov and M. C. Zolotorev, JETP Lett. 26, 379 (1978).

16. H. Fritzsch and M. Gell-Mann, Proc. 16th Intl. Conf. on High Energy Physics, Vol. 2, 135 (Batavia, Illinois: National Accelerator Lab); H. Fritzsch, M. Gell-Mann and H. Leutwyler, Phys. Lett. 47B, 365 (1973); S. Weinberg, Phys. Rev. Lett. 31, 494 (1973); D. J. Gross and F. Wilczek, Phys. Rev. D8, 3633 (1973).

17. C. N. Yang and R. Mills, Phys. Rev. 96, 191 (1954).

18. S. L. Glashow, Phys. Rev. Letters 45, 1914 (1981). Experiments at PETRA reveal that the tt analog state of J/ψ and Ψ does not exist at a mass less than ~36 GeV. Glashow predicts the mass to be 38 ± 2 GeV.

19. H. D. Politzer, Phys. Rev. Lett. 30, 1346 (1973); see also REF. 16.

20. R. P. Feynman, Phys. Rev. Lett. 23, 1415 (1969); J. D. Bjorken, "In Proceedings of 3rd International Symposium on Electron and Photon Interactions, Stanford, California; J. D. Bjorken and E. A. Paschos, Phys. Rev. 185, 1975 (1969); For reviews of the Parton model see R. P. Feynman, "Photon Hadron Interactions" (Benjamin, New York 1972); F. E. Close, "An introduction to Quarks and Partons", (Academic Press, London 1979).

21. Excellent reviews of deep inelastic processes and scaling violation can be found in A. Peterman, Phys. Rep. 53C, 157 (1979); A. J. Buras, Rev. of Modern Phys. 52, 199 (1980).

22. M. Moshe, "Hunting for Higher Twists", TECHNION-PH-80-50, September 1980 (unpublished).

23. Excellent reviews on e^+e^- annihilation into hadrons can be found in: B. H. Wiik, "New e^+e^- Physics", DESY 80/124 December 1980. A. Ali, "A QCD Analysis of Jets in e^+e^- Annihilation", DESY 80/103, October 1980 (unpublished); G. Wolf, "Jets in e^+e^- Annihilation at High Energies", DESY 80/85, September 1980, (unpublished); B. R. Webber, "Quark and Gluon Jets in Quantum Chromodynamics", (to appear in Physica Scripta). T. F. Walsh, "Jets, Gluons, QCD", DESY 80/48, June 1980 (unpublished); T. F. Walsh, "Phenomenology of Jets", DESY 80/45, May 1980, (unpublished); G. Flügge, "Recent e^+e^- Physics", Karlsruhe preprint, KfK 2995, March 1980, (unpublished); B. H. Wiik, "Recent Results from PETRA", DESY 79/84 December 1979, (unpublished).

24. R. Brandelik et al., Phys. Letters 86B, 243 (1979); D. P. Barber et al., Phys. Rev. Letters 43, 830 (1979); Ch. Berger et al., Phys. Letters 86B, 418 (1979); W. Bartel et al., Phys. Letters 91B, 142 (1979).

25. M. L. Laursen, K. O. Mikaelian and M. A. Samuel, to be published in Phys. Rev. D23, Rapid Communications (June, 1981).

26. M. L. Laursen, K. O. Mikaelian and M. A. Samuel, "Electron Positron Annihilation into Three Gluons", Lawrence Livermore Preprint, March, 1981.

27. M. L. Perl, "e^+e^- Physics Today and Tomorrow", SLAC-PUB-2615, September 1980 (unpublished); C. H. Llewellyn Smith," e^+e^- Physics beyond PETRA energies", LEP Summer Study/1-2, October 1978 (unpublished).

28. G. Schierholz, "Higher order QCD Corrections in e^+e^- Annihilation into Hadrons", DESY 80/120, December 1980; K. Fabricius, I. Schmitt, G. Schierholz and G. Kramer, DESY 80/91, September 1980 (to be published in Phys. Letters B); R. K. Ellis, D. R. Ross and A. E. Terrano, Caltech Preprint Calt-68-785 (1980).

CHAPTER II

STATUS OF THE ANOMALOUS MAGNETIC MOMENTS OF THE LEPTONS

Introduction

In this chapter we will review the experimental-as well as the theoretical situation for the electron, positron and the positive and negative muon magnetic moments.

From atomic spectroscopy the term g-factor or Landé-factor is well-known, and we shall adopt the same definition for the g_ℓ-factors of the leptons. These are dimensionless numbers which relate their magnetic dipole moments to their intrinsic angular momentum (spin). We can therefore write $\mu_\ell = g_\ell(\frac{e}{2mc})$, and if the leptons obey the Dirac equation, then $g_\ell=2$ exactly.[1]

An eventual substructure would lead to a deviation from the point-like structure, implied by the Dirac equation, and therefore to a g_ℓ value different from two. For other spin-½ particles such as the proton and neutron, the substructure leads to a substantial change in their magnetic moments, namely $g_p = 2.79$ and $g_n = -1.91$. Based on the present level of agreement between g_e^{Theory} and $g_e^{Experiment}$ (5×10^{-10}) fermionic substructure could occur only at distances smaller than 2×10^{-16} cm,[2] which is roughly a factor 10^{-5} smaller than the Compton wave length of the electron.

However, even in the absence of an intrinsic structure of the leptons, the electromagnetic interaction leads to a modification of the g_ℓ-factor of the order 10^{-3}. One then defines the so called anomalous magnetic moment a_ℓ, in such a way, that $g_\ell = 2(1+a_\ell)$ or $a_\ell = \frac{1}{2}(g_\ell - 2)$ and, hence, the name "g-2 experiments".

Experimental Status

When leptons are placed in a circular orbit in a plane perpendicular to a uniform static magnetic field, the spin will rotate faster than the momentum vector with a relative frequency (anomaly frequency) $\bar{\omega}_a = \bar{\omega}_L - \bar{\omega}_c = a_\ell(\frac{e\bar{B}}{mc})$. Here $\bar{\omega}_c = \frac{e\bar{B}}{mc}$ is the cyclotron frequency and $\bar{\omega}_L = g_\ell(\frac{e\bar{B}}{2mc})$ is the Larmor spin frequency. In principle, by measuring ν_a and ν_c, we can determine the anomaly $a_\ell = \frac{\nu_a}{\nu_c} = \frac{\nu_L - \nu_c}{\nu_c}$.

We shall begin by describing the latest g-2 experiment of the electron, which is basically a radiofrequency experiment.[3] A non-relativistic electron (1 meV) is stored and kept in a so-called Penning trap. The axial oscillatory resonance frequency $\nu_Z \simeq 60$ MHZ is easily detected.

The electron is bound to the earth, (through the axial magnetic field and the electric quadrupole field) in a superheavy atom called "Geonium". The Breit-Rabi energy levels are given as ($m = \pm \frac{1}{2}$, $n,k,q = 0,1,2,\ldots$)

$$\frac{1}{h} E_{mnkq} = m\nu_s + (n+\tfrac{1}{2})(\nu_c - \delta_e) + (k+\tfrac{1}{2})\nu_Z - (q+\tfrac{1}{2})\nu_m . \qquad (1\text{-}1)$$

Due to the electric field, the cyclotron frequency has been changed to $\nu_c - \delta_e$ where $\delta_e = \frac{1}{2}\nu_Z^2/(\nu_c - \delta_e)$. ν_m is the magnetron frequency, which for ideal axial symmetry is equal to δ_e.

Spin flips at the anomaly frequency and excitation of the cyclotron

resonance are detected by making ν_Z slightly dependent on m and n. Use of a magnetic bottle leads to $\delta\nu_Z(m,n) = (m+n+1)$Hz.

Now by monitoring the axial frequency the cyclotron resonance is measured via excitation to n>>1, while spin-flips and therefore ν_a is measured as changes $\delta\nu_Z = \pm$ 1.0 HZ when $\Delta m = \pm$ 1 (n=0) occur.

This leads to the incredibly precise value

$$a_{e-} = 1159\ \ 652\ \ 200(40) \times 10^{-12}$$

and, hence,

$$g_{e-} = 2.002319304400(80)$$

which is one of the most accurate measurements of any physical quantity ever determined.

This experimental set up can also be used to determine the positron anomaly a_{e+} very accurately. A preliminary result for a_{e+} has recently been obtained,[4] with the value

$$a_{e+} = 1159\ \ 652\ \ 222(50) \times 10^{-12}\ .$$

Together with a_{e-} this give a weighted average value

$$a_e = 1159\ \ 652\ \ 211(32) \times 10^{-12}\ .$$

This gives an extremely good test of the CPT-theorem, which states that $g_{e+} = g_{e-}$. From above follows $|a_{e-} - a_{e+}|/a_e \simeq 19 \times 10^{-9}$ or $|g_{e-} - g_{e+}|/g_e \simeq 11 \times 10^{-12}$! This is an improvement of a factor 10^{+3} compared with an earlier Russian experiment[5] which gave $|g_{e-} - g_{e+}|/g_e \simeq 12 \times 10^{-9}$.

Next we describe the latest CERN muon (g-2) experiment,[6] which provides us also with a test of Einstein's theory of special relativity (time dilation), and the CPT-theorem.

First we notice that the anomaly frequency is unaffected by time dilation. Consider namely a high energy muon with $\gamma = (1-\beta^2)^{-\frac{1}{2}} >> 1$. The cyclotron frequency is $\bar{\omega}_c = \frac{e\bar{B}}{\gamma mc}$. The circular motion of the particle leads to a relativistic effect in which the particle rest frame appears to rotate with precession frequency $\bar{\omega}_T = (1 - \frac{1}{\gamma})\frac{e\bar{B}}{mc}$ (Thomas Precession).[7] The net angular rotation frequency of the spin is $\bar{\omega}_s = \bar{\omega}_L - \bar{\omega}_T = (a_\mu + \frac{1}{\gamma})\frac{e\bar{B}}{mc}$ and therefore $\bar{\omega}_a = a_\mu \frac{e\bar{B}}{mc}$. Indeed ν_a is unaffected by time-dilation.

If we add a transverse electric field $\bar{E}$, (to provide vertical focusing), we find

$$\bar{\omega}_a' = \bar{\omega}_a + (\frac{1}{\gamma^2-1} - a_\mu)\bar{\beta}x\bar{E}\frac{e}{mc} . \qquad (1\text{-}2)$$

However, by choosing a $\gamma = (1 + 1/a_\mu)^{\frac{1}{2}} \simeq 29.3$, or equivalently, a momentum 3.094 GeV/c, the effect of $\bar{E}$ can be reduced to zero, leaving $\bar{\omega}_a$ unchanged.

The anomaly frequency is determined by looking at the observed electron counting rate as a function of time

$$N(t) = N_o \exp\{-t/\tau\}\{1 - A[\cos(\omega_a t + \phi)]\} \qquad (1\text{-}3)$$

where $t = \gamma\tau_o$ is the dilated muon lifetime.

In the same experiment the effective mean proton resonance frequency ω_p' is determined leading to a known ratio $R = \omega_a/\omega_p'$. If this is combined with measurements of $\lambda = \omega_\mu'/\omega_p' = (g_\mu/g_p)$ of muon to proton

frequencies in liquid Bromid,[8] the anomaly can be determined from $a_\mu = R(R-\lambda)^{-1}$. This leads to

$$a_{\mu-} = 1165\ 936(12) \times 10^{-9},$$

$$a_{\mu+} = 1165\ 910(12) \times 10^{-9}$$

with an overall weighted value

$$a_\mu = 116\ 5923(9) \times 10^{-9}\ .$$

The CPT-theorem is tested very accurately by $|g_{\mu-} - g_{\mu+}|/g_\mu = 2.6 \times 10^{-8}$.

Since the counting rate is damped exponentially we can also determine the lifetimes of $\mu^{\pm}$. In this experiment $\gamma = 29.326$, and using the best value of muon life time at rest $\tau_o = 2.1\ 9711\ \mu s$, yields a "theoretical" lifetime $\tau = 64.435\ \mu s$. From the counting rate it was found $\tau^{exp} = 64.378\ \mu s$, thus leading to an accuracy of order 10^{-3} of the time transformation. The CPT theorem was tested by measuring $\tau_{\mu-}$ and $\tau_{\mu+}$. It was found $|\tau_{\mu-} - \tau_{\mu+}|/\tau_\mu \lesssim 3.0 \times 10^{-3}$ giving a stronger limit on any possible CPT violation.

Theoretical Status

First, we would like to show how the anomaly can be obtained formally in Quantum field theory. We shall restrict ourselves to QED, and we will show that the anomaly $a = F_2(0)/F_1(0)$, where $F_{1,2}(q^2)$ are the electric and magnetic form factors respectively.[10]

Let $\hat{J}_\mu(x)$ be the current operator. By definition the charge operator $\hat{Q}$ and the magnetic moment operators $\hat{\vec{M}}_\ell$ are:

$$\hat{Q} = \int d^3\bar{r}\, J_o(\bar{r},t)$$

and (1-4)

$$\hat{\bar{M}}_\ell = \int d^3\bar{r}\, \frac{1}{2}\, \bar{r} \times \bar{J}(\bar{r},t).$$

If we let $\Phi(x)$ be a "one electron" state, then the charge and the magnetic moment are the expectation values

$$e' = \langle\Phi|\hat{Q}|\Phi\rangle$$

and (1-5)

$$\bar{\mu}'_\ell = \langle\Phi|\hat{\bar{M}}_\ell|\Phi\rangle .$$

Next we expand $\Phi(x)$ on a complete set of states with a given momentum $\bar{p}$ and spin $\bar{\sigma}$:

$$\Phi(x) = \sum_{p\sigma} \phi_{\bar{p}\bar{\sigma}}\, \bar{U}_{\bar{p}\sigma}\, e^{-ip\cdot x} \tag{1-6}$$

where $U_{\bar{p}\sigma}$ are bispinors satisfying the Dirac equation

$$(\not{p}-m)U_{\bar{p}\sigma} = 0. \tag{1-7}$$

The problem is then reduced to evaluating the matrix element $\langle p'|J_\mu|p\rangle$. Using gauge invariance, parity and charge conjugation conservation, the most general matrix element is of the form

$$\langle p'|J_\mu|p\rangle = e\bar{U}_{\bar{p}'\sigma'}\{\gamma_\mu[F_1(q^2)+F_2(q^2)] - \frac{(p+p')_\mu}{2m} F_2(q^2)\}\, \bar{U}_{\bar{p}\sigma} \tag{1-8}$$

where $q = p'-p$ is the momentum transfer.

For the charge, one finds easily:

$$\langle p'|\hat{Q}|p\rangle = eF_1(o)\ \langle \bar{p}'\sigma'|\bar{p}\sigma\rangle \tag{1-9}$$

and therefore $e' = eF_1(o)$.

That is, the charge is defined at zero momentum transfer. This is the so-called Thompson limit. For QCD this limit does not exist and one will instead have to define a "running coupling constant" $e'(q^2)$. We shall return to this point in Chapter VI.

To obtain the interpretation of $F_2(q^2)$ we will consider the non-relativistic limit $q^2 \to o$. Then we can write

$$\Phi(x) = \begin{pmatrix} \chi(\bar{r}) \\ o \end{pmatrix} \tag{1-10}$$

where $\chi(\bar{r})$ is an ordinary spinor. After a tedious calculation one ends up with

$$\bar{\mu}'_\ell = \frac{eF_1(o)}{2m}\ \langle \bar{L}\rangle + \frac{e}{2m}\, 2[F_1(o)+F_2(o)]\langle \bar{S}\rangle$$

where the orbital angular momentum

$$\langle \bar{L}\rangle = \int d^3\bar{r}\ \ \chi^+(\bar{r})\,(\bar{r} \times \frac{1}{i}\bar{\nabla})\chi(\bar{r}) \tag{1-11}$$

and the spin angular momentum

$$\langle \bar{S}\rangle = \int d^3\bar{r}\ \chi^+(\bar{r})\ \frac{1}{2}\,\bar{\sigma}\ \chi(\bar{r})$$

Since the Bohr magneton now is $\frac{e'}{2m} = \frac{eF_1(o)}{2m}$ we have

$$\bar{\mu}'_\ell = \frac{e'}{2m}\langle \bar{L}\rangle + \frac{e'}{2m}\, g_\ell\, \langle \bar{S}\rangle \tag{1-12}$$

where the g_ℓ-factor is $2(1+a_\ell)$ with $a_\ell = F_2(o)/F_1(o)$.

If we switch off the EM interactions, then $F_2(o) = 0$ and the g-factor is indeed equal to two. The reason $a \neq 0$ in field theory is due to quantum fluctuations in the field associated with emission and absorption of virtual photons and the polarization of the vacuum by these photons into virtual particle-antiparticle pairs.

This self interaction between the particle and its field leads to infinities in QED. However, these infinities are less severe (diverges at most logarithmically), than the ones in classical EM.

There are two types of infinities in QED. Ultraviolet divergencies (UV) due to large momenta in the loop integrals, and infrared divergencies (IR) due to the vanishing mass of the photon. The UV-divergencies can be removed, order by order in perturbation theory, by adding appropriate counter terms, such that the charge $e'=e(F_1(o)=1)$ and therefore $a_\ell = F_2(o)$. This is known as renormalization. To handle the IR-divergencies one gives the photon a fictitious mass $\lambda << m$, and drops terms of order $\frac{\lambda}{m}$ and smaller. For each gauge invariant set of diagrams and, in particular, in each order of perturbation theory, the divergencies cancel, leaving a finite answer.

The anomaly can now be written formally as a power series expansion in $\alpha = e^2/4\pi$

$$a_\ell = A_\ell^{(2)} \left(\frac{\alpha}{\pi}\right) + A_\ell^{(4)} \left(\frac{\alpha}{\pi}\right)^2 + A_\ell^{(6)} \left(\frac{\alpha}{\pi}\right)^3 + A_\ell^{(8)} \left(\frac{\alpha}{\pi}\right)^4 + \ldots . \qquad (1\text{-}13)$$

and a_ℓ arises only from vertex diagrams. Unfortunately, not only does the number of diagrams go like N!, in N'th order, but each diagram leads to a (N+1)-dimensional parametric integral. These are usually very singular along the edges of the integration region, and

great care must be taken if one is doing numerical integration.

In lowest order (N=2) there is only one diagram (Figure 1). This was first calculated by Schwinger in 1948[11] with the result

$$a_e^{(2)} = a_\mu^{(2)} = \frac{1}{2}\left(\frac{\alpha}{\pi}\right). \tag{1-14}$$

In fourth order (N=4) there are seven mass-independent diagrams (Figure 2). Here the contribution is also known exactly[12]

$$a_e^{(4)} = \left[\frac{197}{144} + \frac{\pi^2}{12} - \frac{1}{2}\pi^2 \log 2 + \frac{3}{4}\zeta(3)\right]\left(\frac{\alpha}{\pi}\right)^2. \tag{1-15}$$

In this order (and higher) there are also mass dependent diagrams (Figure 3) due to vacuum polarization insertions. Usually the contribution from muon vacuum polarization insertion into the electron vertex is negligible. One has

$$a^{(4)}\left(\frac{m_e}{m_\mu}\right) = \frac{1}{45}\left(\frac{m_e}{m_\mu}\right)^2\left(\frac{\alpha}{\pi}\right)^2$$

and (1-16)

$$a^{(4)}\left(\frac{m_\mu}{m_e}\right) = \left[\frac{1}{3}\log\frac{m_\mu}{m_e} - \frac{25}{36} + \frac{\pi^2}{4}\frac{m_e}{m_\mu} - 4\left(\frac{m_e}{m_\mu}\right)^2 \log\frac{m_\mu}{m_e} + \frac{134}{45}\left(\frac{m_e}{m_\mu}\right)^2\right]\left(\frac{\alpha}{\pi}\right)^2$$

$$= 1.094\left(\frac{\alpha}{\pi}\right)^2$$

It is customary to quote the difference between a_μ and a_e which in general is much easier to evaluate.

$$a_\mu - a_e = a\left(\frac{m_\mu}{m_e}\right) - a\left(\frac{m_e}{m_\mu}\right) \simeq a\left(\frac{m_\mu}{m_e}\right). \tag{1-17}$$

In sixth-order (N=6) we have 72 mass-independent diagrams (Figure 4),

Figure 1. Second-Order Contribution to the Lepton Anomaly

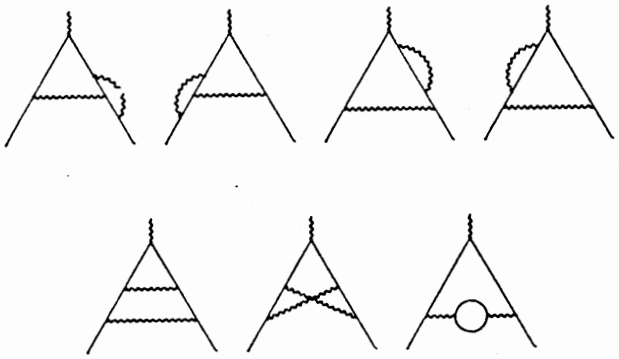

Figure 2. Mass-Independent Fourth-Order Contributions to the Lepton Anomaly

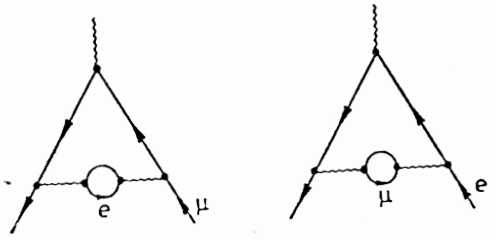

Figure 3. Mass-Dependent Fourth-Order Contribution to the Lepton Anomaly

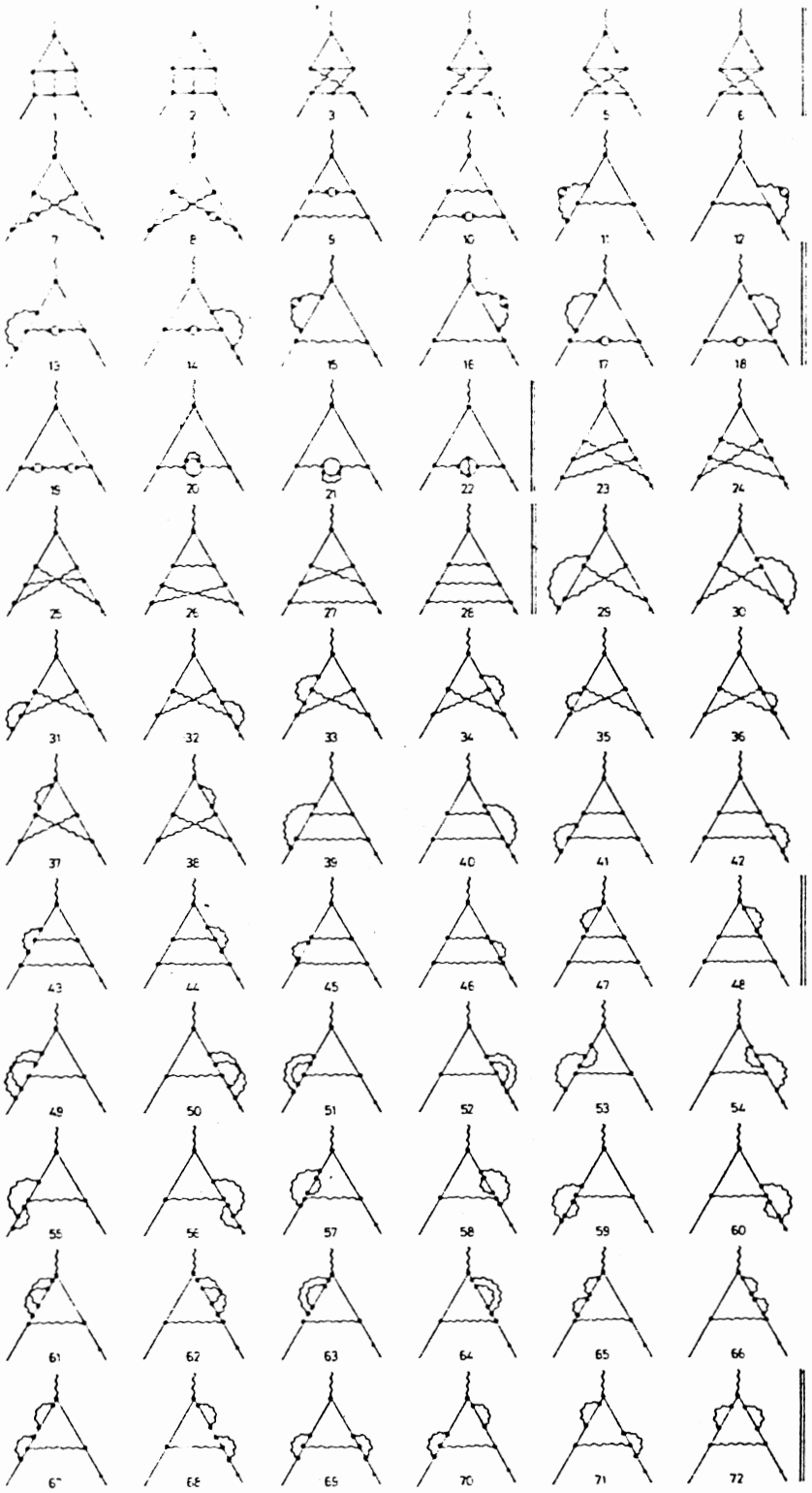

Figure 4. Mass-Independent Sixth-Order Contributions to the Lepton Anomaly

of which 51 diagrams are known exactly and the rest are known numerically with the answer[14]

$$a_e^{(6)}(\mathrm{I}) = [1.184(7)]\left(\frac{\alpha}{\pi}\right)^3 .$$

However an alternate but uncorroborated calculation of the photon-photon scattering contribution to $a_e^{(6)}$ yields[15]

$$a_e^{(6)}(\mathrm{II}) = [1.213(14)]\left(\frac{\alpha}{\pi}\right)^3 .$$

There are 24 mass-dependent diagrams also. (Figure 5). Of these, the six light by light diagrams are known numerically to O(1), and account for the biggest contribution[16]

$$a_\mu^{(6)}(\gamma\gamma) = \left[\frac{2\pi^2}{3}\log\frac{m_\mu}{m_e} - 13.68\right]\left(\frac{\alpha}{\pi}\right)^3 = 21.32\left(\frac{\alpha}{\pi}\right)^3 . \qquad (1\text{-}18)$$

The other 18 diagrams are known analytically[17] to $O\left(\frac{m_e}{m_\mu}\right)$.

$$\left[\frac{2}{9}\log^2\frac{m_\mu}{m_e} + \left(\frac{31}{27} + \frac{\pi^2}{9} - \frac{2\pi^2}{3}\log 2 + \zeta(3)\right)\log\frac{m_\mu}{m_e} + \left(\frac{1075}{216} - \frac{25}{18}\pi^2\right.\right.$$

$$\left. + \frac{5\pi^2}{3}\log 2 - 3\zeta(3) + \frac{11}{216}\pi^4 - \frac{2}{9}\pi^2\log^2 2 - \frac{1}{9}\log^4 2 - \frac{8}{3}a_4\right) \qquad (1\text{-}19)$$

$$\left. + \left(\frac{3199}{1080}\pi^2 - \frac{16}{9}\pi^2\log 2 - \frac{13}{18}\pi^3\right)\frac{m_e}{m_\mu}\right]\left(\frac{\alpha}{\pi}\right)^3 = 1.92\left(\frac{\alpha}{\pi}\right)^3 .$$

Therefore

$$a_\mu^{(6)} - a_e^{(6)} = 23.24\left(\frac{\alpha}{\pi}\right)^3 .$$

Since $a_e^{(6)} \simeq \left(\frac{\alpha}{\pi}\right)^3$ we see clearly the importance of the mass-dependent diagrams.

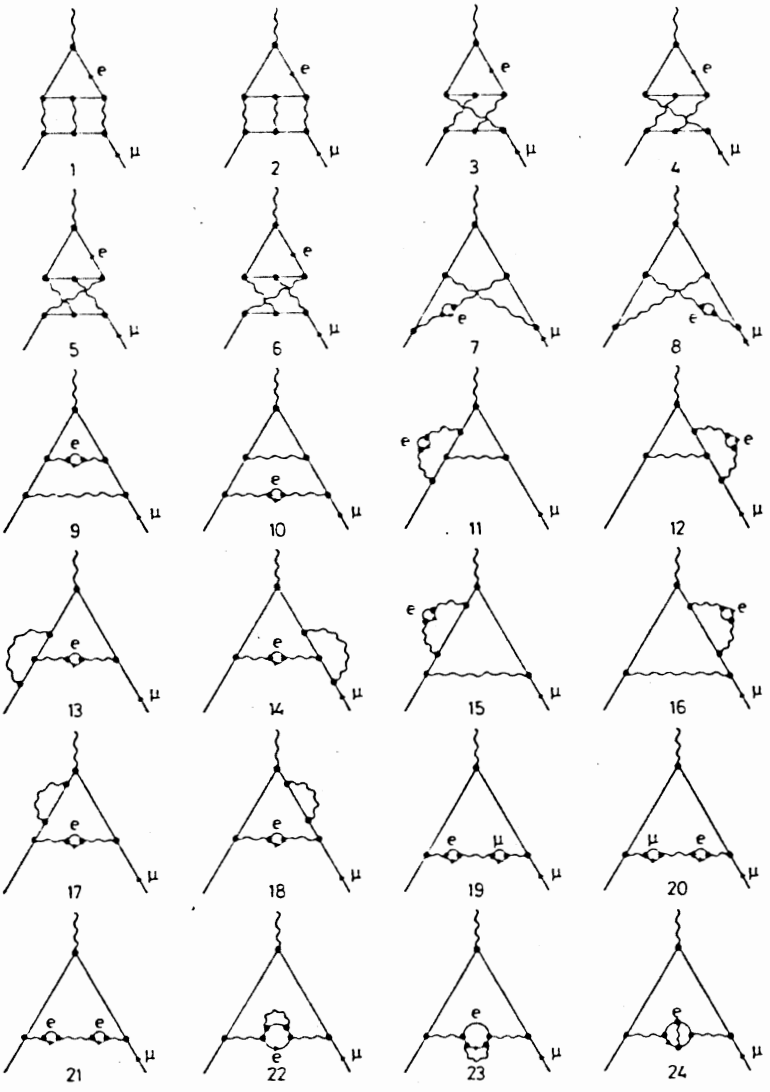

Figure 5. Mass-Dependent Sixth-Order Contributions to the Muon Anomaly

In eighth-order (N=8) there are altogether 891 mass independent diagrams (not shown). These can be classified into five different groups.[14] The first group (25 diagrams) consists of second-order vertex diagrams with second, fourth and sixth-order vacuum polarization insertions. Numerical integration gives $a_e^I = 0.08(\frac{\alpha}{\pi})^4$. The second group (54 diagrams) contains fourth-order vertex diagrams with fourth-order vacuum polarization insertions. Numerically $a_e^{II} = -0.52\ (\frac{\alpha}{\pi})^4$. The other three groups: (III) sixth-order vertex diagrams with second-order vacuum polarization insertions (150 diagrams, (IV) vertex diagrams with photon-photon scattering sub-diagrams (144 diagrams) and (V) diagrams containing no vacuum polarization loops (518 diagrams) are unknown yet. However an answer is expected within the next year.

There are 469 mass-dependent diagrams (Figure 6). Of these, 304 diagrams (group A to F') give contributions, which can be obtained by renormalization group techniques. The contribution to the $\log^n \frac{m_\mu}{m_e}$ terms[18] (n = 1,2,3) is

$$a_{A-F'}^{(8)} = \left[C \log \frac{m_\mu}{m_e} + D \log^2 \frac{m_\mu}{m_e} + E \log^3 \frac{m_\mu}{m_e}\right](\frac{\alpha}{\pi})^4 = 17.2(\frac{\alpha}{\pi})^4 . \quad (1\text{-}20)$$

The group G contains 18 diagrams[19]

$$a_G^{(8)} = \left[\frac{2\pi^3}{3} \log^2 \frac{m_\mu}{m_e} - 15.1 \log \frac{m_\mu}{m_e}\right](\frac{\alpha}{\pi})^4 = 117.5(\frac{\alpha}{\pi})^4 \quad (1\text{-}21)$$

The groups H (18 diagrams) and J (3 diagrams) have been shown to not have any $\log \frac{m_\mu}{m_e}$.[11] The last three groups I(18 diagrams), K(48 diagrams) and K'(60 diagrams) can be estimated to give[11]

$$\pm 63(\frac{\alpha}{\pi})^4 .$$

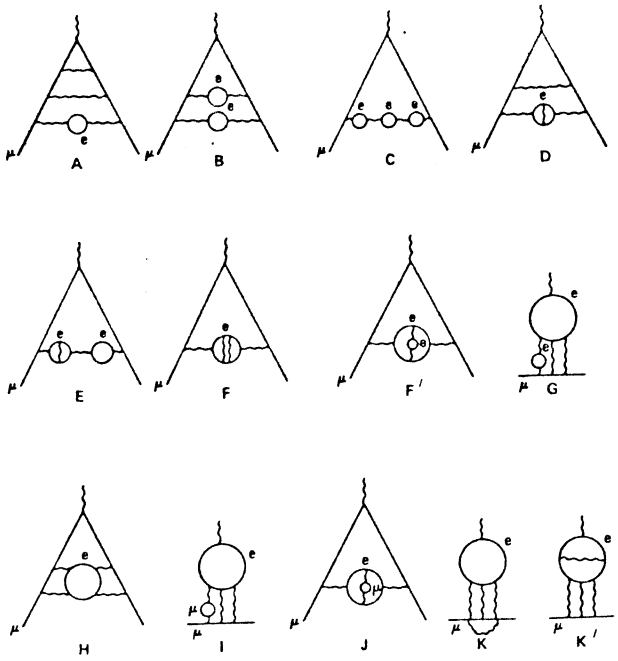

Figure 6. Mass-Dependent Eighth-Order Contributions to the Muon Anomaly

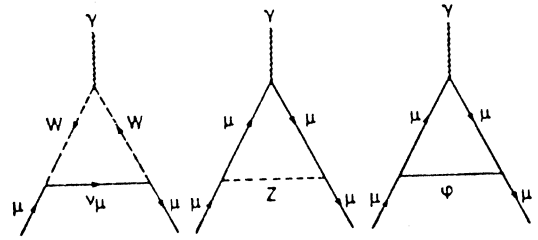

Figure 7. The Weak Contribution to the Muon Anomaly

This yields an estimate

$$a_\mu^{(8)} - a_e^{(8)} = (135 \pm 63)\left(\frac{\alpha}{\pi}\right)^4 = (3.7 \pm 2.1) \times 10^{-9} .$$

Notice again the very large coefficient! This is due to the fact that the main contribution arises from diagrams with electron insertion, in which the expansion parameter is $\alpha \log \frac{m_\mu}{m_e}$ rather than α itself.

Also since the muon is fairly heavy, hadronic and weak contributions will add to a_μ.

The dominant part (order $\left(\frac{\alpha}{\pi}\right)^2$) of the hadronic contribution (Figure 8) comes from hadronic vacuum polarization insertion into the lowest-order muon vertex.[20] The muon anomaly is expressed as a spectral integral over the total cross section for e^+e^- annihilation into hadrons $\sigma_H(s)$, where s is the CM-energy.

$$a_\mu^{(H)} = \frac{m_\mu^2}{4\pi^3} \int_{4m_\pi^2}^{\infty} ds\ \sigma_H(s)\ K_\mu^{(2)}(s)$$

where (1-22)

$$K_\mu^{(2)}(s) = \int_0^1 dx\ \frac{x^2(1-x)}{x^2 m_\mu^2 + (1-x)s} \to \frac{1}{3s} \text{ for } s \to \infty$$

One finds

$$a_\mu^{(H)} = (70.2 \pm 8.0) \times 10^{-9} .$$

In higher order $\left(\frac{\alpha}{\pi}\right)^3$ (Figure 9) one obtains[20]

$$a_\mu^{(H)} = (-3.5 \pm 1.4) \times 10^{-9}$$

giving a total

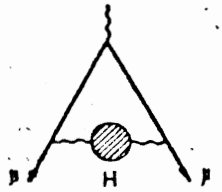

Figure 8. Hadronic Vacuum Polarization Correction to Lowest-Order Contribution to a_μ

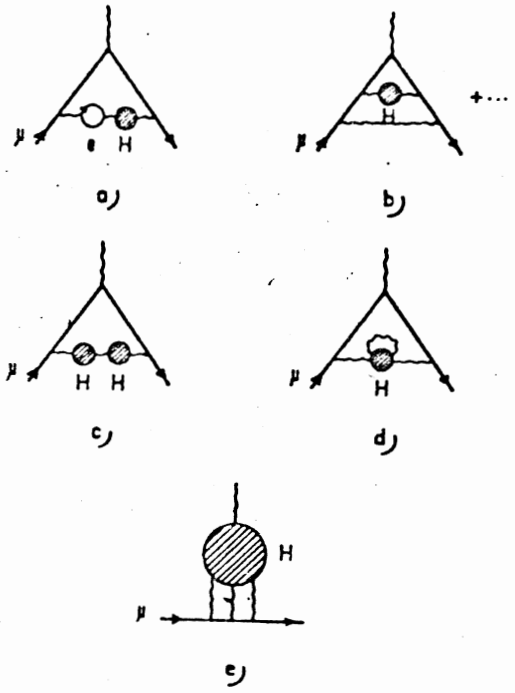

Figure 9. Hadronic Contributions to a_μ of Order $(\frac{\alpha}{\pi})^3$

$$a_\mu^{(H)} \simeq (66.7 \pm 9.4) \times 10^{-9}.$$

The contribution to $a_e^{(H)}$ is indeed very small since

$$a_e^{(H)} \simeq \left(\frac{m_e}{m_\mu}\right)^2 a_\mu^{(H)} = 1.6 \times 10^{-12}.$$

Finally for the weak contributions in the W-S model we have[21]

$$a_\mu^{(W)} = (2.1 \pm 0.2) \times 10^{-9}$$

and

$$a_e^{(W)} \simeq \left(\frac{m_e}{m_\mu}\right)^2 a_\mu^{(W)} = 0.05 \times 10^{-12}.$$

In Table I and II we have given the different contributions to a_e and a_μ using the latest value of $\alpha^{-1} = 137.035963(15)$ (obtained from the Josephson effect).[22] By comparison with the experimental values we see that, in the case of the muon, theory and experiment agree beautifully.

In the case of the electron, there is a fair agreement (2.4 σ) provided one uses $a_e^{(6)}$(I). If, however a_e^{6}(II) is correct, there is a 3.3 standard deviation discrepancy between theory and experiment. Assuming $a_e^{(8)} \simeq \left(\frac{\alpha}{\pi}\right)^4 = 29 \times 10^{-12}$, this could mean a breakdown of pure QED. But before drawing such a conclusion, we must, of course, know the $a_e^{(6)}$ term analytically, in particular the light by light contribution. This would also determine which of the two $a_e^{(6)}$(I) and $a_e^{(6)}$(II) is correct.

TABLE I

CONTRIBUTIONS TO a_e^{THEORY} AND COMPRISON WITH $a_e^{EXPERIMENT}$

$a_e^{(2)}$	$(1161410039 \pm 130) \times 10^{-12}$
$a_e^{(4)}$	$(-1772303 \pm 1) \times 10^{-12}$
$a_e^{(6)}$ (I)	$(14838 \pm 88) \times 10^{-12}$
$a_e^{(6)}$ (II)	$(15202 \pm 176) \times 10^{-12}$
$a_e^{(8)}$	$? (29) \times 10^{-12}$
$a_e^{(4)}$ (muon)	2.8×10^{-12}
$a_e^{(4)}$ (tauon)	0.01×10^{-12}
$a_e^{(4)}$ (hadron)	1.6×10^{-12}
$a_e^{(2)}$ (weak)	0.05×10^{-12}
a_e^{Theory} (I)	$(1159652567 \pm 150) \times 10^{-12}$
a_e^{Theory} (II)	$(1159652931 \pm 220) \times 10^{-12}$
$a_e^{Experiment}$	$(1159652200 \pm 40) \times 10^{-12}$

TABLE II

CONTRIBUTIONS TO a_μ^{THEORY} AND COMPARISON WITH $a_\mu^{EXPERIMENT}$

$a_\mu^{(2)}$	$(1161410.0 \pm 1.3) \times 10^{-9}$
$a_\mu^{(4)}$	$(-1772.3) \times 10^{-9}$
$a_\mu^{(6)}$	$(306.3 \pm 0.8) \times 10^{-9}$
$a_\mu^{(8)}$	$(3.7 \pm 2.1) \times 10^{-9}$
$a_\mu^{(4)}$ (electron)	$(5904.1) \times 10^{-9}$
$a_\mu^{(4)}$ (tauon)	0.4×10^{-9}
$a_\mu^{(4)}$ (hadron)	$(70.2 \pm 8.0) \times 10^{-9}$
$a_\mu^{(6)}$ (hadron)	$(-3.5 \pm 1.4) \times 10^{-9}$
$a_\mu^{(2)}$ (weak)	$(2.1 \pm 0.2) \times 10^{-9}$
a_μ^{Theory}	$(1165920.0 \pm 13.8) \times 10^{-9}$
$a_\mu^{Experiment}$	$(1165923 \pm 12) \times 10^{-9}$

REFERENCES

1. P. A. M. Dirac, Proc. Roy. Soc. A117, 610 (1928); ibid A118, 351 (1928).

2. S. J. Brodsky and S. D. Drell, Phys. Rev. D22, 2236 (1980).

3. R. S. Van Dyck, Jr., Bull. Am. Phys. Soc. 24, 758 (1979); see also R. S. Van Dyck, Jr., P. B. Schwinberg and H. G. Dehmelt, Phys. Rev. Lett. 38, 310 (1977).

4. R. S. Van Dyck, Jr., P. B. Schwinberg and H. G. Dehmelt, Bull. Am. Phys. Soc. 26, 597 (1981).

5. S. I. Serednyakov et al., Phys. Lett. 66B, 102 (1977).

6. F. Combley, F. J. M. Farley and E. Picasso, Phys. Reports 68C, 93 (1981).

7. L. H. Thomas, Nature 117, 514 (1926).

8. K. M. Crowe et al., Phys. Rev. D5, 2145 (1972).

9. M. P. Balandin et al., Sov. Phys. JETP 40, 1645 (1974).

10. B. E. Lautrup, "Lecture Notes in QED", Niels Bohr Institute 1973-1974.

11. For many of the theoretical results up to 1977 we refer to the excellent review articles by J. Calmet et al., Rev. of Modern Physics Vol. 49, 21 (1977); B. E. Lautrup, A. Peterman and E. de Rafael, Phys. Rep. 3C, 193 (1972).

12. J. S. Schwinger, Phys. Rev. 73, 416 (1948).

13. The fourth order anomaly was first calculated erroneous by R. Karplus and N. Kroll, Phys. Rev. 77, 536 (1950); and was later corrected by C. Sommerfield, Phys. Rev. 107, 328 (1954), Ann. Phys. 5, 26 (1958); A. Peterman, Nucl. Phys. 3, 689 (1957), Helv. Phys. Acta 30, 407 (1957); and by M. V. Terent'ev, using dispersion technique, Sov. Phys. JETP 16 444 (1963).

14. The latest updates on a_e and a_μ are given in G. P. Lepage, "Theoretical Advances in Quantum Electrodynamics", CLNS-80/474, November 1980; T. Kinoshita, "Anomalous Magnetic Moment of an Electron and High Precision Test of Quantum Electrodynamics," CLNS-79/437,

October 1979; T. Kinoshita, "What can one learn from very Accurate Measurements of the Lepton Magnetic Moments," CLNS-390, March, 1978.

15. M. A. Samuel and C. Chlouber, Phys. Rev. D18, 613 (1978).

16. C. Chlouber and M. A. Samuel, Phys. Rev. Lett. 36, 442 (1976).

17. M. L. Laursen, M. A. Samuel, and A. K. Ray, Zeit. für Physic 6C, 3 (1980).

18. M. A. Samuel, Phys. Rev. D9, 2913 (1974); B. E. Lautrup and E. de Rafael, Nucl. Phys. B70, 317 (1974); see also Ref. 10.

19. C. Chlouber and M. A. Samuel, Phys. Rev. D16, 3596 (1977); B. E. Lautrup and M. A. Samuel, Phys. Lett. 72B, 114 (1977).

20. J. Calmet et al., Phys. Lett. B61, 283 (1976); see also Ref. 10.

21. W. A. Bardeen, R. Gastmans and B. E. Lautrup, Nucl. Phys. B46, 319 (1972); see also Ref. 10 for comparison with other models.

22. E. R. Williams and P. T. Olsen, Phys. Rev. Lett. 24, 1575 (1979).

CHAPTER III

CORRECTIONS TO THE SIXTH-ORDER ANOMALOUS MAGNETIC MOMENT OF THE MUON

Introduction

In sixth-order, the difference between the muon and electron magnetic moments can be expressed, for $m_\mu/m_e \gg 1$, as

$$a_\mu^{(6)} - a_e^{(6)} = \left(\frac{\alpha}{\pi}\right)^3 \{A\ln^2(m_\mu/m_e) + B\ln(m_\mu/m_e) + C + D(m_e/m_\mu) + O[(m_e/m_\mu)^2 \ln^2(m_\mu/m_e)]\} . \quad (3\text{-}1)$$

A and B are completely known analytically.[1,2]

$$A = 2/9.$$

$$B = 31/27 + 7\pi^2/9 - \frac{2\pi^2}{3}\ln 2 + \zeta(3). \quad (3\text{-}2)$$

All contributions to C, except the light-by-light contribution $C^{(\gamma\gamma)}$, are also known analytically.[3] ($C^{(\gamma\gamma)}$ is known numerically.[4,5])

$$C = \frac{1075}{216} - \frac{25\pi^2}{18} + \frac{5\pi^2}{3}\ln 2 - 3\zeta(3) + 3C_4 + C^{(\gamma\gamma)}$$

where

$$C_4 = \frac{11}{648}\pi^4 - \frac{2}{27}\pi^2 \ln^2 2 - \frac{1}{27}\ln^4 2 - \frac{8}{9}a_4$$

and

$$a_4 = \sum_1^\infty \frac{1}{2^n n^4} \tag{3-3}$$

The only contribution to D which is known analytically is the double-bubble contribution[6] (diagram (d) of Figure 10)

$$D^{(d)} = -4\pi^2/45 \tag{3-4}$$

The contribution to D due to the other diagrams of Figure 10 is known numerically,

$$D^{(a+b+c)} = -5.6776256$$

$$D^{(e+f)} = 0. \tag{3-5}$$

In this paper we present an analytic calculation of $D_{(a+b+c)}$, the contribution to D from fourth-order electron vacuum polarization (the proper diagrams a, b and c of Figure 10).

This quantity is given by the following expression.[7,8]

$$D^{(a+b+c)} = \frac{\pi}{2} - 2\pi \int_0^1 \frac{dx\,x}{(1-x^2)^{3/2}} \left[\frac{1}{\pi} \mathrm{Im}\pi^{*(4)}(x) - \frac{1}{\pi} \mathrm{Im}\pi^{*(4)}(1)\right] / \left(\frac{\alpha}{\pi}\right)^2 \tag{3-6}$$

where

$$\frac{1}{\pi} \mathrm{Im}\pi^{*(4)}(x) = \left(\frac{\alpha}{\pi}\right)^2 \left\{\left[\frac{5x}{8} - \frac{3x^3}{8}\right] + x\left(\frac{-1}{2} + \frac{x^2}{6}\right) \ln\left(\frac{64x^4}{(1-x^2)^3}\right) + \left(\frac{11}{16} + \frac{11}{24}x^2 - \frac{7}{48}x^4\right) \ln\left(\frac{1+x}{1-x}\right) + \left(\frac{1}{2} + \frac{x^2}{3} - \frac{x^4}{6}\right) \ln\left(\frac{(1+x)^3}{8x^2}\right) \ln\left(\frac{1+x}{1-x}\right) - \left(\frac{1}{2} + \frac{x^2}{3} - \frac{x^4}{6}\right) \cdot \left[4\,\Phi\left(-\frac{1-x}{1+x}\right) + 2\,\Phi\left(\frac{1-x}{1+x}\right) + \frac{\pi^2}{2}\right]\right\} \tag{3-7}$$

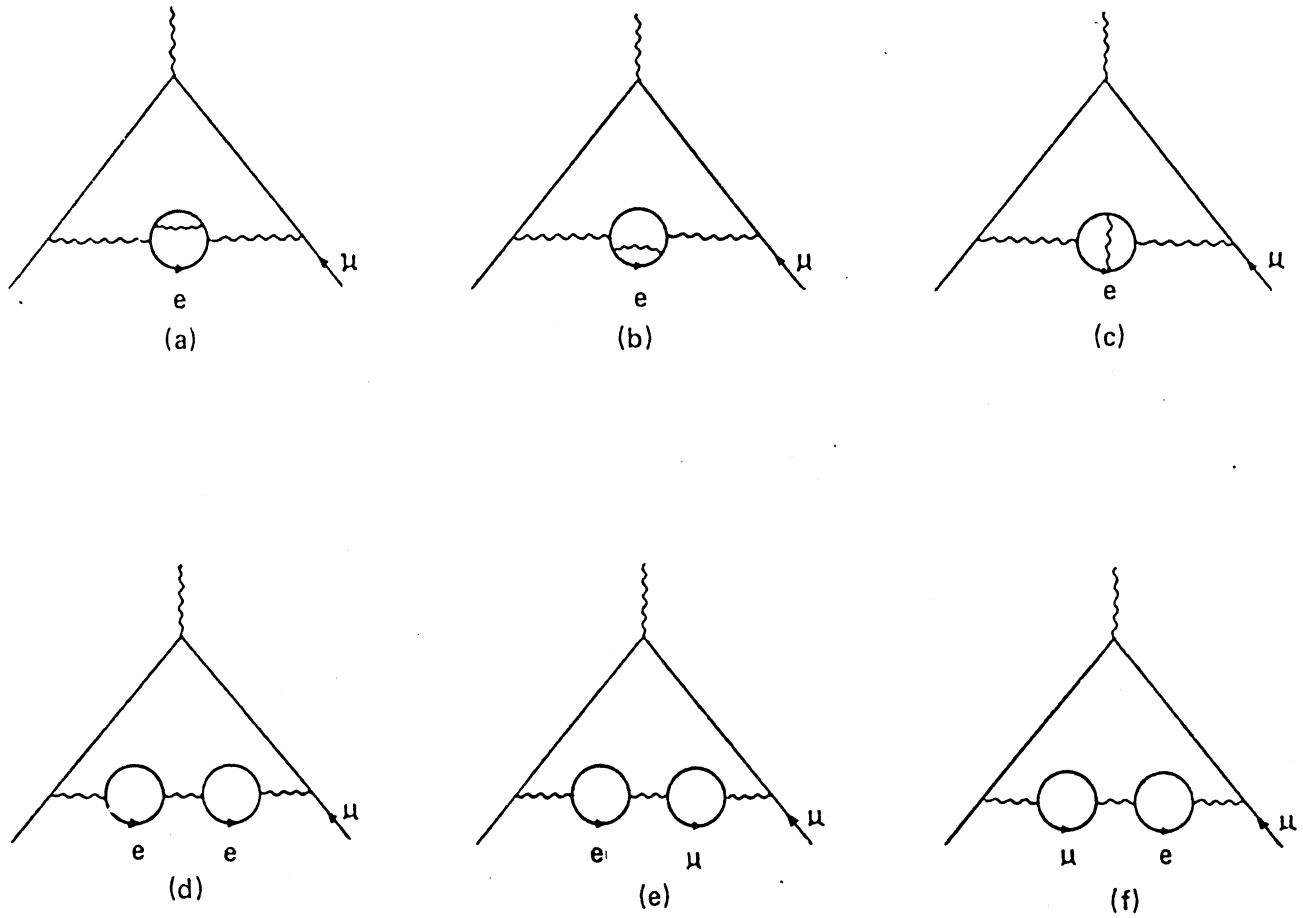

Figure 10. Feynman Diagrams Representing the Fourth-Order Vacuum Polarization Contribution to the Sixth-Order Muon Anomaly

and

$$\frac{1}{\pi}\,\mathrm{Im}\pi^{*(4)}(1) = \frac{1}{4}\left(\frac{\alpha}{\pi}\right)^2 . \tag{3-8}$$

So we can write

$$D^{(a+b+c)} = \frac{\pi}{2} - 2\pi\left[R_1 + R_2 + R_3 + R_4 + R_5 - \frac{1}{4}\int_0^1 \frac{dxx}{(1-x^2)^{3/2}}\right] \tag{3-9}$$

where the five R_i correspond to the five terms in Eqn. (3-7). It is easy to see that $R_2 + R_3$, R_4 and R_5 are finite and the combination

$$R_1' = R_1 - \frac{1}{4}\int_0^1 \frac{x}{(1-x^2)^{3/2}} \tag{3-10}$$

is also finite.

We now evaluate the integrals. Our results are as follows:

$$R_1' = \frac{1}{4} - \frac{\pi}{32} \tag{3-11}$$

$$R_2 + R_3 = \pi\ln 2 - \frac{211\pi}{288} \tag{3-12}$$

and

$$R_4 + R_5 = \frac{13\pi^2}{36} - \frac{\pi}{9}\ln 2 - \frac{151\pi}{216} . \tag{3-13}$$

Adding the terms in Eqns. (3-11), (3-12) and (3-13) and substituting into Eqn. (3-9), we obtain our result.

$$D^{(a+b+c)} = -\frac{13\pi^3}{18} - \frac{16\pi^2}{9}\ln 2 + \frac{79\pi^2}{27} = -5.6776257 \tag{3-14}$$

This is in excellent agreement with the numerical value in Eqn. (3-5):

Interestingly, although the term proportional to π cancels out, there remains a π^3 term. This is the first time an odd power of π occurs in a g-2 contribution.

Using Eqns. (3-4), (3-5) and (3-14), the contribution to D from all the graphs of Figure 10 can be written,

$$D^{(a+b+c)} + D^{(d)} + D^{(e+f)} = -\frac{13\pi^3}{18} - \frac{16\pi^2}{9}\ln 2 + \frac{383\pi^2}{135} . \qquad (3\text{-}15)$$

We would like to mention that the above result in Eqn. (3-15) can be also obtained from the vacuum polarization potential of muonic atoms in order $\alpha^2(Z\alpha)$. For more on this point see Reference 9.

REFERENCES

1. T. Kinoshita, Nuovo Cimento 51B, 140 (1967).

2. B. E. Lautrup and M. A. Samuel, Physics Letts. 72B, 114 (1977).

3. R. Barbieri and E. Remiddi, Nuclear Physics B90, 233 (1975).

4. M. A. Samuel and C. Chlouber, Phys. Rev. Letts. 36, 442 (1976).

5. C. Chlouber and M. A. Samuel, Phys. Rev. D16, 3596 (1977).

6. M. A. Samuel, Nuclear Physics B70, 351 (1974).

7. C. Chlouber and M. A. Samuel, Phys. Rev. D17, 2817 (1978).

8. B. E. Lautrup and E. de Rafael, Phys. Rev. 174, 1835 (1968).

9. M. L. Laursen and M. A. Samuel, to be published in Zeit. für Physik C (1981).

CHAPTER IV

MORE CORRECTIONS TO THE SIXTH-ORDER ANOMALOUS MAGNETIC MOMENT OF THE MUON

Introduction

The contributions to $a_\mu^{(6)} - a_e^{(6)}$ (in units of $(\frac{\alpha}{\pi})^3$) from the graphs in Figures 11 and 12 are respectively:[1]

$$I_L = 2 \int_{4m_e^2}^{\infty} \frac{dt}{t} \frac{1}{\pi} \mathrm{Im}\pi_e^{(2)}(t)\ L_\mu^{(4)}(t),$$

$$I_M = 2 \int_{4m_e^2}^{\infty} \frac{dt}{t} \frac{1}{\pi} \mathrm{Im}\pi_e^{(2)}(t)\ M_\mu^{(4)}(t) \qquad (4\text{-}1)$$

with the total given by

$$I_K = 2 \int_{4m_e^2}^{\infty} \frac{dt}{t} \frac{1}{\pi} \mathrm{Im}\pi_e^{(2)}(t)\ K_\mu^{(4)}(t)$$

where

$$K_\mu^{(4)}(t) \equiv L_\mu^{(4)}(t) + M_\mu^{(4)}(t).$$

Here $\frac{1}{\pi} \mathrm{Im}\pi_e^{(2)}(t)$ is the second-order spectral function

$$\frac{1}{\pi} \mathrm{Im}\pi_e^{(2)}(t) = x(\frac{1}{2} - \frac{1}{6} x^2)\ \theta(t - 4m_e^2)$$

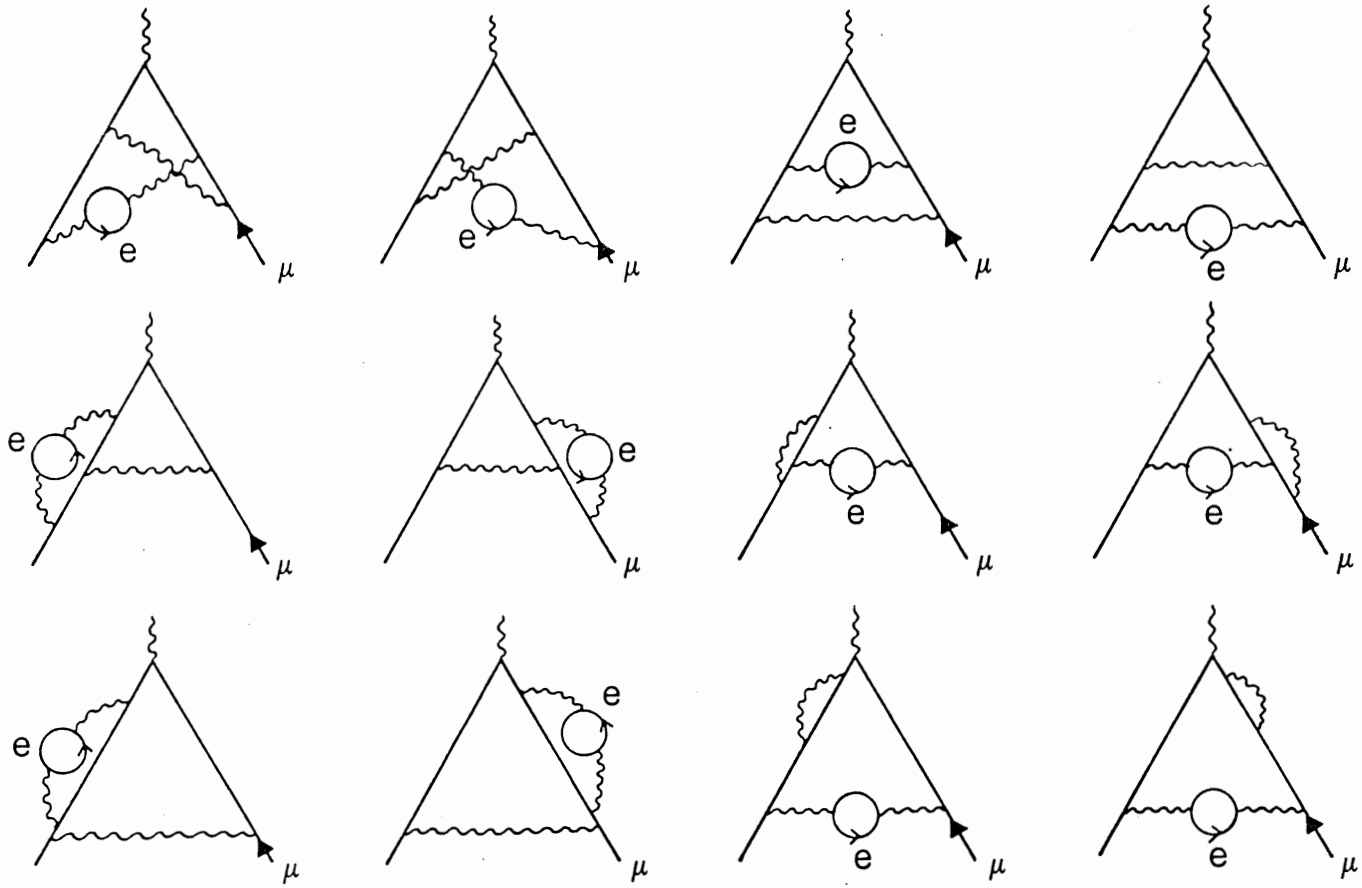

Figure 11. Sixth-Order Vertex Graphs With a Single Second-Order Vacuum Polarization Insertion

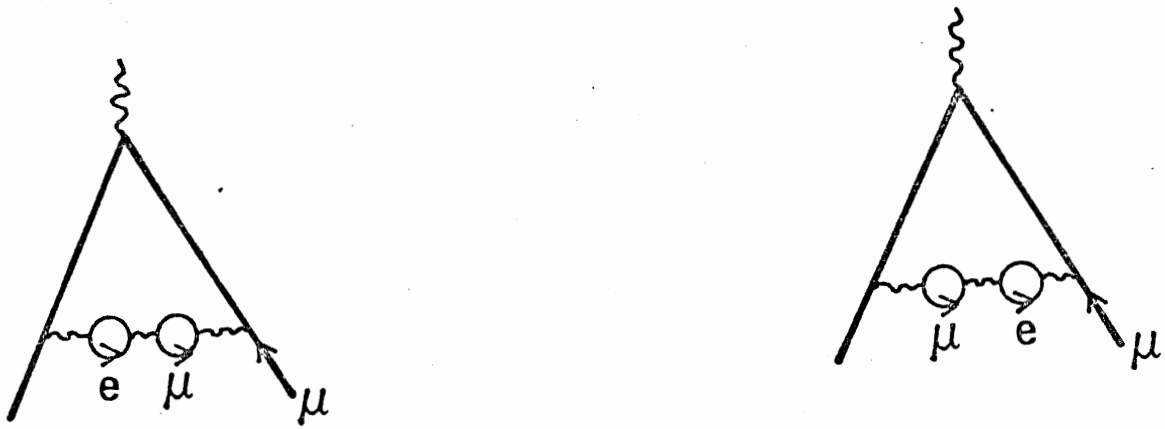

Figure 12. Sixth-Order Vertex Graphs With Mixed Fourth-Order Vacuum Polarization Insertion

with

$$x = \left(1 - \frac{4m_e}{t}\right)^{1/2} \tag{4-2}$$

while $K_\mu^{(4)}(t)$ and $L_\mu^{(4)}(t)$ are one half of the fourth-order anomaly, with a heavy photon of mass $\sqrt{t}$, with and without vacuum polarization insertions, respectively.

For $b \equiv \frac{t}{m_\mu^2} \geq 4$ we have[1]

$$K_\mu^{(4)}(b) = -\frac{139}{144} + \frac{115}{72}\,b + \left(\frac{19}{12} - \frac{7}{36}\,b + \frac{23}{144}\,b^2 + \frac{1}{b-4}\right)\log b$$

$$+ \left[-\frac{4}{3} + \frac{127}{36}\,b - \frac{115}{72}\,b^2 + \frac{23}{144}\,b^3\right]\frac{\log y}{\sqrt{b(b-4)}} + \left(\frac{9}{4} + \frac{5}{24}\,b - \frac{1}{2}\,b^2 - \frac{2}{b}\right)\zeta(2)$$

$$+ \frac{5}{96}\,b^2\log^2 b + \left(-\frac{1}{2}\,b + \frac{17}{24}\,b^2 - \frac{7}{48}\,b^3\right)\frac{\log y \log b}{\sqrt{b(b-4)}}$$

$$+ \left(\frac{19}{24} + \frac{53}{48}\,b - \frac{29}{96}\,b^2 - \frac{1}{3b} + \frac{2}{b-4}\right)\log^2 y$$

$$+ \left(-2b + \frac{17}{6}\,b^2 - \frac{7}{12}\,b^3\right)\frac{D_p(b)}{\sqrt{b(b-4)}}$$

$$+ \left(\frac{13}{3} - \frac{7}{6}\,b + \frac{b^2}{4} - \frac{b^3}{6} - \frac{4}{b-4}\right)\frac{D_m(b)}{\sqrt{b(b-4)}}$$

$$+ \left(\frac{1}{2} - \frac{7}{6}\,b + \frac{1}{2}\,b^2\right)T(b) \tag{4-3}$$

and

$$M_\mu^{(4)}(b) = \frac{35}{36} + \frac{8}{9}\,b + \left(\frac{4}{3} - \frac{b}{9} - \frac{5}{18}\,b^2\right)\log b$$

$$+ \left(-\frac{4}{3} + \frac{19}{9}\,b + \frac{4b^2}{9} - \frac{5}{18}\,b^3\right) \frac{\log y}{\sqrt{b(b-4)}}$$

$$+ \left(1 + \frac{b}{3} - \frac{b^2}{6} - \frac{2}{b}\right)\zeta(2) + \left(\frac{1}{2} + \frac{b}{6} - \frac{b^2}{12} - \frac{1}{3b}\right)\log^2 y$$

$$+ \left(\frac{16}{3} - \frac{4b}{3} - \frac{4b^2}{3} + \frac{b^3}{3}\right) \frac{D_m(b)}{\sqrt{b(b-4)}} \qquad (4\text{-}4)$$

with

$$y = \frac{\sqrt{b} - \sqrt{b-4}}{\sqrt{b} + \sqrt{b-4}}\,,$$

$$D_p(b) = \mathrm{Li}_2(y) + \log y \log(1-y) - \frac{1}{4}\log^2 y - \zeta(2),$$

$$D_m(b) = \mathrm{Li}_2(-y) + \frac{1}{4}\log^2 y + \frac{1}{2}\zeta(2) \qquad (4\text{-}5)$$

and

$$T(b) = -6\mathrm{Li}_3(y) - 3\mathrm{Li}_3(-y) + \log^2 y \log(1-y)$$

$$+ \frac{1}{2}\left[\log^2 y + 6\zeta(2)\right]\log(1+y)$$

$$+ 2\log y\left[\mathrm{Li}_2(-y) + 2\mathrm{Li}_2(y)\right].$$

Outline of Calculation

The integral I_K in Eqn. (4-1) can be written as follows:

$$I_K = \frac{2}{\pi}\,\mathrm{Im}\pi_e^{(2)}(\infty)\int_{4m_e^2}^{\infty}\frac{dt}{t}\,K_\mu^{(4)}(t)$$

$$+ 2K_\mu^{(4)}(o)\int_{4m_e^2}^{\infty}\frac{dt}{t}\left[\frac{1}{\pi}\,\mathrm{Im}\pi_e^{(2)}(t) - \frac{1}{\pi}\,\mathrm{Im}\pi_e^{(2)}(\infty)\right] + R_K$$

$$= Q_K + R_K + S_K \tag{4-6}$$

where[1]

$$Q_K = \left[\frac{197}{108} + \frac{\pi^2}{9} - \frac{2\pi^2}{3}\log 2 + \zeta(3)\right]\log\frac{m_\mu}{m_e}$$

$$+ \left[\frac{2861}{648} - \frac{77}{54}\pi^2 + \frac{5\pi^2}{3}\log 2 - \frac{7}{2}\zeta(3) + \frac{11}{216}\pi^4 - \frac{2\pi^2}{9}\log^2 2\right.$$

$$\left. - \frac{1}{9}\log^4 2 - \frac{8}{3}a_4\right],$$

$$a_4 = \sum_{n=1}^{\infty}\frac{1}{2^n n^4}$$

$$R_K = 2\int_{4m_e^2}^{\infty}\frac{dt}{t}\left[\frac{1}{\pi}\mathrm{Im}\pi_e^{(2)}(t) - \frac{1}{\pi}\mathrm{Im}\pi_e^{(2)}(\infty)\right]\left[K_\mu^{(4)}(t) - K_\mu^{(4)}(o)\right]$$

and

$$S_K = -\frac{2}{\pi}\mathrm{Im}\pi_e^{(2)}(\infty)\int_o^{4m_e^2}\frac{dt}{t}\left[K_\mu^{(4)}(t) - K_\mu^{(4)}(o)\right].$$

We will show in Appendix A that, in the limit $b \to 0$,

$$K_\mu^{(4)}(b) = K_\mu^{(4)}(o) - \frac{\pi}{8}\sqrt{b} - \frac{1}{2}b\log b + O(b)$$

with the fourth-order result having been verified to be

$$K_\mu^{(4)}(o) = \frac{197}{144} + \frac{\pi^2}{12} - \frac{\pi^2}{2}\log 2 + \frac{3}{4}\zeta(3). \tag{4-7}$$

Since the result in Eqn. (4-7) plays a crucial role in our calculation, we have performed a numerical check. The results of our numerical

computations are shown in Figures 13 and 14. In Figure 13 we have plotted $K_\mu^{(4)}(o) - K_\mu^{(4)}(b) - \frac{b}{2}\log b$ versus $\sqrt{b}$. One can see that in the limit $b \to 0$, the computed points asymptotically approach a straight line through the origin of slope .39 = $\pi/8$, in agreement with the result of Eqn. (4-7). In Figure 14 we have a semi-log plot of b versus $\frac{1}{b}\left[K_\mu^{(4)}(b) - K_\mu^{(4)}(o) + \frac{\pi}{8}\sqrt{b}\right]$. Again, in the limit $b \to 0$, the computed points asymptotically approach a straight line. The line intercepts the vertical axis at b = 1 (log b = 0). The slope is - 1.15, which becomes on conversion to the natural log, - 1.15/log 10 = - 1.15/2.30 = - .50, in agreement with the result of Eqn. (4-7).

Using Eqns. (4-6) and (4-7) one finds to order $\frac{m_e}{m_\mu}$

$$R_K = \left[-\frac{\pi}{3} + \frac{\pi^2}{8}\right] \frac{m_e}{m_\mu}$$

and

$$S_K = \frac{\pi}{3} \frac{m_e}{m_\mu}$$

or

$$R_K + S_K = \frac{\pi^2}{8} \frac{m_e}{m_\mu} . \qquad (4\text{-}8)$$

Similarly, we have

$$I_M = Q_M + R_M + S_M$$

with[2]

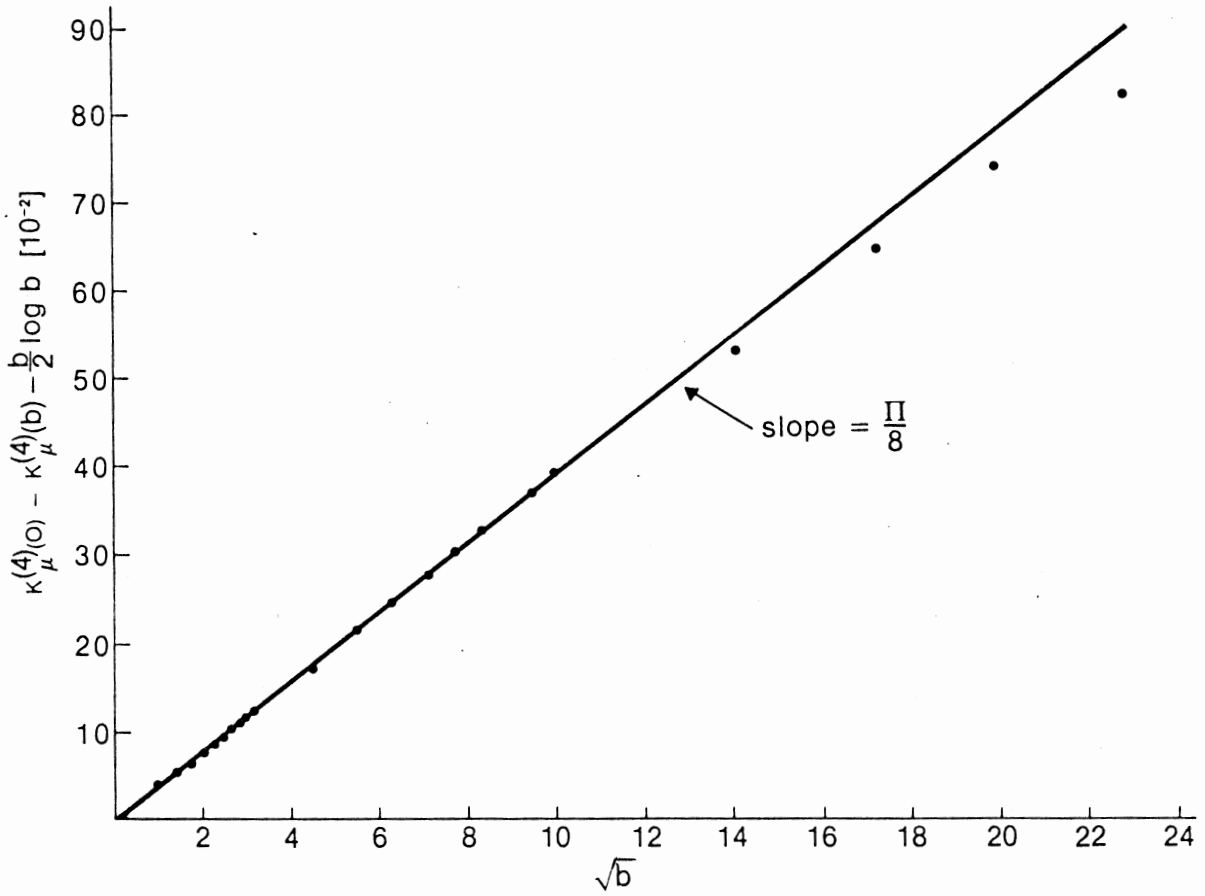

Figure 13. $K_\mu^{(4)}(o) - K_\mu^{(4)}(b) - \frac{b}{2}\log b$ Plotted Versus $\sqrt{b} \times 10^2$. The Fact That the Computed Points Approach A Straight Line Through the Origin With the Correct Slope Provides a Numerical Verification of Eqn. (4-7)

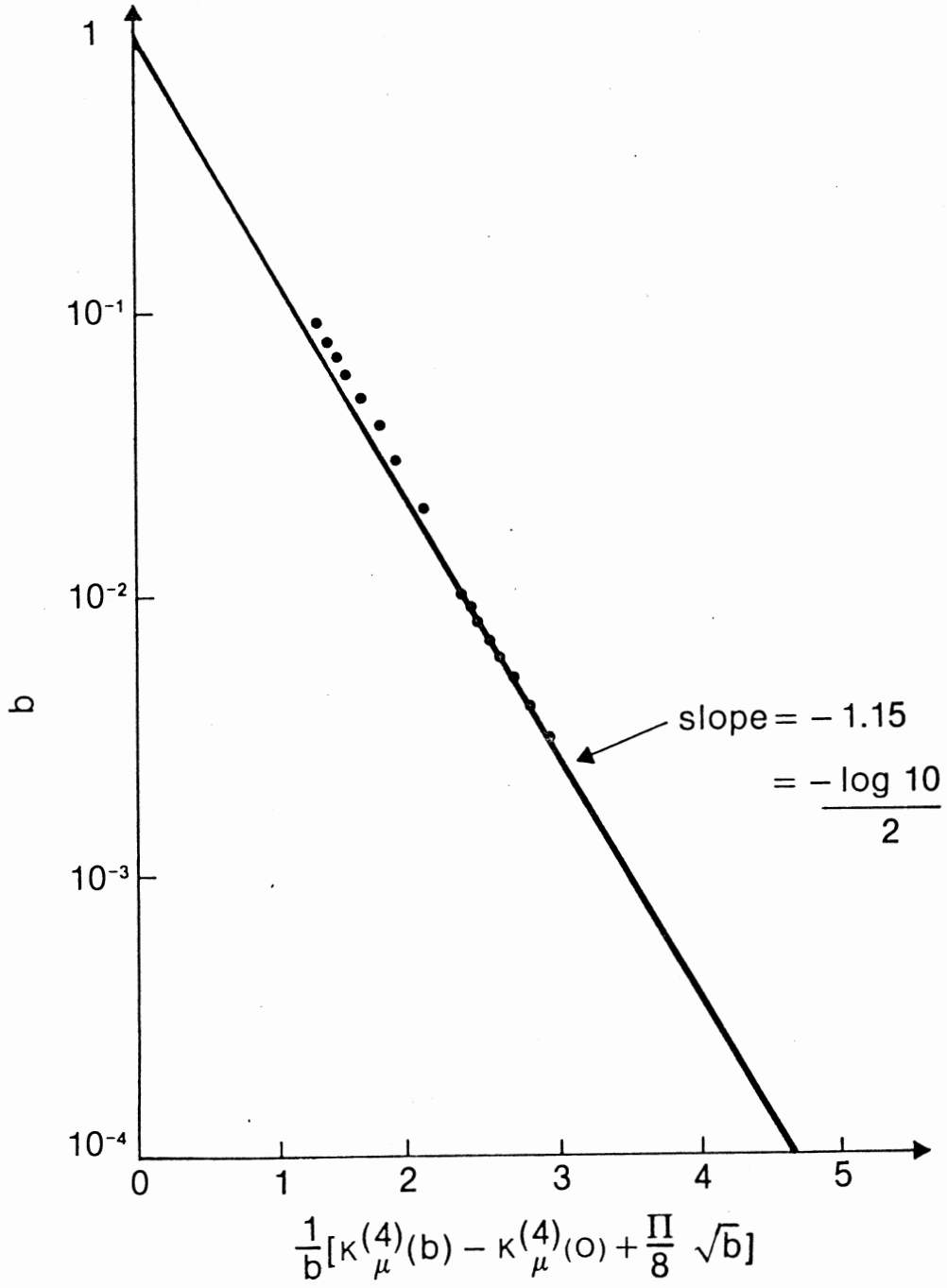

Figure 14. Semi-Log Plot of b Versue $\frac{1}{b}\left[K_{\mu}^{(4)}(b) - K_{\mu}^{(4)}(o) + \frac{\pi}{8}\sqrt{b}\right]$. The Fact That the Computed Points Approach a Straight Line With the Correct Slope and the Vertical Intercept a b=1 Provides a Numerical Verification of Eqn. (4-7)

$$Q_M = \left[\frac{119}{27} - \frac{4\pi^2}{9}\right] \log \frac{m_\mu}{m_e} + \left[\frac{\pi^2}{27} - \frac{61}{162}\right] .$$

$R_M + S_M$ is known numerically[3] to be of order $\left(\frac{m_e}{m_\mu}\right)^2$.

We find easily, in the limit $b \to 0$,

$$M_\mu^{(4)}(b) = M_\mu^{(4)}(o) + \left[\frac{115}{108} - \frac{\pi^2}{9}\right] b + O(b^{3/2})$$

with

$$M_\mu^{(4)}(o) = \frac{119}{36} - \frac{\pi^2}{3} . \qquad (4\text{-}9)$$

Eqn. (4-9) now shows that only the order $\left(\frac{m_e}{m_\mu}\right)^2$ term is present in $R_M + S_M$.

Summary of Results for $a_\mu^{(6)} - a_e^{(6)}$

The total contribution from all graphs in sixth order, to the difference between the muon and electron magnetic moments, for $m_\mu/m_e \gg 1$, is given by

$$a_\mu^{(6)} - a_e^{(6)} = \left(\frac{\alpha}{\pi}\right)^3 \left[A \log^2 \frac{m_\mu}{m_e} + B \log \frac{m_\mu}{m_e} + C \right.$$

$$\left. + D \frac{m_e}{m_\mu} + O\left(\left(\frac{m_e}{m_\mu}\right)^2 \log^2 \frac{m_\mu}{m_e}\right)\right]$$

All coefficients are now completely known analytically[4] except for the light-by-light contributions to C and D, denoted by $C^{(\gamma\gamma)}$ and $D^{(\gamma\gamma)}$, respectively. (The light-by-light contribution is known numerically[5]). The results are:

$$A = \frac{2}{9},$$

$$B = \frac{31}{27} + \frac{7\pi^2}{9} - \frac{2\pi^2}{3} \log 2 + \zeta(3),$$

$$C = \frac{1075}{216} - \frac{25}{18}\pi^2 + \frac{5\pi^2}{3} \log 2 - 3\,\zeta(3) + 3C_4 + C^{(YY)}$$

with

$$C_4 = \frac{11}{648}\pi^4 - \frac{2}{27}\pi^2 \log^2 2 - \frac{1}{27}\log^4 2 - \frac{8}{9}a_4$$

and

$$D = \frac{3199}{1080}\pi^2 - \frac{16}{9}\pi^2 \log 2 - \frac{13}{18}\pi^3 + D^{(YY)} . \qquad (4\text{-}10)$$

REFERENCES

1. R. Barbieri and E. Remiddi, Nucl. Phys. B90, 233 (1975).

2. B. Lautrup and E. de Rafael, Nucl. Phys. B70, 317 (1974).

3. C. Chlouber and M. A. Samuel, Phys. Rev. D17, 2817 (1978).

4. M. Laursen and M. A. Samuel, Phys. Rev. D19, 1281 (1979); C. Chlouber and M. A. Samuel, Phys. Rev. D16, 3596 (1977); B. E. Lautrup and M. A. Samuel, Phys. Lett. 72B, 114 (1977); T. Kinoshita, Nuovo Cimento 51B, 140 (1967).

5. M. A. Samuel and C. Chlouber, Phys. Rev. Lett. 36, 442 (1976).

6. L. Lewin, "Dilogarithms and Associated Functions", MacDonald, London (1958).

CHAPTER V

BOREL TRANSFORM TECHNIQUE AND THE n-BUBBLE DIAGRAM CONTRIBUTION TO THE LETPON ANOMALY

Introduction

In calculating the mass-dependent contribution to the muon g-2, it has been customary for many years to use the large mass ratio $m_\mu/m_e \sim 207$ as a good expansion parameter.[1,2] We restrict ourselves to the class of diagrams with electron vacuum polarization insertions into the lowest order muon vertex (see Figure 15).

One considers the asymptotic part of the photon's self-energy $d_R^\infty(q^2/m_e^2)$, that is, terms of order $O(m_e^2/q^2)$ are neglected.[3] From this one can, in principle, calculate the anomaly to O(1). Another possibility is to use the Kinoshita-method.[4] For low order perturbation theory this approximation seems to work very well. The question is whether this will be valid in high order n>>1, and how strongly the approximation depends on m_μ/m_e.

It is the purpose of this paper to investigate this question for a simple class of diagrams, namely the mass-dependent n-bubble diagram (see Figure 16).

Our analysis shows that the expansion breaks down for $n \geq n_o$, where n_o is dependent on the mass ratio m_μ/m_e. In particular we show that the answer starts oscillating like $(-1)^n$ in disagreement with the exact anomaly which is positive for all n.

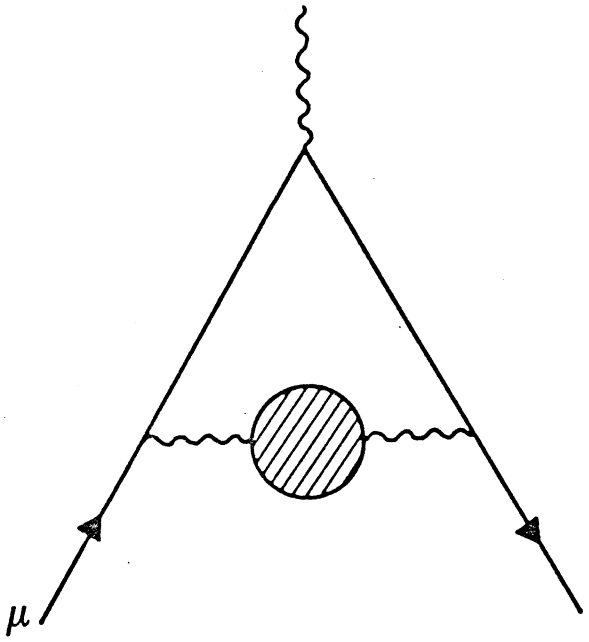

Figure 15. Electron Vacuum Polarization Insertion Into the Lowest-Order Muon Vertex

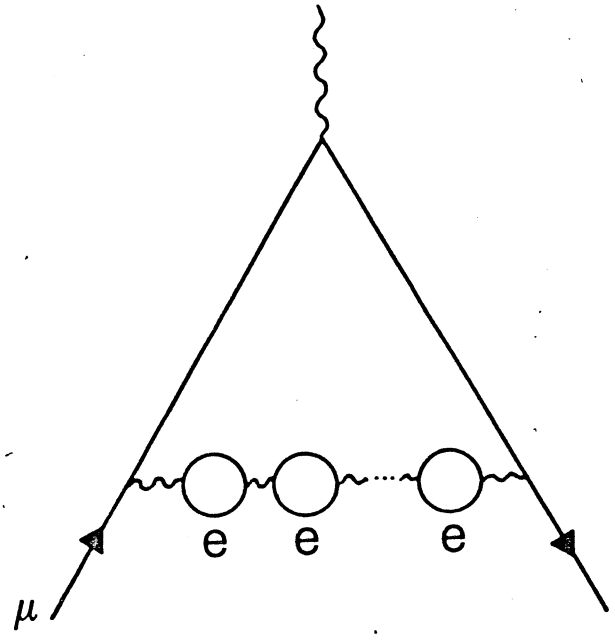

Figure 16. The Mass-Dependent n-Bubble Diagram Contributing to g-2 of the Muon

It is possible to explain why this so-called "false expansion" breaks down. We have neglected terms like m_e^2/q^2. Now to get the full anomaly one must integrate $d_R(q^2/m_e^2)$ with $q^2 = -\, m_\mu^2\, x^2/(1-x)$ over the range $0 \leq x \leq 1$. Clearly, the term m_e^2/q^2 contains a singularity at x=0, and so the neglected terms may become important! The full anomaly does not have such a problem since d_R goes to zero for $x \to 0$.

It has been shown earlier that d_R^∞ satisfies a homogenous Callan-Symanzik equation,[3] and since the asymptotic anomaly is a linear functional of d_R^∞, it itself satisfies a CS-equation. This equation is then solved to all orders, but in view of the above, one might question the validity of this. That is, one can not neglect the right-hand side function $\Delta(q^2/m_e^2)$ in the CS equation even if $\Delta(q^2/m_e^2) \to 0$.

Downstairs we calculate the anomaly exactly for all n, in the limit $m_\mu/m_e \gg 1$, by making use of the Borel transform technique.[5] For large n an approximate expression is obtained. The exact anomaly is evaluated numerically and is compared to the above mentioned anomaly for different mass ratios. We also compare with Lautrup's asymptotic estimate.[6]

Muon Anomaly From the Mass-Dependent n-Bubble Diagram

The exact muon anomaly from the mass-dependent n-bubble diagram is $a_n(\frac{\alpha}{\pi})^{n+1}$ where

$$a_n = \int_0^1 dx(1-x)\left[-\pi^{(2)}\left(-\frac{x^2}{1-x}\,\frac{m_\mu^2}{m_e^2}\right)\right]^n \qquad (5\text{-}1)$$

$\pi^{(2)}$ being the standard second order vacuum polarization function[6] given by

$$\pi^{(2)}\left(\frac{t}{m_e^2}\right) = \frac{8}{9} - \frac{\delta^2}{3} + \left(\frac{1}{2} - \frac{\delta^2}{6}\right)\delta \log\frac{\delta-1}{\delta+1}$$

and

$$\delta = (1 - 4m_e^2/t)^{1/2} .$$

The anomaly (evaluated in the limit $m_\mu/m_e >> 1$) is denoted b_n and uses the asymptotic vacuum polarization function

$$\pi_\infty^{(2)} = \frac{5}{9} - \frac{2}{3} \log \frac{m_\mu}{m_e} - \frac{1}{3} \log \frac{x^2}{1-x} . \qquad (5\text{-}2)$$

Furthermore, let c_n stand for the anomaly with the x^2 in $\pi_\infty^{(2)}$ replaced by 1. c_n represents the true asymptotic value of a_n for large n.

In the following let L stand for $\log m_\mu/m_e$, $a = \frac{5}{9} - \frac{2}{3} L$ and $b = -\frac{1}{3}$. In order to evaluate b_n we will consider the Borel transform $B(\kappa)$ of the series

$$\sum_{n=0}^{\infty} b_n \kappa^n \qquad (5\text{-}3)$$

which is defined as[5]

$$B(\kappa) = \sum_{n=0}^{\infty} \frac{b_n}{n!} \kappa^n . \qquad (5\text{-}4)$$

Using Eqns. (5-1), (5-2) and (5-4) one finds

$$B(\kappa) = e^{-\kappa a} \frac{(1+\kappa b)}{(2-\kappa b)(1-\kappa b)} \frac{\Gamma(1+\kappa b)\Gamma(1-2\kappa b)}{\Gamma(1-\kappa b)} . \qquad (5\text{-}5)$$

To obtain b_n one now differentiates $B(\kappa)$ n times with respect to κ:

$$b_n = \left. \frac{d^n B(\kappa)}{d\kappa^n} \right|_{\kappa=0} \equiv B^{(n)}(0) . \qquad (5\text{-}6)$$

Since it is easier to differentiate log $\Gamma(Z)$, we find it convenient to define $G(\kappa) = \log B(\kappa)$. Using the fact that the Euler-function $\psi(Z)$ satisfies

$$\begin{aligned} \psi(Z) &= \frac{d}{dZ} \log \Gamma(Z) \\ \psi^{(n)}(Z)\Big|_{Z=1} &= (-1)^{n+1} n! \zeta(n+1) \end{aligned} \tag{5-7}$$

we find

$$G^{(1)}(0) = -a + \frac{5}{2} b = \frac{2}{3} L - \frac{25}{18}$$

$$G^{(n)}(0) = b^n (n-1)! \{(-1)^{n-1} + \frac{1}{2^n} + 1$$

$$+ \zeta(n)[(-1)^n + 2^n - 1]\}, \quad n \geq 2. \tag{5-8}$$

Asymptotically for large n, $G^{(n)}(0)$ approaches

$$G^{(n)}(0) \simeq (2b)^n (n-1)! \tag{5-9}$$

To obtain b_n we first notice that the following recursion formula holds (easily proved by differentiation of $B(\kappa) = \exp\{G(\kappa)\}$):

$$B^{(n)}(\kappa) = \sum_{k=0}^{n-1} \binom{n-1}{k} G^{(n-k)}(\kappa) B^{(k)}(\kappa) \tag{5-10}$$

and, therefore,

$$b_n = \sum_{k=0}^{n-1} \binom{n-1}{k} G^{(n-k)}(0) b_k \, . \tag{5-11}$$

If we further write

$$b_n = \sum_{m=0}^{n} b_{n,m} L^m , \tag{5-12}$$

Eqn. (5-11) gives easily

$$b_{n,m} = \frac{2}{3} b_{n-1,m-1} - \frac{25}{18} b_{n-1,m} + \sum_{k=m}^{n-2} \binom{n-1}{k} G^{(n-k)}(0) b_{k,m} \tag{5-13}$$

with the requirement $b_{o,m} = \frac{1}{2} \delta_{o,m}$. We now have a recursion relation allowing us to calculate the coefficients $b_{n,m}$ of L^m for arbitrary n. Using "REDUCE",[7] we have calculated $b_{n,m}$ up to n=18. Table III shows the results up to n=5. The n=0,1,2,3 values are well-known.[1,2,3,4]

To get an asymptotic estimate for b_n for n>>1, we go back to Eqn. (5-2). We notice that the singularity at x=0 is stronger than the x=1 singularity. Putting x=0, and using the Method of Steepest Descents we obtain for large n

$$b_n \simeq \left(-\frac{2}{3}\right)^n n! e^{5/6} \left(\frac{m_e}{m_\mu}\right), \quad n>>1 . \tag{5-14}$$

Notice that the answer is of $O(m_e/m_\mu)$ and so is comparable with the neglected terms. For a mass ratio $m_\mu/m_e = 10$, we checked that this estimate was good to within 2% for $n \gtrsim 6$ (see Table IV). To see how good b_n approximates a_n we evaluated a_n by numerical integration. The results for a_n, b_n and c_n where[6]

$$c_n \simeq \left(\frac{1}{6}\right)^n n! e^{-10/3} \left(\frac{m_\mu}{m_e}\right)^4 \tag{5-15}$$

are shown in Tables V and VI for the mass ratios $m_\mu/m_e = 207$ and $m_\mu/m_e = 10$.

TABLE III

THE COEFFICIENTS $b_{n,m}$ UP TO n=5

$$b_{0,0} : \frac{1}{2}$$

$$b_{1,0} : -\frac{25}{36}$$

$$b_{1,1} : \frac{1}{3}$$

$$b_{2,0} : \frac{2}{9}\,\zeta(2) + \frac{317}{324}$$

$$b_{2,1} : -\frac{25}{27}$$

$$b_{2,2} : \frac{2}{9}$$

$$b_{3,0} : -\frac{2}{9}\,\zeta(3) - \frac{25}{27}\,\zeta(2) - \frac{8609}{5832}$$

$$b_{3,1} : \frac{4}{9}\,\zeta(2) + \frac{317}{162}$$

$$b_{3,2} : -\frac{25}{27}$$

$$b_{3,3} : \frac{4}{27}$$

$$b_{4,0} : \frac{16}{27}\,\zeta(4) + \frac{8}{27}\,\zeta^2(2) + \frac{100}{81}\,\zeta(3) + \frac{634}{243}\,\zeta(2) + \frac{64613}{26244}$$

$$b_{4,1} : -\frac{16}{27}\,\zeta(3) - \frac{200}{81}\,\zeta(2) - \frac{8602}{2187}$$

$$b_{4,2} : \frac{16}{27}\,\zeta(2) + \frac{634}{243}$$

$$b_{4,3} : -\frac{200}{243}$$

$$b_{4,4} : \frac{8}{81}$$

TABLE III (Continued)

$$b_{5,0} : -\frac{40}{27}\zeta(5) - \frac{80}{81}\zeta(3)\,\zeta(2) - \frac{1000}{243}\zeta(4) - \frac{500}{243}\zeta^2(2) - \frac{3170}{729}\zeta(3) - \frac{43045}{6561}\zeta(2) - \frac{2182775}{472392}$$

$$b_{5,1} : \frac{160}{81}\zeta(4) + \frac{80}{81}\zeta^2(2) + \frac{1000}{243}\zeta(3) + \frac{6340}{729}\zeta(2) + \frac{323065}{39366}$$

$$b_{5,2} : -\frac{80}{81}\zeta(3) - \frac{1000}{243}\zeta(2) - \frac{43045}{6561}$$

$$b_{5,3} : \frac{160}{243}\zeta(2) + \frac{6340}{2187}$$

$$b_{5,4} : -\frac{500}{729}$$

$$b_{5,5} : \frac{16}{243}$$

TABLE IV

CHECK OF ASYMPTOTIC EXPRESSION FOR b_n FOR THE MASS RATIO $\frac{m_\mu}{m_e} = 10$

n	b_n	b_n(Asympt)
0	0.500	0.230
1	0.072	- 0.153
2	0.390	0.205
3	- 0.180	- 0.409
4	1.36	1.09
5	- 3.23	- 3.64
6	1.51×10^1	1.45×10^1
7	$- 6.70 \times 10^1$	$- 6.78 \times 10^1$
8	3.64×10^2	3.62×10^2
9	$- 2.17 \times 10^3$	$- 2.17 \times 10^3$
10	1.45×10^4	1.45×10^4
11	$- 1.06 \times 10^5$	$- 1.06 \times 10^5$
12	8.52×10^5	8.49×10^5
13	$- 7.38 \times 10^6$	$- 7.36 \times 10^6$
14	6.89×10^7	6.87×10^7
15	$- 6.89 \times 10^8$	$- 6.87 \times 10^8$

TABLE V

THE QUANTITIES a_n, b_n AND c_n UP TO n = 15 FOR THE PHYSICAL MASS RATIO $\frac{m_\mu}{m_e} = 207$

n	a_n	b_n	c_n
0	0.500	0.5	3.27×10^7
1	1.09	1.08	5.45×10^6
2	2.72	2.72	1.82×10^6
3	7.23	7.19	9.10×10^5
4	2.02×10^1	2.02×10^1	6.06×10^5
5	5.85×10^1	5.81×10^1	5.05×10^5
6	1.75×10^2	1.75×10^2	5.05×10^5
7	5.40×10^2	5.34×10^2	5.90×10^5
8	1.71×10^3	1.71×10^3	7.86×10^6
9	5.53×10^3	5.40×10^3	1.18×10^6
10	1.83×10^4	1.89×10^4	1.97×10^6
11	6.20×10^4	5.65×10^4	3.60×10^6
12	2.14×10^5	2.54×10^5	7.21×10^6
13	7.55×10^5	3.96×10^5	1.56×10^7
14	2.71×10^6	6.06×10^6	3.64×10^7
15	9.93×10^6	-2.36×10^7	9.11×10^7

TABLE VI

THE QUANTITIES a_n, b_n AND c_n UP TO n = 20
FOR THE MASS RATIO $\frac{m_\mu}{m_e} = 10$

n	a_n	b_n	c_n
0	0.500	0.500	1.78×10^{2}
1	0.248	0.072	2.97×10^{1}
2	0.217	0.390	9.90
3	0.236	- 0.180	4.95
4	0.293	1.36	3.30
5	0.405	- 3.23	2.75
6	0.610	1.51×10^{1}	2.75
7	0.990	$- 6.70 \times 10^{1}$	3.21
8	1.72	3.64×10^{2}	4.28
9	3.19	$- 2.17 \times 10^{3}$	6.42
10	6.30	1.45×10^{4}	1.07×10^{1}
11	1.31×10^{1}	$- 1.06 \times 10^{5}$	1.96×10^{1}
12	2.92×10^{1}	8.52×10^{5}	3.93×10^{1}
13	6.84×10^{1}	$- 7.38 \times 10^{6}$	8.50×10^{1}
14	1.69×10^{2}	6.69×10^{7}	1.98×10^{2}
15	4.42×10^{2}	$- 6.89 \times 10^{8}$	4.96×10^{2}
16	1.21×10^{3}	7.35×10^{9}	1.32×10^{3}
17	3.54×10^{3}	$- 8.33 \times 10^{10}$	3.75×10^{3}
18	1.08×10^{4}	9.99×10^{11}	1.12×10^{4}
19	3.45×10^{4}	$- 1.27 \times 10^{13}$	3.56×10^{4}
20	1.15×10^{5}	1.69×10^{14}	1.17×10^{5}

We see that for the physical mass ratio $m_\mu/m_e = 207$ the approximation $a_n \simeq b_n$ is good up to $n \simeq 10$, while for the ratio $m_\mu/m_e = 10$, the approximation is totally wrong for all $n \geq 1$. That is, in the latter case, the neglected terms of $O(m_e/m_\mu)$ are now bigger than the logarithmic terms and the O(1) term together! On the other hand for $n \gtrsim 18$, the approximation $a_n \simeq c_n$ is very good.

To summarize, for very large mass ratios, b_n provides a good approximation for low n, while c_n is good for very large n. In the region in between, neither is valid, and one must, therefore, use the full anomaly. This might have some relevance for the τ-lepton anomaly with muon bubble insertions since $(m_\tau/m_\mu) = 16.9$.

REFERENCES

1. T. Kinoshita, Nuovo Cimento 51B, 140 (1967).

2. H. Suura and E. Wichmann, Phys. Rev. 105, 1930 (1957); A Petermann, Phys. Rev. 105, 1931 (1957).

3. B. E. Lautrup and E. de Rafael, Nucl. Phys. B70, 317 (1974).

4. M. A. Samuel, Phys. Rev. D9, 2913 (1974).

5. R. Coquereaux, "Fermionic Expansion in QED", to be published in Phys. Rev. D23 (1981).

6. B. E. Lautrup, Phys. Lett. 69B, 109 (1977).

7. A Hearn, "Interactive Systems for Experimental Applied Mathematics", edited by M. Klerer and J. Reinfelds, Academic Press, N.Y. (1968).

CHAPTER VI

ELEMENTS OF GAUGE THEORIES

The Need for Color

Soon after the quark model was introduced by Gell-Mann and Zweig in 1964,[1] an apparent paradox arose concerning the properties of the quarks. We recall from Chapter I that the baryons are three quark states $|qqq\rangle$ and the mesons are quark-antiquark pairs, $|q\bar{q}\rangle$. These quarks come in 5(6) different flavors denoted u,d,s,c,b(t). The problem has to do with the spin-statistics theorem. Consider the Δ^{++} made of three u-quarks or Ω^- made of three s-quarks. Now, since the spin of the quarks is $J=\frac{1}{2}$, and Δ^{++}, Ω^- have $J = \frac{3}{2}$, they should satisfy Fermi-Dirac statistics. However, in the ground state (S-wave), the Δ^{++} and Ω^- are totally symmetric in interchanging the quarks.

The easiest way out of this puzzle, is to introduce a new quantum number called "color".[2] Each quark flavor now comes in three varieties "red", "green" or "blue." We shall later see that "color" is the non-Abelian counterpart of electric charge. The wave function is now made totally antisymmetric in the color indices (ijk).

$$|\Delta^{++}, J = \frac{3}{2}\rangle = \frac{1}{\sqrt{6}} \sum_{i=R,G,B} \varepsilon_{ijk} |u_i u_j u_k\rangle .$$

In group theoretical language, this state now forms a singlet under SU(3)-color, which is easily seen from the decomposition

$$3 \otimes 3 \otimes 3 = 1 \oplus 8 \oplus 8 \oplus 10 .$$

Similarly for the mesons $|q\bar{q}>$, we have the decomposition

$$3 \otimes \bar{3} = 1 \oplus 8.$$

Notice, however, that a diquark $|qq>$ can not exist in a singlet state:

$$3 \otimes 3 = 6 \oplus \bar{3} \neq 1 .$$

We have chosen three colors, for which there is good experimental evidence. If we had chosen, say, four colors, the lowest singlet state would have been a four quark state $|qqqq>$[3]. This "exotic" state has not been seen in nature.

We could have chosen instead an SO(3)-color group. However, this would have allowed a diquark, and moreover, it would lead to no asymptotic freedom for $N_f > 2$, and we know already that $N_f \geq 5$.

The reason we choose the color singlet state, is that free quarks have not been observed in any high energy experiment, and it is natural to postulate "color" confinement. However, there is an experiment by Fairbank et al., in which they claim to see fractional charges of $\pm$ 1/3 e.[4] Whether these charges can be identified with quarks is too early to say, and if it does, would it mean that QCD is wrong? Clearly other experiments would be important to confirm Fairbank's experiment.

There is additional experimental evidence for N=3 colors. First consider the decay $\pi^0 \to \gamma\gamma$. Using PCAC,[5] one can relate this decay to the axial vector coupling to two photons, which in lowest order proceeds via a virtual quark loop (VVA - triangle diagram).

The decay rate is then given as:

$$\Gamma^{TH}(\pi^{o}\to\gamma\gamma) \doteq N^2\ 0.89\ \text{eV} = 8.01\ \text{eV}$$

for N = 3 colors. The experimental value is

$$\Gamma^{EXP}(\pi^{o}\to\gamma\gamma) = (7.95 \pm 0.55)\ \text{eV}$$

This is clearly an indication of N = 3 colors.

Evidence for N = 3 colors is also obtained by considering the so-called R value, which is defined in electron-positron annihilation into hadrons as:[6]

$$R \equiv \frac{\sigma_T(e^+e^- \to \text{hadrons})}{\sigma\ (e^+e^- \to \mu^+\mu^-)}\ .$$

In the asymptotic high-energy region one has

$$R = N \sum_i q_i^2,$$

where q_i is the quark charge. Below "charm", one has experimentally $R \simeq 2 - 2.5$ (u,d,s), while $R^{TH} = 3\cdot\frac{2}{3} = 2(N=3)$. Above the "charm" threshhold, $R \simeq 4.5$-5. Now, allowing one unit of R^{EXP} for τ lepton production, the value $R^{TH} = \frac{10}{3}$ is in good agreement with R^{EXP}. For CM energies above 13 GeV, the data shows R to be constant with $\langle R\rangle = 3.94$. With five flavors $R^{TH} = 3.7$. Including radiative corrections, this value is actually lifted to $R^{TH} = 3.92$.

The last reason we give for color is of a theoretical nature, and has to do with cancellation of the Adler-Bell-Jackiw anomalies (VVA triangle diagrams).[7] It is required, that these anomalies, which are independent of the masses of the leptons and quarks, cancel in order to have a renormalization theory.[8] In the Standard Model of electro-weak and strong interactions,

the condition reads $Tr[\hat{Q}_{lep} + \hat{Q}_{had}] = 0$,[3,9] where $\hat{Q}_{lep}$ and $\hat{Q}_{had}$ are the charge matrices for leptons and quarks.

We shall assume lepton-hadron universality, so that to each weak-isospin doublet corresponds a quark doublet:

$$\begin{pmatrix} \nu_e \\ e^- \end{pmatrix}, \quad \begin{pmatrix} \nu_\mu \\ \mu^- \end{pmatrix}, \quad \begin{pmatrix} \nu_\tau \\ \tau^- \end{pmatrix}$$
$$\updownarrow \qquad \updownarrow \qquad \updownarrow$$

and

$$\begin{pmatrix} u \\ d \end{pmatrix}, \quad \begin{pmatrix} c \\ s \end{pmatrix}, \quad \begin{pmatrix} t \\ b \end{pmatrix}.$$

Since $Q(\nu_{e,\mu,\tau}) = 0$, $Q(e,\mu,\tau) = 1$, $Q(u,c,t) = \frac{2}{3}$ and $Q(d,s,b) = -\frac{1}{3}$ we find

$$Tr[\hat{Q}_{lep} + \hat{Q}_{had}] = -3 + N$$

In order for this to vanish, we must have precisely N=3. We shall discuss the Standard-Model later.

Gauge Invariance of Abelian QED and Non-Abelian QCD

We begin with the free field Lagrangian for a massive fermionic field $\psi(x)$:[9,10]

$$L_F = \bar{\psi}(x)\,(i\partial\!\!\!/ - m)\psi \tag{6-1}$$

where the slashed notation $a\!\!\!/ \equiv a_\mu \gamma^\mu$, γ^μ being the usual gamma matrices.

Clearly L_F is invariant under the global transformation

$$\psi(x) \rightarrow \psi'(x) = \exp\{-i\theta\}\psi(x)$$

and leads to a conserved current $j_\mu(x) = \bar{\psi}(x)\gamma_\mu\psi(x)$.

This is not very exciting, since we are just multiplying the wave-function by a phase factor, which is a non-observable. So let us instead try to make L_F invariant under a local transformation $\psi(x) \to U(x)\psi(x) = \exp\{-i\theta(x)\}\psi(x)$.

However, we discover that since

$$\partial_\mu \psi(x) \to U(x)\{\partial_\mu\psi - i\,\partial_\mu\theta\} \tag{6-2}$$

L_F is no longer invariant. The way to remedy this, is to introduce an Abelian gauge field A_μ, and define a covariant derivative $D_\mu = \partial_\mu - igA_\mu$, and require A_μ to transform as

$$A_\mu \to A'_\mu = UA_\mu U^{-1} - \frac{i}{g}(\partial_\mu U)U^{-1} = A_\mu - \frac{1}{g}\partial_\mu\theta\,. \tag{6-3}$$

A little algebra now shows that $D_\mu\psi$ transforms as

$$(D_\mu\psi) \to (D_\mu\psi)' = (\partial_\mu - igA'_\mu)\psi'$$

$$= (\partial_\mu - igA_\mu + i\partial_\mu\theta)U(x)\psi(x) = U(x)(D_\mu\psi)\,. \tag{6-4}$$

and the Lagrangian

$$L_F = \bar{\psi}(i\not{\partial}_\mu - m)\psi \tag{6-5}$$

is indeed invariant. Notice that we have introduced the minimal coupling to the electromagnetic field: $L_I = gj_\mu(x)A^\mu(x)$.

To get the total QED Lagrangian, we must add the kinetic term:

$$L_{Kin} = -\frac{1}{4}F_{\mu\nu}F^{\mu\nu}$$

where the electromagnetic field tensor $F_{\mu\nu} = \partial_\mu A_\nu - \partial_\nu A_\mu$ is clearly invariant. To summarize, the QED Lagrangian is

$$\begin{aligned} L_{QED} &= L_F + L_I + L_{Kin} \\ &= \bar{\psi}(x)(i\not{\partial}-m)\psi(x) - \frac{1}{4} F_{\mu\nu} F^{\mu\nu}, \end{aligned} \tag{6-6}$$

with one conserved current. This is the Abelian U(1) symmetry.

We will now try to generalize QED by imposing an SU(N) symmetry instead.[3,9,10] Each fermion (quark) is now represented as a $(N \otimes 1)$ color matrix $(\psi_i)_{i=1,2,\ldots,N}$ and the fermion Lagrangian is

$$L_F = \bar{\psi}_i (i\not{\partial}\delta_{ij} - \hat{M}_{ij})\psi_j \tag{6-7}$$

where $\hat{M}_{ij}$ is the mass matrix.

Again we will consider the local transformation

$$\psi_i(x) \to \psi_i'(x) = U(x)\psi_i(x) = \exp\{-i\, T_a \theta_a(x)\}\psi(x) \ .$$

Notice that since we require SU(N) symmetry, we need N^2-1 generators T_a and, therefore, N^2-1 parameters $\theta_a(x)$.

For N=2, we have $T_a = \frac{1}{2}\tau_a$, τ_a being the ordinary Pauli-matrices, and for N=3 we have $T_a = \frac{1}{2}\lambda_a$, λ_a being the Gell-Mann matrices.

The generators T_a no longer commute, but satisfy $[T_a, T_b] = i\, f_{abc}\, T_c$ where f_{abc} are the structure constants of SU(N). For N=2, $f_{abc} = \varepsilon_{abc}$. T_a now represents the non-Abelian charge.

For each generator, we introduce a Non-Abelian field A_μ^a and define the covariant derivative $D_\mu^{ij} = \delta^{ij}\partial_\mu - ig(T^a)^{ij} A_\mu^a$, with A_μ^a transforming as

$$T^a A_\mu^a \to (T^a A_\mu^a)' = U(T^a A_\mu^a)U^{-1} - \frac{i}{g}(\partial^\mu U)U^{-1}. \tag{6-8}$$

Then we find again $(D_\mu^{ij}\psi)' = U(D_\mu^{ij}\psi)$. If $\theta_a(x)$ is infinitesimal, we obtain

$$(T^a A_\mu^a)' \simeq [1 - iT^b\theta^b]T^a A_\mu^a[1 + iT^c\theta^c] - \frac{1}{g} T^a \partial_\mu \theta^a$$

$$= T^a A_\mu^a + i\theta^b A_\mu^a [T^a, T^b] - \frac{1}{g} T^a \partial_\mu \theta^a \ . \tag{6-9}$$

Using $[T_a, T_b] = if_{abc} T_c$ yields

$$A_\mu^{a'} = A_\mu^a + f^{abc}\, \theta^b A_\mu^c - \frac{1}{g} \partial_\mu \theta^a \tag{6-10}$$

The second term represents an isospin rotation. Eqn. (6-10) also shows that the transformation of A_μ^a is representation independent.

How should we define $F_{\mu\nu}^a$ this time. It must transform as

$$T^a F_{\mu\nu}^a \to U\, T^a\, F_{\mu\nu}^a\, U^{-1} \tag{6-11}$$

which, for infinitesimal transformations, reads

$$[1 - iT^b\theta^b]T^a F_{\mu\nu}^a [1 + iT^c\theta^c] \tag{6-12}$$

and, using the technique as above, we find

$$F_{\mu\nu}^a \to F_{\mu\nu}^{a'} = F_{\mu\nu}^a + \theta^b f^{abc}\, F_{\mu\nu}^c \ . \tag{6-13}$$

which is an isospin rotation. Clearly.

$$F_{\mu\nu}^{a'}\, F^{a\mu\nu'} = F_{\mu\nu}^a\, F^{a\mu\nu} + 2\theta^b f^{abc} F_{\mu\nu}^a\, F^{c\mu\nu}$$

$$= F_{\mu\nu}^a\, F^{a\mu\nu} \tag{6-14}$$

due to the antisymmetry of f_{abc}.

We claim that

$$F^a_{\mu\nu} \equiv \partial_\mu A^a_\nu - \partial_\nu A^a_\mu + g\, f^{abc}\, A^b_\mu A^c_\nu$$

will do the job.

After some trivial algebra one finds

$$F^{a'}_{\mu\nu} = F^a_{\mu\nu} + f^{abc}\,\theta^b\,(\partial_\mu A^c_\nu - \partial_\nu A^c_\mu) \qquad (6\text{-}15)$$

$$+ g f^{abc}\,\theta^d\,(f^{bde}\, A^a_\mu A^e_\nu + f^{ade}\, A^e_\mu A^b_\nu).$$

The last parenthesis can be written as

$$g(f^{abd}\, f^{aec} + f^{abe}\, f^{adc})\theta^b A^d_\mu A^e_\nu$$

$$= - g\, f^{abc}\, f^{cde}\,\theta^b\, A^d_\mu\, A^e_\nu \qquad (6\text{-}16)$$

where we have used the Jacobi identity

$$[[T_a,T_b],T_c] + [[T_b,T_c],T_a] + [[T_c,T_a],T_b] = 0 \qquad (6\text{-}17)$$

and $[T_a,T_b] = i\, f_{abc}\, T_c$.

It follows that $F^{a'}_{\mu\nu}$ can be written as in Eqn. (6-13)

$$F^{a'}_{\mu\nu} = F^a_{\mu\nu} + \theta^b f^{abc}\, F^c_{\mu\nu} \qquad (6\text{-}18)$$

The QCD Lagrangian is then

$$L_{QCD} = \bar{\psi}_i (i\not{\partial}_{ij} - \hat{M}_{ij})\psi_j - \frac{1}{4} F^a_{\mu\nu}\, F^{a\mu\nu} . \qquad (6\text{-}19)$$

The Standard Model

For completeness we would like to describe the Weinberg-Salam model of the electro-weak interactions. The gauge group is here $SU(2)_L \otimes U(1)$ where SU(2) is the weak isospin group.[9,10] If we also include quarks with the gauge group $SU(3)_c$, we call this the Standard Model.

We begin with the W-S model, which consists of a weak isospin doublet of a left-handed electron and neutrino

$$L \equiv \begin{pmatrix} \nu_L \\ e_L^- \end{pmatrix}$$

where $e_L \equiv \frac{1}{2}(1+\gamma_5)e$, and also a right handed electron (singlet) $e_R = \frac{1}{2}(1-\gamma_5)e$. We shall assume that these particles are massless from the beginning.

Let the generator for the U(1) symmetry be denoted weak hypercharge Y, so that the charge $Q = T_3 + \frac{1}{2}Y$. Clearly $Y(e_L) = Y(\nu_L) = -1$ and $Y(e_R) = -2$.

Assuming the $SU(2)_L \otimes U(1)$ symmetry, the fermion Lagrangian must be invariant under the combined transformations.

$$L \to L' = \exp\{-\frac{i}{2}\tau^a\theta^a(x)\}L$$

and (6-20)

$$R \to R' = \exp\{-i\,\theta'(x)\}R$$

and we must add four gauge bosons A_μ^a (a=1,2,3) and B_μ giving the Lagrangian

$$\mathcal{L}_F = \bar{L}(i\partial\!\!\!/ + \frac{1}{2}g\,\tau^a A\!\!\!/^a - \frac{1}{2}g'B\!\!\!/)L + \bar{R}(i\partial\!\!\!/ - g'B\!\!\!/)R$$

along with the kinetic term

$$L_{Kin} = -\frac{1}{4} F^a_{\mu\nu} F^{a\mu\nu} - \frac{1}{4} G_{\mu\nu} G^{\mu\nu} \tag{6-21}$$

where

$$F^a_{\mu\nu} = \partial_\mu A^a_\nu - \partial_\nu A^a_\mu + g \varepsilon^{abc}_a A^b_\mu A^c_\nu$$

and (6-22)

$$G_{\mu\nu} = \partial_\mu B_\nu - \partial_\nu B_\mu$$

The τ_a's are the usual Pauli matrices

$$\tau^1 = \begin{pmatrix} 0 & 1 \\ 1 & 0 \end{pmatrix}, \tau^2 = \begin{pmatrix} 0 & -i \\ i & 0 \end{pmatrix} \text{ and } \tau^3 = \begin{pmatrix} 1 & 0 \\ 0 & -1 \end{pmatrix} . \tag{6-23}$$

The first step is to change (A^1_μ, A^2_μ) to two other fields (W^+_μ, W^-_μ) (charged vector bosons):

$$\begin{aligned} A^1_\mu &= \frac{1}{\sqrt{2}} (W^+_\mu + W^-_\mu) \\ A^2_\mu &= \frac{i}{\sqrt{2}} (W^+_\mu - W^-_\mu). \end{aligned} \tag{6-24}$$

We also introduce the "charge currents" $j^+_\mu = (j^-_\mu)^+$

$$j^-_\mu = \bar{\nu}_L \gamma_\mu e_L = \bar{\nu} \gamma_\mu e_L, \tag{6-25}$$

where the last equality follows from the fact that γ_5 anticommutes with γ_μ and $P = \frac{1}{2}(1 + \gamma_5)$ is a projection operator. It follows easily from Eqns. (6-23) and (6-25) that

$$\begin{aligned} \bar{L} \gamma_\mu \tau^1 L &= j^-_\mu + j^+_\mu \\ \bar{L} \gamma_\mu \tau^2 L &= -i(j^-_\mu - j^+_\mu) \end{aligned} \tag{6-26}$$

and, therefore, the part of the Lagrangian containing A_μ^1 and A_μ^2 is

$$\frac{g}{2}\bar{L}\gamma^\mu(\tau^1 A_\mu + \tau^2 A_\mu^2)\, L = \frac{g}{\sqrt{2}}\left[j_\mu^- W^{+\mu} + j_\mu^+ W^{-\mu}\right] \tag{6-27}$$

The rest of the Lagrangian is

$$\frac{1}{2}\left[\gamma^\mu(g\tau^3 A_\mu^3 - g' B_\mu)L - g'\bar{R}\gamma^\mu B_\mu R\right] = g\, j_\mu^3 A^{3\mu} + \frac{1}{2} g'\, j_\mu^n B^\mu \tag{6-28}$$

where we defined

$$j_\mu^3 \equiv \frac{1}{2}\bar{L}\,\gamma_\mu \tau^3 L = \frac{1}{2}(\bar{\nu}\gamma_\mu \nu_L - \bar{e}\gamma_\mu e) \tag{6-29}$$

and the "neutral current"

$$j_\mu^n = -g'\bar{L}\gamma_\mu L - 2g'\bar{R}\gamma_\mu R$$

$$= -g'(\bar{\nu}\gamma_\mu \nu_L + \bar{e}\,\gamma_\mu\, e_L + 2\bar{e}_R\,\gamma_\mu\, e_R)$$

It is convenient to introduce the electromagnetic current

$$j_\mu^{e.m.} = j_\mu^3 + \frac{1}{2} j_\mu^n = -\bar{e}\gamma_\mu e, \tag{6-30}$$

so that Eqn. (6-28) becomes

$$g j_\mu^3 A^{3\mu} + g'(j_\mu^{e.m.} - j_\mu^3)B^\mu \,. \tag{6-31}$$

We then introduce a rotation of $(A_\mu^3, B_\mu) \to (A_\mu, Z_\mu)$, in such a way so that the "photon field" A_μ couples only to the electromagnetic current:

$$\begin{pmatrix} B_\mu \\ A_\mu^3 \end{pmatrix} = \begin{pmatrix} \cos\theta_w & -\sin\theta_w \\ \sin\theta_w & \cos\theta_w \end{pmatrix} \begin{pmatrix} A_\mu \\ Z_\mu \end{pmatrix} \tag{6-32}$$

with

$$\tan\theta_w = \frac{g'}{g} .$$

θ_w is called the Weinberg angle.

We find easily from Eqns. (6-31) and (6-32)

$$g'\cos\theta_w \, j_\mu^{e.m.} \, A^\mu + \frac{g}{\cos\theta_w} \, j_\mu^n \, Z^\mu$$

Therefore, we can identify the electric charge $e = g \sin\theta_w = g'\cos\theta_w$. We have also defined the neutral current j_μ^n as

$$j_\mu^n = j_\mu^3 - \sin^2\theta_w j_\mu^{e.m.} = \frac{1}{2}(\bar{\nu}\gamma_\mu \nu_L - \bar{e}\gamma_\mu e_L) + \sin^2\theta_w(\bar{e}\gamma_\mu e) . \qquad (6\text{-}33)$$

The fermion Lagrangian reads

$$L_F = \frac{g}{\sqrt{2}} (j_\mu^- W^{+\mu} + j_\mu^+ W^{-\mu}) + \frac{g}{\cos\theta_w} j_\mu^n \, Z^\mu + j_\mu^{e.m.} \, A^\mu . \qquad (6\text{-}34)$$

Next, how do we include quarks? We will assume again a lefthanded doublet

$$L = \begin{pmatrix} u_L \\ d_L \end{pmatrix},$$

and, in this case, two right-handed singlets (u_R) and (d_R). Since $Q(u) = \frac{2}{3}$ and $Q(d) = -\frac{1}{3}$, the hypercharges in this case are $Y(u_L) = Y(d_L) = \frac{1}{3}$, $Y(u_R) = \frac{4}{3}$ and $Y(d_R) = -\frac{2}{3}$. The Lagrangian is written in exactly the same way. The $W_\mu^\pm$ now changes a u-quark into a d-quark and vice versa.

$$j_\mu^- = \bar{u}\gamma_\mu d_L$$

$$j_\mu^n = \frac{1}{2}(\bar{u}\,\gamma_\mu\, u_L - \bar{d}\,\gamma_\mu\, d_L) + e \sin^2\theta_w \, (\frac{2}{3}\,\bar{u}\,\gamma_\mu u - \frac{1}{3}\,\bar{d}\,\gamma_\mu d). \qquad (6\text{-}35)$$

This is the Standard Model.

The next question is how do we generate the mass of the electron while keeping the neutrino massless? This is done through a mechanism known as spontaneous symmetry breaking (SBB).[11]

We introduce an SU(2) doublet of complex scalar fields (all together four fields).

$$\phi = \begin{pmatrix} \phi_+ \\ \phi_o \end{pmatrix}$$

The scalar Lagrangian is

$$L_{SCA} = \left| \partial_\mu \phi + \frac{i}{2} g \tau^a A^a_\mu \phi + \frac{i}{2} g' B_\mu \phi \right|^2 - V(\phi^+\phi) \tag{6-36}$$

where the scalar potential is assumed to be ($\mu^2 < o$)

$$V(\phi^+\phi) = \mu^2(\phi^+\phi) + \lambda(\phi^+\phi)^2 . \tag{6-37}$$

The Yukawa interaction must be $SU(2)_L \otimes U(1)$ invariant and reads

$$L_{Yu} = - G_e(\bar{R}\phi^+ L + (\bar{L}\phi)R) . \tag{6-38}$$

The potential $V(\phi^+\phi)$ has a minimum at $|\phi| = (-\mu^2/2\lambda)^{\frac{1}{2}}$. Due to the SU(2) symmetry we can choose this minimum such that only the neutral component ϕ_o has a non-vanishing expectation value.

$$\phi_o = \langle o|\phi|o\rangle = \frac{1}{\sqrt{2}} \begin{pmatrix} o \\ v \end{pmatrix} \tag{6-39}$$

with

$$v = (-\mu^2/\lambda)^{\frac{1}{2}} .$$

Instead of expanding $\phi = \phi_o + \phi_1$ we will parametrize ϕ in terms of

4 new fields ξ^o(a=1,2,3) and η which for infinitesimal fields reduces

$$U(\xi) = \exp\{-\frac{t^a\xi^a(x)}{2v}\}$$

$$\phi = U^{-1}(\xi)\ \frac{1}{\sqrt{2}}\ \begin{pmatrix} o \\ v+\eta \end{pmatrix},$$

to $\frac{1}{\sqrt{2}}$ $(v+\eta+i\xi)$. This eliminates unwanted massless Goldstone Bosons. Since we have SU(2) symmetry we can transform

$$\phi \to \phi' = U(\xi)\ \phi = \frac{1}{\sqrt{2}}\ \begin{pmatrix} o \\ v+\eta \end{pmatrix} \qquad (6\text{-}40)$$

while changing A_μ^a

$$\tau^a A_\mu^{a'} = U(\xi)\tau^a A_\mu^a U^{-1}(\xi) - \frac{i}{g}\ (\partial_\mu U(\xi))U^{-1}(\xi)\ .$$

The quadratic part of the scalar Lagrangian becomes simply

$$\frac{1}{2}\ (\partial_\mu\eta)^2 + \mu^2\eta^2 + \frac{v^2}{8}\ \{g^2[(A_\mu^1)^2 + (A_\mu^2)^2] + (gA_\mu^3 - g'B_\mu)^2\} \qquad (6\text{-}41a)$$

while the quadratic part of the kinetic Lagrangian is

$$-\frac{1}{2}|\partial_\mu W_\nu^+ - \partial_\nu W_\mu^+|^2 - \frac{1}{4}(\partial_\mu Z_\nu - \partial_\nu Z_\mu)^2 - \frac{1}{4}(\partial_\mu A_\nu - \partial_\nu A_\mu)^2 \qquad (6\text{-}41b)$$

Introducing ($W^\pm$, Z, A) we obtain for the quadratic part of the total Lagrangian

$$L_o = -\frac{1}{2}|\partial_\mu W_\nu^+ - \partial_\nu W_\mu^+|^2 + \frac{1}{4}(gv)^2|W_\mu^+|^2$$

$$-\frac{1}{4}(\partial_\mu Z_\nu - \partial_\nu Z_\mu)^2 + \frac{v^2}{8}\ (g^2+g'^2)\ (Z_\mu)^2 \qquad (6\text{-}42)$$

$$-\frac{1}{4}(\partial_\mu A_\nu - \partial_\nu A_\mu)^2 - \frac{1}{2}(\partial_\mu \eta)^2 + \mu^2\eta^2 \qquad (6\text{-}42)$$

From this we see that three of the gauge bosons have acquired masses, while the photon remains massless:

$$M_{W^\pm} = \frac{1}{2} gv,$$

$$M_Z = \frac{v}{2}(g^2 + g'^2)^{1/2}, \quad M_A = 0 \qquad (6\text{-}43)$$

with

$$\frac{M_W}{M_Z} = \cos\theta_W$$

The last term; in Eqn. (6-42) represents a heavy scalar particle called the "Higgs" boson with mass $m_H = |\mu|2^{\frac{1}{2}}$.

What has happened is that three of the originally four massless "Goldstone" Bosons have been eaten up by giving longitudinal terms to the three vector bosons, which then acquire masses. One of the left-over bosons has also acquired mass.

Finally, we would like to relate the coupling constants (g,g') to the four fermion coupling constant $G = 1.2 \times 10^{-5}$ GeV^{-2}.

Since the W propagator for small q^2 is simply $\frac{1}{M_W^2} g_{\mu\nu}$ this give an effective Lagrangian

$$\frac{1}{2}\left(\frac{g}{M_W}\right)^2 (j_\mu^+ j^{-\mu})$$

while the four fermion Lagrangian is $2\sqrt{2}\, G(j_\mu^+ j^{-\mu})$. It follows

$\frac{G}{\sqrt{2}} = \frac{g^2}{8M_W^2} = \frac{1}{2v^2}$ and therefore

$$M_W = \left(\frac{\pi\alpha}{\sqrt{2}\,G}\right)^{\frac{1}{2}} \frac{1}{\sin\theta_W} = \frac{37.3}{\sin\theta_W} \simeq 78 \text{ GeV} \qquad (6\text{-}44)$$

$$M_Z = \frac{M_W}{\cos\theta_W} = \frac{37.3}{\cos\theta_W \cdot \sin\theta_W} \simeq 90 \text{ GeV}$$

using the value $\sin^2\theta_w = 0.23$ obtained from experiment. We also find $L_{Yu} = -\frac{1}{2} v\, G_e(\bar{e}e)$ which gives a mass $m_e = \frac{1}{2} G_e V$, while the neutrino remains massless.

Propagators and Vertices

Once the Lagrangian is given the socalled propagators and vertices can be found. This can be done rigorously using Feynman path integral formalism or canonical quantization. Here we shall adopt a method by t'Hooft and Veltman, from which we can read off the propagators and vertices in a very simple way.[12]

Consider any field ϕ_i and look at the bilinear part of the Lagrangian

$$L = \phi_i \Gamma_{ij} \phi_j$$

The propagator G_{ij} is then defined as

$$G_{ij} \Gamma_{jk} = \delta_{ik}$$

if it exists, always considered in momentum space. That is, a derivative ∂_μ is replaced by $-ik_\mu$, for example.

The vertices are defined as the trilinear or quartic terms in $L = \phi_i \phi_j \phi_k \Gamma_{ijk}$.

Consider QED first and recall that

$$L_{QED} = -\frac{1}{4}(\partial_\mu A_\nu - \partial_\nu A_\mu)^2 + \bar{\psi}(i\not{\partial} - m)\psi + e\bar{\psi}\gamma_\mu \psi A^\mu \qquad (6\text{-}45)$$

The fermion propagater is simply given by

$$S(\not{k}) = \frac{1}{i\not{\partial} - m} \rightarrow \frac{1}{\not{k} - m} \qquad (6\text{-}46)$$

and the vertex is $\Gamma_\mu = e\gamma_\mu$.

The photon propagater is tricky, since the inverse does not exist! We can avoid this problem, however, by adding a gauge-breaking term $-\frac{1}{2\alpha}(\partial_\mu A^\mu)^2$[2,3,10,13] so that

$$L_{Kin} = -\frac{1}{2} A^\mu \{\overleftarrow{\partial}\cdot\overrightarrow{\partial}\, g_{\mu\nu} - \overleftarrow{\partial}_\nu\overrightarrow{\partial}_\mu + \frac{1}{\alpha}\overleftarrow{\partial}_\mu\overrightarrow{\partial}_\nu\} A^\nu$$

where we have defined (6-47)

$$f\overleftarrow{\partial}_\mu g = (\partial_\mu f)g \text{ and } f\overrightarrow{\partial}_\mu g = f(\partial_\mu g).$$

The term in the bracket (in momentum space) reads $\Gamma_{\mu\nu} = -k^2 g_{\mu\nu} + (1 - \frac{1}{\alpha})k_\mu k_\nu$.

Due to gauge invariance the propagater must have the form $G_{\mu\nu} = Ag_{\mu\nu} + B\, k_\mu k_\nu$. By solving $\Gamma_{\mu\nu} G^{\nu\lambda} = g_\mu{}^\lambda$ we find easily

$$G_{\mu\nu} = -\frac{g_{\mu\nu}}{k^2} + (1-\alpha)\frac{k_\mu k_\nu}{k^4} \tag{6-48}$$

The case $\alpha=1$ gives the Feynman gauge, $\alpha=0$ the Landau gauge, and finally $\alpha\to\infty$ corresponds to the unitary gauge.

Although we have spoiled the gauge invariance, it turns out to be harmless, since $\partial_\mu A^\mu$ is a free field. This property allows one to show that the unphysical degree of polarization of the photon, decouples from the theory and the S-matrix is gauge invariant and unitary.

We can also find the $W^\pm$ and Z^o propagators quite easily. Recall the bilinear part of the Lagrangian L_o in Eqn. (6-42) is

$$-\frac{1}{2}|\partial_\mu W_\nu^+ - \partial_\nu W_\mu^+|^2 + M_W{}^2|W_\mu^+|^2 \tag{6-49}$$

$$= -\{W_\mu^-\{(M_W{}^2 + \overleftarrow{\partial}\overrightarrow{\partial})g_{\mu\nu} - \overleftarrow{\partial}_\mu\overrightarrow{\partial}_\nu\}W^{+\nu}$$

giving $\Gamma_{\mu\nu} = (M_w^2 - k^2)g_{\mu\nu} + k_\mu k_\nu$.

Following steps as above, we obtain

$$G_{\mu\nu} = \frac{-g_{\mu\nu} + k_\mu k_\nu / M_w^2}{k^2 - M_w^2} \qquad (6\text{-}50)$$

and similarly for the Z^o-propagator. Notice, we do not have to add gauge breaking terms, since we already have longitudinal terms in the Lagrangian.

Now let us go to QCD.

Again we must break the gauge invariance by adding a term $-\frac{1}{2\alpha}(\partial_\mu A^\mu_a)^2$. Except for color factors, the fermion and gluon propagator and, also, the quark-quark-gluon vertex are the same as in QED. However, in this case, there are self-couplings among the gluons.

For the trilinear terms, a typical term is

$$g(\partial_\mu A^a_\nu) f^{abc} A^{b\mu} A^{c\nu}$$

giving a trilinear coupling $f_{abc}\, k_{1\mu}\, g_{\nu\lambda}$. Now, due to Bose-Einstein statistics, the trilinear coupling must be symmetric under interchanging the three gluons. By correct symmetrization we find the triple-gluon coupling:

$$\Gamma^{abc}_{\mu\nu\lambda} = g\, f^{abc}\{(k_1-k_2)_\lambda\, g_{\mu\nu} + (k_2-k_3)_\mu\, g_{\nu\lambda} + (k_3-k_1)_\nu\, g_{\mu\lambda}\} \qquad (6\text{-}51)$$

There is also a quartic term

$$g^2\, f^{abc}\, f^{ade}\, A_{b\mu} A_{c\nu} A^\mu_d\, A^\nu_e$$

giving quartic coupling $g^2\, f^{abc}\, f^{ade}\, g_{\mu\nu}\, g_{\rho\sigma}$. By symmetrization, we obtain

$$g^2 \{ f_{abc} f_{cde} (g_{\mu\sigma} g_{\nu\rho} - g_{\mu\rho} g_{\nu\sigma})$$

$$+ f_{ace} f_{bde} (g_{\mu\nu} g_{\sigma\rho} - g_{\mu\rho} g_{\nu\sigma}) \qquad (6\text{-}52)$$

$$+ c_{ade} c_{cbe} (g_{\mu\sigma} g_{\nu\rho} - g_{\mu\nu} g_{\sigma\rho}) \}$$

These are exactly the same as the corresponding couplings $\gamma W^+ W^-$ and $\gamma\gamma W^+ W^-$ in W-S model. There is just one problem with this procedure, namely, the field $\partial_\mu A^{a\mu}$ is no longer a free field, and the unphysical degrees of freedom do not cancel, and therefore unitarity and gauge invariance are no longer preserved. In order to restore the unitarity, one adds two new fields: the Faddeev-Popov ghosts, η^a and ω^a. These are anticommuting objects and appear only in closed loops.

One considers the additional Lagrangian

$$L_{FP} = \partial^\mu \eta^a D_\mu^{ab} \omega^b$$

where (6-53)

$$D_\mu^{ab} = \delta^{ab} \partial_\mu + g f^{abc} A_\mu^c$$

This leads to a ghost propagator, $\frac{1}{k^2} \delta^{ab}$, and a coupling to gluons $g f_{abc} k_\mu$.

Qualitative Difference Between QED and QCD

The essential difference between QED and QCD lies in the behavior of the renormalized coupling constant. It is well-known that the physical coupling constant e in QED, defined at large distances (Thomson limit), is smaller than the effective coupling constant e_{eff}, which one would measure at smaller distances, due to the presence of vacuum polarization effects. The "bare" electron is surrounded by a

cloud of virtual e^+e^- pairs, and will attract the virtual positrons and, thus, shield part of its electric charge. Hence the vacuum behaves as a dielectric.

In lowest-order perturbation theory (Figure 17) the asymptotic behavior of the effective coupling constant is

$$\alpha(q^2) = \alpha(\mu^2)\,\{1 + \frac{\alpha(\mu^2)}{3\pi}\log(-\frac{q^2}{\mu^2})\}. \qquad (6\text{-}54)$$

We have renormalized at $q^2 = -\mu^2$, to prevent any I.R. singularities.

Adding "bubbles" yields a geometrical series, which can be summed up to give,

$$\alpha(q^2) = \frac{\alpha(\mu^2)}{1 - \frac{\alpha(\mu^2)}{\pi}\log(-\frac{q^2}{\mu^2})}. \qquad (6\text{-}55)$$

The coupling constant does indeed grow with increasing q^2, that is, smaller distances.

In QCD, the behavior is different. This is due to the self interaction of the gluons. We will separate the contributions due to transverse gluonic degrees of freedom (Figure 18) and "Coulomb" degrees of freedom, (Figure 19), using the Coulomb gauge.[14]

The contribution of the transverse gluons leads to color charge screening, like e^+e^- contributions in QED

$$\alpha_s^{t.r.}(q^2) = \alpha(\mu^2)\,\{1 + \frac{\alpha(\mu^2)}{4\pi}\log(-\frac{q^2}{\mu^2})\}, \qquad (6\text{-}56)$$

while the "Coulomb" gluons lead to an anti-screening, which is twelve times larger than the screening due to transverse gluons:

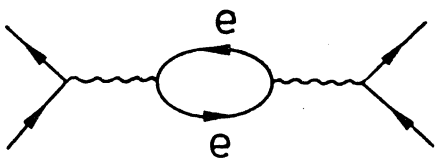

Figure 17. Vacuum Polarization in QED

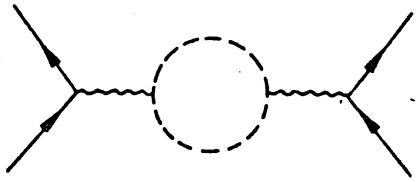

Figure 18. Vacuum Polarization in QCD Due to Transverse Gluons (Dashed Lines)

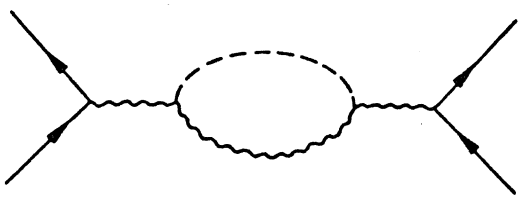

Figure 19. Vacuum Polarization in QCD Due to a Transverse and a "Coulomb" Gluon

$$\alpha_s^c(q^2) = \alpha(\mu^2)\{1 - 12\,\frac{\alpha(\mu^2)}{4\pi}\log(-\frac{q^2}{\mu^2})\}\ . \qquad (6\text{-}57)$$

Each quark flavor contributes

$$\alpha_s(q^2) = \alpha(\mu^2)\{1 + \frac{2}{3}N_f\,\frac{\alpha(\mu^2)}{4\pi}\log(-\frac{q^2}{\mu^2})\}\ . \qquad (6\text{-}58)$$

Altogether

$$\alpha_s(q^2) = \alpha(\mu^2)\{1 - (11 - \frac{2}{3}N_f)\,\frac{\alpha(\mu^2)}{4\pi}\log(-\frac{q^2}{\mu^2})\} \qquad (6\text{-}59)$$

and summing the "bubbles" gives

$$\alpha_s(q^2) = \frac{\alpha(\mu^2)}{1 + \beta_o\,\frac{\alpha(\mu^2)}{4\pi}\log(-\frac{q^2}{\mu^2})} \qquad (6\text{-}60)$$

where we have defined $\beta_o = 11 - \frac{2}{3}N_f$. We see that, if $N_f < 16$, then $\beta_o > 0$ and the coupling constant tends to zero for $q^2 \to -\infty$. This is the so-called asymptotic freedom.

Since the effective coupling constant can not depend on the renormalization point μ^2 we can write

$$\alpha_s(q^2) = \frac{4\pi}{\beta_o\log(-\frac{q^2}{\Lambda^2})},\quad |q^2| >> \Lambda^2 \qquad (6\text{-}61)$$

where the constant $\Lambda \simeq 500$ MeV, has been determined in scaling violations in deep inelastic scattering processes. If we put $|q^2| = \Lambda^2$ in eq. (6-61) the effective coupling constant becomes singular. This occurs at distances around 0.5 fm, which is about the size of the hadrons. We shall see in the next section that it is possible to do perturbation theory in $\alpha_s(q^2)$, rather than using $\alpha(\mu^2)$ which is of order unity. This is

known as renormalization group improved perturbation theory and leads to satisfactory predictions in e^+e^- annihilation into hadrons and also for deep inelastic processes.

Renormalization Group Equation for Massless QED and QCD

Before we introduce the Renormalization Group Equation (RGE), we would like to remind ourselves of what is meant by multiplicative renormalization.[3,13]

Consider for simplicity the Lagrangian for massless QED:

$$L_o = -\frac{1}{4}(\partial_\mu A_\nu - \partial_\nu A_\mu)^2 + \bar{\psi}(i\not{\partial})\psi + e\bar{\psi}\gamma_\mu\psi A^\mu \ . \qquad (6\text{-}62)$$

In the tree approximation, there are no loop integrals and everything is finite. But in the 1-loop approximation and higher infinities arise due to divergent loop integrals. These can be regulated by introducing a momentum cut-off Λ.

The infinities are then cancelled by adding a suitable counter term L_c to the old Lagrangian L_o.

Now, since QED is renormalizable, L_c will take the form:

$$L_c = -\frac{1}{4}(Z_3-1)(\partial_\mu A_\nu - \partial_\nu A_\mu)^2 + (Z_2-1)\bar{\psi}(i\not{\partial})\psi + (Z_1-1)e\bar{\psi}\gamma_\mu\psi A^\mu \qquad (6\text{-}63)$$

where the Z_i's are dependent on the cut-off Λ.

If we do a rescaling (renormalization) of the photon field A_μ, the fermion field and the charge e in the following way,

$$A_\mu = Z_3^{-1/2} A_\mu^B \ ,$$

$$\psi = Z_2^{-1/2} \psi^B \qquad (6\text{-}64)$$

and

$$e = \frac{Z_2}{Z_1} Z_3^{1/2} e^B \tag{6-64}$$

then $L_0 + L_c$ is simply equal to the old Lagrangian, now evaluated using the "bare" fields A_μ^B, ψ^B and coupling e^B. This process can now be repeated to any finite order and we say that QED is renormalizable to any finite order. We would like to mention here that the so-called Ward identity exists, namely that $Z_1 = Z_2$ and therefore $e = Z^{1/2} e_B$.

In connection with the QCD Lagrangian, we shall later define the renormalization constants uniquely.

A necessary condition for a theory to be renormalizable follows. Consider the mass dimension d of the coupling constant g, which we denote $[g]$.

If $d \geq 0$, the theory is renormalizable and it is non-renormalizable if $d < 0$. Example: QED. Since $[L] = 4$ we find easily that $[A_\mu] = 1$ and $[\psi] = \frac{3}{2}$ and, therefore, $[e] = 4 - 2\,\frac{3}{2} - 1 = 0$; and QED has a dimensionless coupling constant and is, hence, renormalizable. QCD and the W-S also have dimensionless couplings and are renormalizable. Examples of non-renormalizable theories are the old 4-fermion theory and gravity since $[G_F] = -2$ and the Newtonian constant $[G_N] = -2$.

For QCD, we write the counter terms as follows:

$$\begin{aligned} &- Z_3 \frac{1}{4} \bar{G}_{\mu\nu} \cdot \bar{G}^{\mu\nu} - Z_1 \frac{g}{2} \bar{G}_{\mu\nu} \cdot (\bar{A}_\mu x \bar{A}_\nu) - Z_4 \frac{g^2}{4} (\bar{A}_\mu x \bar{A}_\nu)^2 \\ &- \frac{1}{2\alpha} (\partial_\mu \bar{A}^\mu)^2 - \tilde{Z}_3 \partial^\mu \bar{\eta} \cdot \partial_\mu \bar{\omega} - \tilde{Z}_1 g^\mu \bar{\eta} \cdot (\bar{A}_\mu x \bar{\omega}) \\ &+ Z_2^F \bar{\psi}(i\partial\!\!\!/)\psi + g Z_1^F \bar{\psi} \bar{T} \cdot \bar{A} \psi \,. \end{aligned} \tag{6-65}$$

We have introduced the notation $G^a_{\mu\nu} = \partial_\mu A_\nu{}^a - \partial_\nu A^a_\mu$ with $\bar{G}_{\mu\nu} \cdot \bar{G}^{\mu\nu} =$

$G^a_{\mu\nu} G^{a\mu\nu}$ and also $(\bar{A}_\mu \times \bar{A}_\nu)^a = f^{abc} A^b_\mu A^c_\nu$.

Adding L_0 and L_c, and writing it as the old Lagrangian in the "bare" fields, gives us the scale transformations:

$$\begin{aligned}
\bar{A}_\mu &= Z_3^{-1/2} \bar{A}_\mu^B , \\
(\bar{\eta}, \bar{\omega}) &= \tilde{Z}_3^{-1/2} (\bar{\eta}^B, \bar{\omega}^B) , \\
\psi_i &= (Z_2^F)^{-1/2} \psi_i^B , \\
g &= \frac{Z_3^{3/2}}{Z_1} g^B , \\
\frac{Z_4}{Z_3} &= \left(\frac{Z_1}{Z_3}\right)^2
\end{aligned} \tag{6-66}$$

and

$$\alpha = Z_3^{-1} \alpha_B$$

along with the so-called Slavnor-Taylor identities,

$$\frac{Z_1}{Z_3} = \frac{\tilde{Z}_1}{\tilde{Z}_3} = \frac{Z_1^F}{Z_2^F}$$

so that $g = Z_2^F (Z_1^F)^{-1} Z_3^{1/2} g_B$, as in QED.

The renormalization constants are now defined as follows[3] (U refers to unrenormalized and μ is the renormalization point).

The gluon propagator (transverse):

$$U_{D\mu\nu}^{ab(Tr)}(k)\Big|_{k^2=-\mu^2} = \frac{i}{\mu^2} Z_3 \left(g_{\mu\nu} + \frac{k_\mu k_\nu}{\mu^2}\right) \delta^{ab}$$

The ghost propagator:

$$U_{\tilde{G}}^{ab}(k)\Big|_{k^2=-\mu^2} = \frac{-i}{\mu^2}\tilde{Z}_3\,\delta^{ab}$$

The fermion propagator:

$$U_S^{ij}(k)\Big|_{k^2=-\mu^2} = \frac{i}{\not{k}}Z_2^F\,\delta^{ij}$$

The triple-gluon vertex:

$$U_{\Gamma\,\mu\nu\lambda}^{abc}(k_1)k_2,k_3)\Big|_{k_1^2=k_2^2=k_3^2=-\mu^2} = Z_1^{-1}\,\Gamma_{\mu\nu\lambda}^{abc}(k_1,k_2,k_3)\Big|^B. \tag{6-67}$$

The ghost-ghost-gluon vertex:

$$U_{\Gamma\,\mu}^{abc}(k_1,k_2,k_3)\Big|_{k_1^2=k_2^2=k_3^2=-\mu^2} = \tilde{Z}_1^{-1}\,k_{1\mu}\,f^{abc}$$

and finally the quark-quark-gluon vertex

$$U_{\Gamma\,\mu}^{a}(k_1,k_2,k_3)\Big|_{k_1^2=k_2^2=k_3^2=-\mu^2} = (Z_1^F)^{-1}\,\gamma_\mu T^a\,.$$

We are now ready to discuss the Renormalization Group equation.[3,13,15] Consider first a renormalized one-particle irreducible Greens function (all external propagators removed) $R_\Gamma^{(n)}(k_i)$, with n external gluons. Inclusion of fermions is trivial. $R_\Gamma^{(n)}(k_i)$ can be obtained from the unrenormalized amplitude $U_\Gamma^{(n)}(k_i)$ via multiplicative renormalization. The unrenormalized amplitude depends on the cut off Λ, the bare coupling

constant g_B and the gauge parameter α_B, while the renormalized amplitude depends on the renormalization point μ, the renormalized coupling constant g and the gauge parameter α.

We now suppress the external momenta k_i and write

$$R_\Gamma^{(n)}(\mu,g,\alpha) = Z_3^{n/2}(\Lambda,\mu g_B,\alpha_B)\, U_\Gamma^{(n)}(\Lambda, g_B,\alpha_B). \tag{6-68}$$

Z_3 depends on Λ and μ through the combination $\frac{\Lambda}{\mu}$.

Now since the unrenormalized Greens function does not depend on μ, any variation with respect to μ must vanish, i.e.,

$$\mu \frac{d}{d\mu} \Gamma^{(n)}(\Lambda,g_B,\alpha_B) = 0 . \tag{6-69}$$

We are now interested in the influence of this variation on the renormalized Greens function. We have

$$\mu \frac{d}{d\mu} = \mu \frac{\partial}{\partial\mu} + \beta(g,\alpha) \frac{\partial}{\partial g} + \delta(g,\alpha) \frac{\partial}{\partial\alpha} \tag{6-70}$$

where the β-function:

$$\beta(g,\alpha) \equiv \mu \left.\frac{\partial g}{\partial\mu}\right|_{\Lambda,g_B,\alpha_B} = - g \frac{\partial}{\partial \log\Lambda} \log(Z_3^{3/2} Z_1^{-1}),$$

the anomalous dimension γ:

$$\gamma(g,\alpha) \equiv - \frac{1}{2} \frac{\partial}{\partial \log\Lambda} \log Z_3 \Big|_{\Lambda,g_B,\alpha_B}$$

and

$$\delta(g,\alpha) = - 2\alpha\, \gamma(g,\alpha).$$

Notice that in the Landau gauge, $\alpha=0$, and, therefore, $\delta(g,\alpha)$ vanishes. One can prove that β and γ depends only on g, and we have

$$\left[\mu \frac{\partial}{\partial \mu} + \beta(g) \frac{\partial}{\partial g} - n\, \gamma(g)\right] R_\Gamma^{(n)}(g,\mu) = 0. \tag{6-71}$$

To "solve" this equation, we perform a scaling of all momenta $k_i \to \lambda k_i$ and write $t = \log \lambda$. We also define the "running coupling constant" $\bar{g}(g,t)$ with initial value $\bar{g}(g,o)=g$ through $\frac{d\bar{g}}{dt} = \beta(\bar{g})$.

One finds[3,13,15]

$$R_\Gamma^{(n)}(\lambda k_i, g, \mu) = R_\Gamma^{(n)}(k_i, \bar{g}, \mu)\lambda^{4-n} \exp\{-n \int_g^{\bar{g}} \frac{\gamma(g')}{\beta(g')} dg'\}. \tag{6-72}$$

Now we see that the large momentum ($\lambda \to \infty$) behavior is governed by the amplitude with g replaced by the running coupling constant $\bar{g}$. The β function and the anomalous dimension can both be calculated in perturbation theory and, hence, $\bar{g}$ can be obtained.

$$\beta(g) = -\beta_o g^3 + \beta_1 g^5 + \cdots$$

$$\gamma(g) = c_o g^2 + c_1 g^4 + \cdots \tag{6-73}$$

In the 1-loop approximation, the renormalization constants are[16] (Figure 20)

$$Z_3^{YM} = 1 + \frac{g^2}{16\pi^2}\{(\frac{13}{3} - \alpha)C_2(G) - \frac{8}{3}T(N)\}\log\frac{\Lambda}{\mu},$$

$$Z_1^{YM} = 1 + \frac{g^2}{16\pi^2}\{(\frac{17}{6} - \frac{3\alpha}{2})C_2(G) - \frac{8}{3}T(N)\}\log\frac{\Lambda}{\mu} \tag{6-74}$$

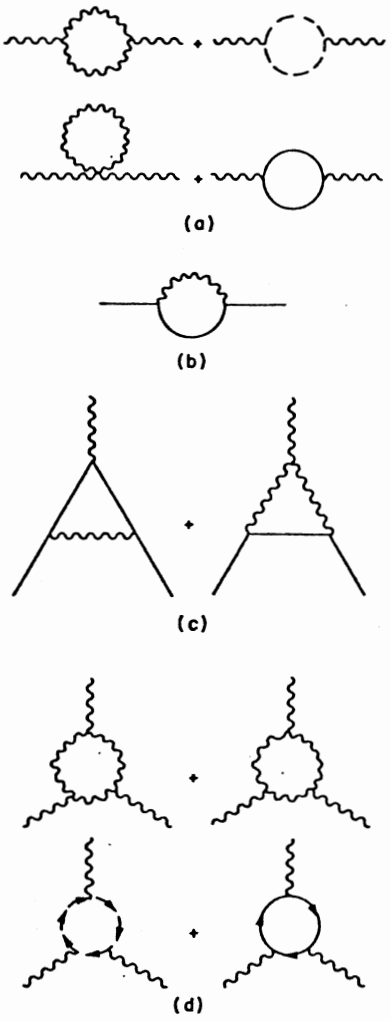

Figure 20. Feynman Diagrams Contributing the g^2 Corrections to (a) Z_3, (b) Z_2^F, (c) Z_1^F and (d) Z_1

$$\tilde{Z}_3 = 1 + \frac{g^2}{16\pi^2}\left(\frac{3}{2} - \frac{\alpha}{2}\right)C_2(G)\log\frac{\Lambda}{\mu} ,$$

$$\tilde{Z}_1 = 1 - \frac{g^2}{16\pi^2}\alpha C_2(G)\log\frac{\Lambda}{\mu} ,$$

$$Z_2^F = 1 - \frac{g^2}{16\pi^2}(2\alpha)C_2(N)\log\frac{\Lambda}{\mu}$$

and

$$Z_1^F = 1 - \frac{g^2}{16\pi^2}\left\{\left(\frac{3}{2} + \frac{\alpha}{2}\right)C_2(G) + (2\alpha)C_2(N)\right\}\log\frac{\Lambda}{\mu}$$

where $C_2(G) = N$ is the Quadratic Casimir invariant for the adjoint representation of G, while $C_2(N) = \frac{N^2-1}{2N}$ and $T(N) = \frac{1}{2}$ are the Casimir invariants for the fundamental fermionic representation.

$$C_2(G)\delta_{ab} = \sum_{c,d} f_{acd} f_{bcd} ,$$

$$T(N)\delta_{ab} = \mathrm{Tr}(T_a T_b) = \frac{1}{2}\delta_{ab} \qquad (6\text{-}75)$$

$$C_2(N) = T_a T_a .$$

Notice that the Slavnov-Taylor identities are satisfied to order g^2. We are now ready to calculate the lowest order β function. We find

$$\frac{Z_3^{3/2}}{Z_1} = 1 + \frac{g^2}{16\pi^2}\left[\frac{11}{3}C_2(G) - \frac{4}{3}T(N)\right]\log\frac{\Lambda}{\mu} \qquad (6\text{-}76)$$

and therefore, $\beta(g) = -\beta_0 g^3$ gives $\beta_0 = \frac{11}{3}C_2(G) - \frac{4}{3}T(N) = 11 - \frac{2}{3}N_f$.[17] This is the famous one-loop β-function, which was first obtained by Gross, Wilczek and Politzer in 1973.[17]

This is the same function as the one found in the previous section.

To summarize, we have seen that the large momentum behavior of the Greensfunction is governed by the running coupling constant, and that QCD leads to an asymptotically-free field theory, provided the number of flavors $N_f \leq 16$.

REFERENCES

1. M. Gell-Mann, Phys. Lett. 8, 214 (1964); G. Zweig, "CERN" Report 182/TH 401 (1964).

2. O. W. Greenberg, Phys. Rev. Lett. 13, 598 (1964); O. W. Greenberg and M. Resnikoff, Phys. Rev. 163, 1844 (1967); M. Gell-Mann, Acta Phys. Austrica Supp. 9, 733 (1967); W. A. Bardeed, H. Fritzsch and M. Gell-Mann in "Scale and Conformal Symmetry in Hadron Physics", (Wiley, New York, 1973).

3. E. Reya, Phys. Rep. 69C, 195 (1981); W. Marciano and H. Pagels, Phys. Rep. 36C, 137 (1978).

4. G. S. LaRue, J. D. Philips and W. M. Fairbank, Phys. Rev. Lett. 46, 967 (1981).

5. S. L. Adler, "Lectures on Particles and Quantum Field Theory", (Brandeis 1970, MIT Press, Cambridge).

6. B. H. Wiik, "New e^+e^- Physics", DESY 80/124, December, 1980.

7. S. L. Adler, Phys. Rev. 177, 2426 (1969); J. S. Bell and R. Jackiw, Nuovo Cim. 60, 47 (1969).

8. H. Giorgi and S. L. Glashow, Phys. Rev. D6 429 (1972); D. J. Gross and R. Jackiw, ibid. D6, 477 (1972).

9. H. Fritzsch and P. Minkowski, "Flavor-dynamics of Quarks and Leptons", Berne preprint 1981.

10. I. J. R. Aitchison, "An informal Introduction to Gauge Theories", Oxford preprint 17/80; E. S. Abers and B. W. Lee, Phys. Rep. 9C, 1 (1973); J. C. Taylor, "Gauge Theories of Weak-interactions", (Cambridge University Press, 1972).

11. G. S. Guralnik, C. R. Hagen and T. W. B. Kibble in "Advances in Particle Physics 2, 567 (1968); G. S. Guralnik et al., Phys. Rev. Lett. 13, 585 (1964); F. Englert and R. Brout, Phys. Rev. Lett. 13, 321 (1964).

12. G. t'Hooft and T. Veltman, "Diagrammar", CERN Yellow Report 73-9 (1973).

13. L. D. Faddeev and A. A. Slavnov, "Gauge Fields, Introduction to Quantum Theory", (Frontiers in Physics Vol. 50) (Benjamin Pub. Company, Massachusetts 1980); C. Nash, "Relativistic Quantum Fields", (Academic Press, London 1978).

14. V. A. Novikov et al., Phys. Rep. 41C, 1, (1978).

15. A. Peterman, Phys. Rep. 53C, 157 (1979).

16. H. Bohr, Ph.D. Thesis, Niels Bohr Institute, Copenhagen (1979).

17. D. J. Gross and F. Wilczek, Phys. Rev. Lett. 30, 1343 (1973); D. Politzer, ibid 30, 1346 (1973).

CHAPTER VII

Z^o DECAY INTO THREE GLUONS

Introduction

The next generation of electron-positron colliders is expected to achieve c.m. energies comparable to the mass of the weak intermediate neutral vector boson Z^o. In the standard Weinberg-Salam model, this mass is around 90 GeV/c^2 and the SLAC single pass collider, the Cornell e^+e^- ring, and LEP are all projected to reach or exceed this energy.[1] The purpose is to take advantage of the very large resonant cross section at $\sqrt{s} = M_z$ and study rare decays of the Z^o.

Calculations[2,3,4,5] have been reported on several decay modes: $\ell\bar{\ell}$, $\ell\bar{\ell}\gamma$, $q\bar{q}$, $q\bar{q}\gamma$, $q\bar{q}g$, $H\gamma$, etc. Here we report on a new decay channel, namely $Z^o \to ggg$, and also discuss $Z^o \to gg\gamma$ and $Z^o \to \gamma\gamma\gamma$. One of the reasons to study these processes is that the corresponding two body decay modes $Z^o \to \gamma\gamma$, $g\gamma$ and gg vanish (Figure 21): the first by Yang's theorem,[6] the second by color conservations ($Tr[T_a]=o$), and the third because the two gluons have to carry the same color ($Tr[T_aT_b] = \frac{1}{2}\delta_{a,b}$), and, therefore, Yang's theorem again applies. As usual $T_a = \frac{1}{2}\lambda_a$ where λ_a is the Gell-Mann SU(3) color matrices.

This three-gluon decay is a high-order QCD process of order $(\frac{\alpha_s}{\pi})^3 \approx 10^{-4}$ relative to the $q\bar{q}$ decay mode, and with such a small ratio one might worry about the experimental significance. However, with a proposed luminosity $L=10^{32}cm^{-2}s^{-1}$ at LEP, one can expect approximately 1.5 x 10^5 $q\bar{q}$ events per day, so that in a typical experiment one can obtain some 10^7 $q\bar{q}$ events. Therefore, we should expect a significant number of ggg events, thus providing

a test of higher-order perturbative QCD.

Our calculations are based on the standard W-S model and QCD. Furthermore, to simplify our results, we will consider only the limit of vanishing quark masses, i.e. $m_q/M_Z \to 0$.

The Feynman diagrams can be divided into two sets: box diagrams (Figure 22a), and triangle diagrams (Figure 22b). One must, of course, sum over colors as well as flavors in the quark loops of Figure 22. Then we easily find that the triangle diagrams sum up to zero, because each diagram is found explicitly to be free of any mass singularities; i.e., there are no $\log \frac{m_q}{M_Z}$ terms and is proportional to the axial coupling b^i of the Z^o to $q_i\bar{q}_i$. Thus with $b^i = I_3^i$ (weak isospin) in the standard model, the sum within each SU(2) doublet vanishes ($b^u = -b^d = b^c = -b^s = b^t = -b^b = 1/2$). Needless to say, the vector part of the triangle diagrams vanishes identically due to charge conjugation symmetry.

We are left with the box diagrams which contain both vector and axial vector couplings. The VVVV(AVVV) diagrams involve the symmetric (antisymmetric) part $d_{abc}(f_{abc})$ of the trace over the color matrices: $Tr[T_a T_b T_c] = \frac{1}{4}(d_{abc} + if_{abc})$, since they have charge conjugation C = even(odd) respectively. Again the sum over quark flavors eliminates the AVVV box diagrams by the above argument, and therefore, in the limit of equal masses within each doublet, the decay $Z^o \to ggg$ is proportional to the vector couplings a^i, where $a^a = a^c = a^t = \frac{1}{2} - \frac{4}{3}\sin^2\theta_w$ and $a^d = a^s = a^b = -\frac{1}{2} + \frac{2}{3}\sin^2\theta_w$ in the standard model.

Since we need the box diagram with only one massive external leg, we start with the expressions given by Costantini, De Tollis and Pistoni[7] for photon splitting and take the limit of vanishing fermion mass.

In going from photon splitting to the decay, we have analytical con-

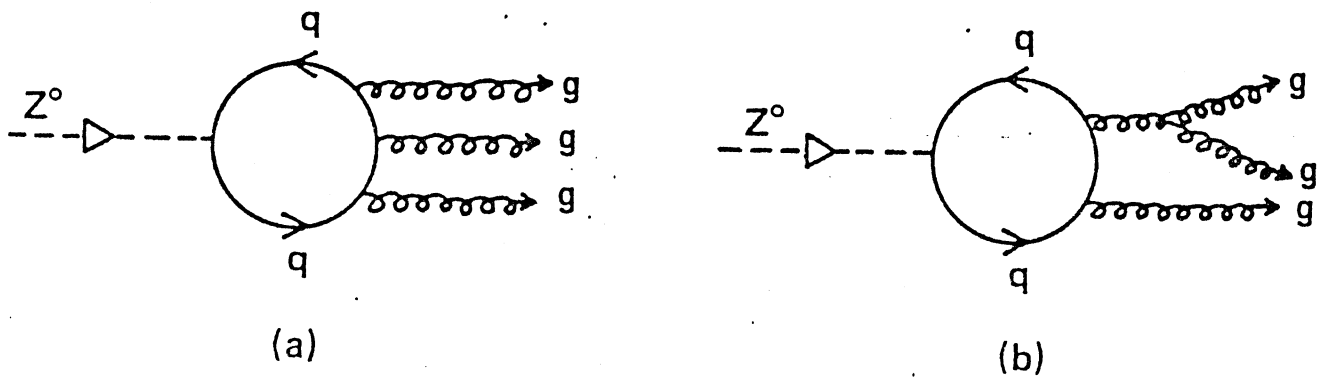

Figure 22. Feynman Diagrams for the Decay $Z^{\circ} \rightarrow ggg$. Permutations Must be Added. For Doublets With Massless Quarks Only the VVVV Part of the Box Diagrams (a) Contribute

tinued from a space-like photon to a time-like Z^o. Normally threshold effects might occur, however, Costantini et al. have shown that their expressions hold for time-like particles also.

Though separate parts of the amplitude contain divergences, the final answer is free of any mass singularity, and can be written as a function of the dimensionless scaling variables $x = 2E_a/M_Z$, $y = 2E_b/M_Z$ and $= 2\ E_c/M_Z$, where the E's refer to the gluon energies in the Z^o rest frame. Only two are independent, since $x + y + z = 2$. We also found, to our surprise, that the imaginary parts add up to zero: there are twenty-four helicity amplitudes and they are all real. A similar result was obtained by Fabricius et al.[8] in their calculation of order α_s^2 correction to $q\bar{q}g$-jets in e^+e^- annihilation.

Forbidden Decays $Z^o \to gg(\gamma\gamma)$

We briefly show why the amplitudes for the two decay modes $Z^o \to gg(\gamma\gamma)$ vanish. As mentioned in the beginning, the two gluons must be identical, and the two decay modes are proportional to each other. We show that they are forbidden follows from a classical symmetry argument, as well as by an explicit calculation, at least in lowest-order perturbation theory, where the decays take place via a virtual triangular quark loop, with only two diagrams contributing (Figure 21). First the classical symmetry argument.[9]

Let the two photons (gluons) have polarization vectors $\bar{\varepsilon}_{1,2}$ and let the relative momentum of them be $\bar{k}$. Any possible final state will be a linear combination in $\bar{\varepsilon}_1$ and $\bar{\varepsilon}_2$ and transform as a vector, if the total final state has spin 1. Only three possibilities exists:

$$\text{(i)}\quad \bar{\varepsilon}_1 \times \bar{\varepsilon}_2,$$

$$\text{(ii)}\quad (\bar{\varepsilon}_1 \cdot \bar{\varepsilon}_2)\bar{k} \tag{7-1}$$

and

$$\text{(iii)}\quad \bar{k} \times (\bar{\varepsilon}_1 \times \bar{\varepsilon}_2)\ .$$

The first two possibilities can be ruled out due to antisymmetry in $1 \leftrightarrow 2$. The last possibility satisfies Bose-Einstein statistics, but it can also be ruled out because of the transversality condition, $\bar{k}\cdot\bar{\varepsilon}=0$. Therefore the two photon(gluon) annihilation is forbidden.

More explicitly, we find for the amplitude $M(Z^o \to gg)$:[10]

$$M(Z^o \to gg) \;\alpha\; S_{\lambda\mu\nu}(k_1,k_2)\; \varepsilon^{\lambda}\; \varepsilon_1^{\mu}\; \varepsilon_2^{\nu}, \tag{7-2}$$

where ε^{λ}, ε_1^{μ} and ε_2^{ν} are the polarization vectors for the Z^o and gluons (photons) respectively, and the tensor $S_{\lambda\mu\nu}$ is:

$$\begin{aligned} S_{\lambda\mu\nu}(k_1,k_2) &= J_{110}(k_1,k_2)\; \varepsilon_{\mu\nu\alpha\beta}\; k_1^{\alpha}k_2^{\beta}(k_1+k_2)_{\lambda} \\ &+ J_{101}(k_1,k_2)\{\varepsilon_{\lambda\nu\alpha\beta}k_1^{\alpha}k_2^{\beta}\; k_{1\mu} + k_1^2\; \varepsilon_{\lambda\mu\nu\alpha}k_2^{\alpha}\} \\ &- J_{011}(k_1,k_2)\{\varepsilon_{\lambda\mu\alpha\beta}k_1^{\alpha}k_2^{\beta}k_{2\nu} + k_2^2\; \varepsilon_{\lambda\mu\nu\alpha}k_1^{\alpha}\}, \end{aligned} \tag{7-3}$$

with the integrals $J_{rst}(k_1,k_2)$ defined as:

$$J_{rst}(k_1,k_2) = -\frac{1}{\pi^2}\int d\alpha_1 d\alpha_2 d\alpha_3 \delta(1-\alpha_1-\alpha_2-\alpha_3) \times \frac{\alpha_1^r\; \alpha_2^s\; \alpha_3^t}{[\alpha_1\alpha_2(k_1+k_2)^2+\alpha_1\alpha_3k_1^2+\alpha_2\alpha_3k_2^2-m_q^2]}\ . \tag{7-4}$$

The integration is over the three-dimensional hypercube. For details leading to the above expressions see Appendix B.

Now for real gluons ($k_1^2 = k_2^2 = 0$), satisfying the transversality con-

ditions $k_1 \cdot \varepsilon_1 = k_2 \cdot \varepsilon_2$ and also using $(k_1+k_2)\cdot\varepsilon=0$, it follows from Eqns. (8-2) and (8-3) that the two gluon (photon) amplitude $M(Z^o \to gg)$ vanishes.

Kinematics and the Three Gluon Decay

We shall follow the notation of Costantini et al.[7], with the exception that we have used the covariant metric instead of the Pauli metric.[11]

Let the 4-momentum of the decaying Z^o be denoted k_1, and the 4-momenta of the three outgoing gluons be k_i (i=2,3,4). Since all four particles are real (on-shell), we have $k_1^2 = M_Z^2 \equiv -4\mu_1$ and $k_i^2 = 0$ (i=2,3,4).

Define three scalar quantities:

$$r = \frac{1}{4}(k_1-k_2)^2$$

$$s = \frac{1}{4}(k_1-k_3)^2 \qquad (7\text{-}5)$$

$$t = \frac{1}{4}(k_1-k_4)^2$$

with the restriction:

$$r + s + t + \mu_1 = 0 .$$

Except for a trivial factor 1/4, r, s and t are the usual Møller-Mandelstam variables s, t and u respectively. Since we have a three-body decay, two of these three variables are sufficient to describe the process. We also define $r_1 \equiv r+\mu_1$ and similarly for s_1 and t_1.

We shall of course work in the rest frame of the decaying particle Z^o. It is customary to introduce the so-called scaling variables:

$$x_i \equiv 2\,\frac{k_i \cdot k_1}{k_1^2} = \frac{2E_i}{M_Z} \quad (i = 2,3,4) \qquad (7\text{-}6)$$

The range of x_i is $0 \le x_i \le 1$, since each gluon can carry at most half the

energy of the Z^o, and energy-conservation is then expressed as $x_2 + x_3 + x_4 = 2$. For convenience, we rename $(x_2, x_3, x_4) \rightarrow (x, y, z)$ in the following.

The variables (r, s, t) now becomes:

$$\begin{aligned} r &= |\mu_1|(1-x) \\ s &= |\mu_1|(1-y) \\ t &= |\mu_1|(1-z). \end{aligned} \tag{7-7}$$

Let each of the outgoing gluons have helicity $\lambda_i = \pm$ (i = 2,3,4) and let ε_1^μ be the polarization vector of the Z^o. The matrix element, for the box diagram with one massive external leg, for a given helicity state is:

$$M_{\lambda_2\lambda_3\lambda_4}(1234) = G_\mu^{(\lambda_2\lambda_3\lambda_4)}(1234)\varepsilon_1^\mu, \tag{7-8}$$

where the vacuum polarization tensor:

$$\begin{aligned} G_\mu^{(\lambda_2\lambda_3\lambda_4)}(1234) &= \frac{-1}{\sqrt{32\Delta}} \{\zeta_\mu^{(\lambda_2\lambda_3\lambda_4)}(1234) \\ &+ E^{(2)}_{\lambda_2\lambda_3\lambda_4}(1234)\, \chi_\mu(1234)\} \end{aligned} \tag{7-9}$$

with

$$\zeta_\mu^{(\lambda_2\lambda_3\lambda_4)}(1234) = E^{(1)}_{\lambda_2\lambda_3\lambda_4}(1234)N_\mu(1234) - E^{(1)}_{\lambda_2\lambda_4\lambda_3}(1243)N_\mu(1243), \tag{7-10}$$

$$N_\mu(1234) = k_{3\mu} - \frac{k_1\cdot k_3}{k_1\cdot k_2} k_{2\mu}, \tag{7-11}$$

$$\chi_\mu(1234) = \varepsilon_{\mu\nu\rho\sigma} k_1^\nu k_2^\rho k_3^\sigma$$

and

$$\Delta = rst .$$

The tensor G_μ is essentially the one used in photonsplitting. As mentioned in the introduction, we have performed an analytical continuation from a space-like γ ($\mu_1 > 0$) to a timelike Z^o ($\mu_1 < 0$). We see that all the tensor structure is present in the N_μ and χ_μ terms, while the real "dynamics" is hidden in the sixteen amplitudes $E^{(i)}_{\lambda_2\lambda_3\lambda_4}$ (i=1,2). Of these sixteen amplitudes, only four are really independent, namely: $E^{(i)}_{\pm++}$(i = 1,2), or equivalently, of the eight amplitudes $M_{\lambda_2\lambda_3\lambda_4}$, only two: $M_{\pm++}$ are independent.

The remaining six amplitudes can be obtained from $M_{\pm++}(1234)$ by using the following general symmetry-properties of G_μ:

$$G_\mu^{(\lambda_2\lambda_3\lambda_4)}(1234) = G_\mu^{(-\lambda_4-\lambda_2\lambda_3)}(1423) = G_\mu^{(-\lambda_3-\lambda_4-\lambda_2)}(1342) =$$

$$- G_\mu^{(\lambda_2\lambda_4\lambda_3)}(1243) = - G_\mu^{(-\lambda_3-\lambda_2\lambda_4)}(1324) = - G_\mu^{(-\lambda_4\lambda_3-\lambda_2)}(1432). \qquad (7\text{-}12)$$

These symmetry relations then yield

$$\begin{aligned} M_{--+}(1234) &= - M_{+++}(1324), \\ M_{-+-}(1234) &= - M_{+++}(1432), \\ M_{++-}(1234) &= - M_{---}(1324) \end{aligned} \qquad (7\text{-}13)$$

and

$$M_{+-+}(1234) = - M_{---}(1432).$$

We also have

$$E^{(1)}_{-\lambda_2-\lambda_3-\lambda_4}(1234) = - E^{(1)}_{\lambda_2\lambda_3\lambda_4}(1234)$$

and

$$E^{(2)}_{-\lambda_2-\lambda_3-\lambda_4}(1234) = E^{(2)}_{\lambda_2\lambda_3\lambda_4}. \qquad (7\text{-}14)$$

For the decay, we shall see that

$$|M_{-\lambda_2-\lambda_3-\lambda_4}|^2 = |M_{\lambda_2\lambda_3\lambda_4}|^2 , \qquad (7\text{-}15)$$

so that, indeed, only $M_{\pm++}$ are independent amplitudes.

We will not give the exact expressions for the four amplitudes $E^{(i)}_{\pm++}(i=1,2)$ here. They are cumbersome and are stated in Appendix C.

We are now ready to evaluate the matrix element squared. Consider first $(\lambda_2\lambda_3\lambda_4) = (+++)$. Wherever possible, we shall drop the (1234) notation.

Using the polarization sum $\varepsilon_1^{*\mu}\varepsilon_1^{\nu} = - g^{\mu\nu} + k_1^{\mu}k_1^{\nu}/M_Z^2$, the condition for gauge invariance $k_1^{\mu}G_{\mu} = 0$, and also $k_i^{\mu}\chi_{\mu} = 0$ we obtain:

$$|M_{+++}|^2 = G^*_{\mu} G_{\nu} \varepsilon_1^{*\mu} \varepsilon_1^{\nu} = - G_{\mu}G^{\mu} =$$
$$- \frac{1}{32\Delta} \{\xi^*_{+++}\cdot\zeta_{+++} + |E^{(2)}_{+++}|^2\chi^2\} . \qquad (7\text{-}16)$$

Remember the amplitudes, in general, are complex, therefore, the asterix on ξ. From Eqns. (7-14) and (7-16) it follows easily that $|M_{+++}|^2 = |M_{---}|^2$ as promised.

The reduction of $\xi^*_{+++}\xi_{+++}$ is straightforward, and using Eqns. (7-10) and (7-11), we obtain

$$\xi^*_{+++}\,\xi_{+++} = - 4\,\frac{st}{r_1}\,|E^{(1)}_{+++}(1234)|^2 - 4\,\frac{st_1}{r_1}|E^{(1)}_{+++}(1243)|^2$$

$$-4\left[\frac{rr_1-ss_1-tt_1}{r_1}\right]\mathrm{Re}\left[E^{(1)}_{+++}(1234)E^{(1)}_{+++}(1243)\right]. \qquad (7\text{-}17)$$

For the χ^2-part we use:

$$\varepsilon^{iklm}\,\varepsilon_{prsm} = -\begin{vmatrix} \delta^i_p & \delta^i_r & \delta^i_s \\ \delta^k_p & \delta^k_r & \delta^k_s \\ \delta^l_p & \delta^l_r & \delta^l_s \end{vmatrix} \qquad (7\text{-}18)$$

yielding easily $\chi^2 = -16\Delta$.

It turns out to be convenient to define the following dimensionless quantities:

$$\hat{E}^{(1)}_{+++}(1234) = \frac{1}{8s}\,E^{(1)}_{+++}(1234) \qquad (7\text{-}19)$$

and

$$\hat{E}^{(2)}_{+++}(1234) = \frac{1}{4}\,E^{(2)}_{+++}(1234).$$

Introducing the scaling variables (x,y,z) we arrive at the exact expression:

$$|M_{+++}|^2 = 8\left\{\frac{y(1-y)}{x(1-x)}\left[\hat{E}^{(1)}_{+++}(x,y,z)\right]^2 + \frac{z(1-z)}{x(1-x)}\left[\hat{E}^{(1)}_{+++}(x,z,y)\right]^2 - \frac{2(1-y)(1-z)}{x(1-x)}\,\hat{E}^{(1)}_{+++}(x,y,z)\hat{E}^{(1)}_{+++}(x,z,y) + \left[\hat{E}^{(2)}_{+++}(x,y,z)\right]^2\right\} \qquad (7\text{-}20)$$

The helicity averaged matrix element squared is then

$$|\bar{M}|^2 = \frac{1}{3}\sum_{pol}|M_{\lambda_2\lambda_3\lambda_4}(1234)|^2 .$$

$$= \frac{2}{3}\{|M_{+++}(x,y,z)|^2 + (x \leftrightarrow y) + x \leftrightarrow z) + |M_{-++}(x,y,z)|^2\} \quad (7\text{-}21)$$

We are now ready to discuss the double differential decay rate.

In the rest frame of the decaying Z^o, the differential decay rate is[12]

$$d\Gamma = \frac{1}{2M_Z} \prod_{i=2}^{4} \frac{d^3k_i}{(2\pi)^3 2E_i} (2\pi)^4 \delta(k_1-k_2-k_3-k_4) |\bar{T}|^2 \quad (7\text{-}22)$$

where $|\bar{T}|^2$ refers to the helicity-averaged matrix element squared.

Performing three angular integrations, we obtain:

$$\frac{d^2\Gamma}{dxdy} = \frac{M_Z^3 G_F \alpha_s^3}{512\sqrt{2}\,\pi^4} (\Sigma a_i)^2 C^{ggg} |\bar{M}|^2 \quad (7\text{-}23)$$

where $|\bar{M}|^2$ is given in Eqn. (7-21). We have used the strong coupling constant g_s for each $q_i\bar{q}_i g$ vertex, and the coupling $2^{1/4} M_Z G_F^{1/2} a_i$ for each $q_i\bar{q}_i Z^o$ vertex. A factor $1/(4\pi)^4$ has been included, since Costantini et al. use a loop momentum d^4k/π^2 instead of $d^4k/(2\pi)^4$. Finally C^{ggg} is the group factor obtained by summing over gluon colors.

$$C^{ggg} = \frac{1}{4} \sum_{a,b,c} d_{abc} d_{abc} = \frac{(N^2-1)(N^2-4)}{4N} = \frac{10}{3} \quad (N=3 \text{ colors}) \quad (7\text{-}24)$$

The corresponding decay $Z^o \to q\bar{q}$ has a width[4]

$$\Gamma_o = \sum_i \Gamma(Z^o \to q_i\bar{q}_i) = \frac{\sqrt{2}\, M_Z^3 G_F}{4\pi} \sum_i (a_i^2 + b_i^2) , \quad (7\text{-}25)$$

which we use for normalization:

$$\frac{1}{\Gamma_o} \frac{d^2\Gamma(Z^o \to ggg)}{dxdy} = \frac{1}{256} \left(\frac{\alpha_s}{\pi}\right)^3 C^{ggg} \frac{(\sum_i a_i)^2}{\sum_i (a_i^2 + b_i^2)} |\bar{M}|^2 \quad (7\text{-}26)$$

In the limit $m_q \to 0$, we find for $|\bar{M}|^2 \equiv d^2F/dxdy$, using Eqns. (7-20) and (8-21) and Appendices C and D,

$$\frac{d^2F}{dxdy} = \frac{16}{3}\{\frac{y(1-y)}{x(1-x)}[\hat{E}^{(1)}_{+++}(x,y,z)]^2 + \frac{z(1-z)}{x(1-x)}[\hat{E}^{(1)}_{+++}(x,z,y)]^2$$

$$- \frac{2(1-y)(1-z)}{x(1-x)}\hat{E}^{(1)}_{+++}(x,y,z)\hat{E}^{(1)}_{+++}(x,z,y) + [\hat{E}^{(2)}_{+++}(x,y,z)]^2\} \quad (7\text{-}27)$$

$$+ (x \leftrightarrow y) + (x \leftrightarrow z) + \frac{64}{3}$$

where

$$\hat{E}^{(1)}_{+++}(x,y,z) = 2(\frac{1-z}{y}) + [3 - \frac{1}{y} + 2(\frac{1-y}{1-x}) - 2(\frac{1-x}{y^2})]\log(1-y)$$

$$+ [-1 + \frac{1}{z} + 2(\frac{1-z}{1-x})]\log(1-z) \quad (7\text{-}28a)$$

$$+ [\frac{y-z}{1-x} + 2\frac{(1-y)(1-z)}{(1-x)^2}]G(y,z) \ .$$

and

$$\hat{E}^{(2)}_{+++}(x,y,z) = [1 - 1/y + 2(1-y)/(1-x)]\ell n(1-y)$$

$$+ [1 - 1/z + 2(1-z)/(1-x)]\ell n(1-z) \quad (7\text{-}28b)$$

$$+ [x/(1-x) + 2(1-y)(1-z)/(1-x)^2]G(y,z) \ .$$

We have also used $\hat{E}^{(1)}_{-++} = 0$ and $\hat{E}^{(2)}_{-++} = -2$.

The function G(y,z) is:

$$G(y,z) = \log(1-y)\log(1-z) + Li_2(y) + Li_2(z) - \frac{\pi^2}{6} \qquad (7\text{-}29)$$

where

$$Li_2(x) = -\int_0^x \frac{dt}{t} \log(1-t).$$

Results

The function $d^2F/dxdy$ is clearly symmetric under $x \leftrightarrow y$, $x \leftrightarrow z$, or $y \leftrightarrow z$, so that it is enough to know the function in one of the six small triangles, shown in Figure 23. Normally we would like to show $d^2F/dxdy$ as a Dalitz plot, but our computations show that the function changes by only a factor two, in going from the center of gravity ($x = y = z = \frac{2}{3}$), where $d^2F/dxdy$ reaches its minimum, to say $x = .99$. This, of course, would make it difficult to see. Instead we decided to plot $d^2F/dxdy$ as a function of x for several values of y. This is done in Figure 24. The range shown is $1.01 \leq x + y \leq 1.98$, or equivalently $.02 \leq z \leq .99$. We characterize the divergence near $z \to 0$ as infrared and near $z \to 1$ as collinear. Both are logarithmic and integrable, $d^2F/dxdy \to \frac{64}{3} \log^2 z$ and $d^2F/dxdy \to \frac{64}{3} \log^2(1-z)$ as $z \to 0$ and $z \to 1$ respectively.

In finding, the asymptotic behavior above, we used the important property $G(y,z) \to 0$ for $x \to 1$. For details see Appendix E. The analytic and numerical results agree within 5%.

Since we have highly divergent ($x \to 1$) terms of the form $1/(1-x)^2$ multiplying G(y,z), we found it necessary in our numerical work to calculate the dilog function and therefore G(y,z) very accurately, in order to see this cancelation. We used the routine "VAC4" developed by Chlouber and Samuel[13] to evaluate $Li_2(x)$ to 13 significant figures. This routine makes use of Padé type II approximants.

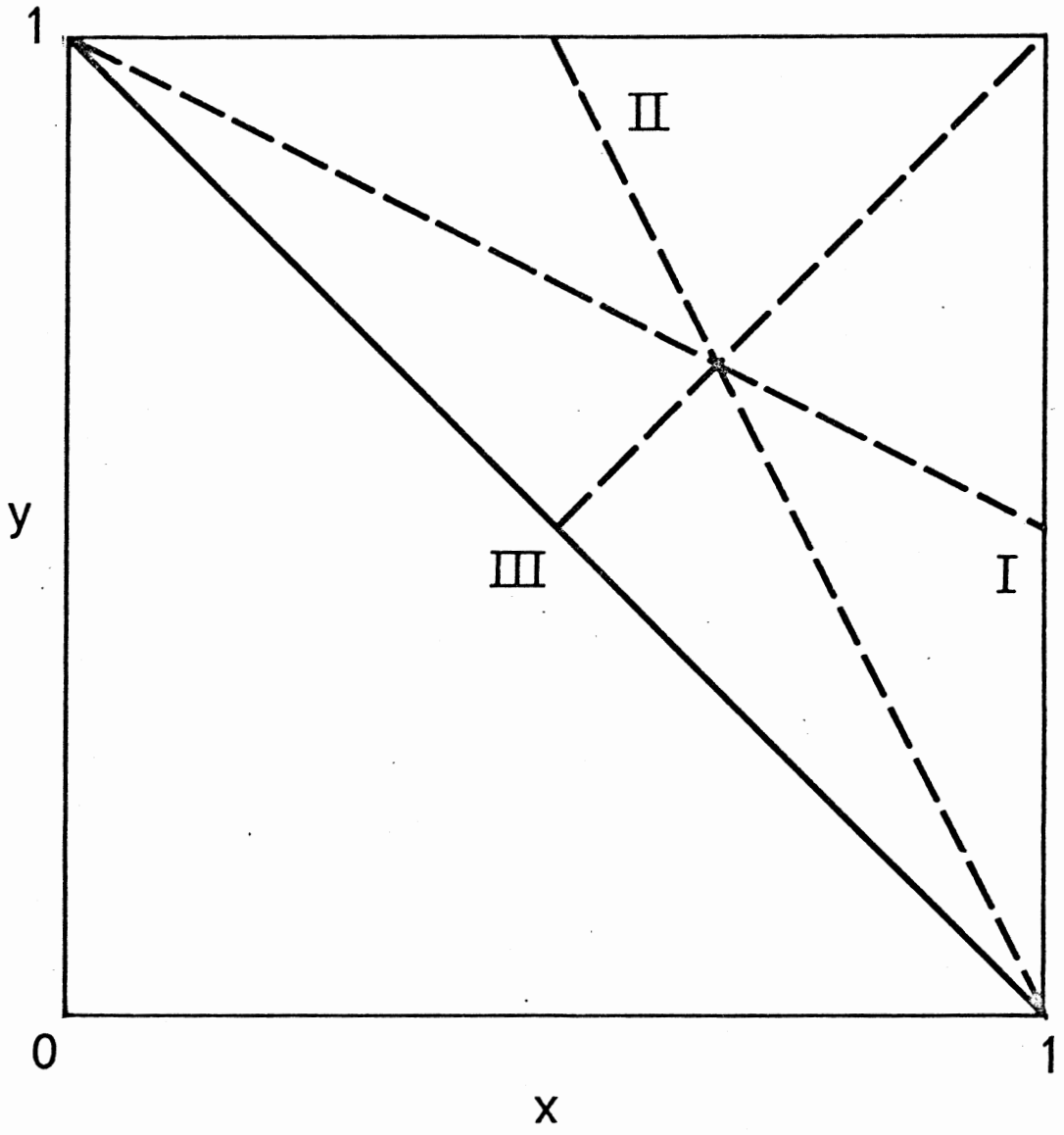

Figure 23. The Dalitz Triangle. The Range of x and y is Such That $0 \leq x, y \leq 1$ and $0 \leq x + y \leq 1$. The Dashed Lines Divides the Triangle Into Six Symmetric Regions. The Roman Numerals I, II and III Refer to the Three Edges Where x, y and $z \rightarrow 1$

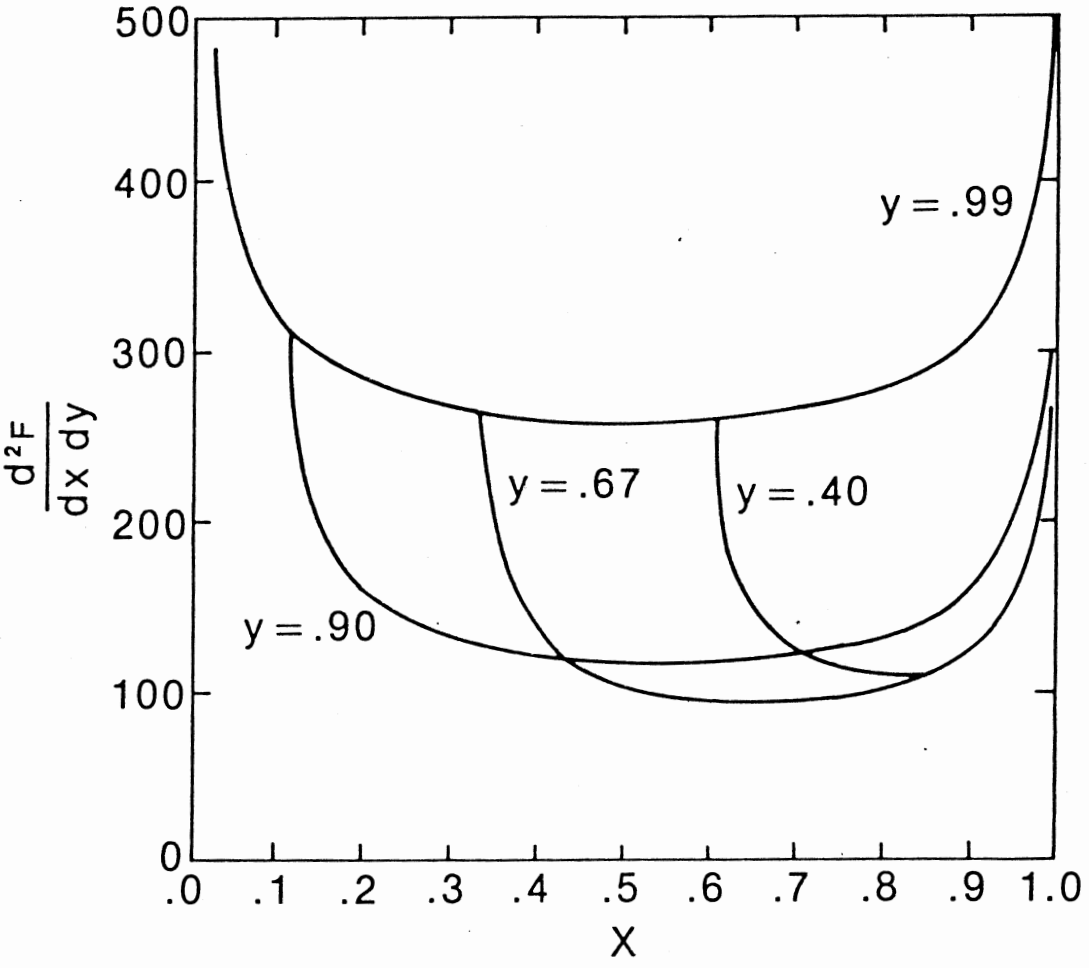

Figure 24. The Double Differential Decay Spectrum $d^2F/dxdy$, as a Function of x, for Several Values of y, in the Physical Region $1.01 \leq x + y \leq 1.98$

Though not necessary, we introduce a cut-off parameter ε in the standard manner[14] of treating 3-jet events in e^+e^- collisions. Experimental cuts will require that each gluon carry a minimum energy of $E \geq \varepsilon M_Z$ for some $0 < \varepsilon \leq \frac{1}{3}$. Following ref. 14 (see also ref. 5) we introduce this cut symmetrically and calculate

$$\frac{dF}{dx} = \int_{1-x+\varepsilon}^{1-\varepsilon} dy \, \frac{d^2F}{dxdy} \tag{7-30}$$

and

$$F(\varepsilon) = \int_{2\varepsilon}^{1-\varepsilon} dx \, \frac{dF}{dx} \, . \tag{7-31}$$

The upper limits guarantee that the opening angle θ between any two gluons satisfies $\sin \frac{\theta}{2} \geq \frac{2\sqrt{\varepsilon}}{1+\varepsilon}$.

In Figure 25 we show dF/dx for several values of ε. Clearly for $x = 2\varepsilon$, $dF/dx = 0$ due to vanishing phase space, and for $x \to 1$, dF/dx diverges like $\log^2(1-x)$. In Figure 26 we plot $F(\varepsilon)$. At $\varepsilon = \frac{1}{3}$, $F(\frac{1}{3}) = 0$, again due to vanishing phase space, and for $\varepsilon \to 0$, $F(\varepsilon)$ approaches a finite value, but with an infinite slope. Analytically one finds (see Appendix F) $F(\varepsilon) - F(0) = -128(1 + \xi(2) - 2\xi(3)\varepsilon \log^2\varepsilon \simeq -30\varepsilon \log^2\varepsilon$. We have therefore plotted $F(\varepsilon)$ as a function of $\varepsilon \log^2\varepsilon$ (see Figure 27). Clearly, as $\varepsilon \to 0$, $F(\varepsilon)$ approaches a straight line with slope $dF/d\varepsilon \simeq -30$ and intercept $F(0) \simeq 80$. We have used the Monte Carlo integration routine "VEGAS" developed by Lepage.[15]

The value of the constant multiplying $d^2F/dxdy$ in Eqn. (7-26) is 2.3×10^{-7} in the standard model with 3 quark doublets,[16] and, therefore, the branching ratio $\Gamma(Z^0 \to ggg)/\Gamma_0 = 1.8 \times 10^{-5}$. With 1.5×10^5 $q\bar{q}$ events per day, hence, we expect approximately 3 ggg events per day.

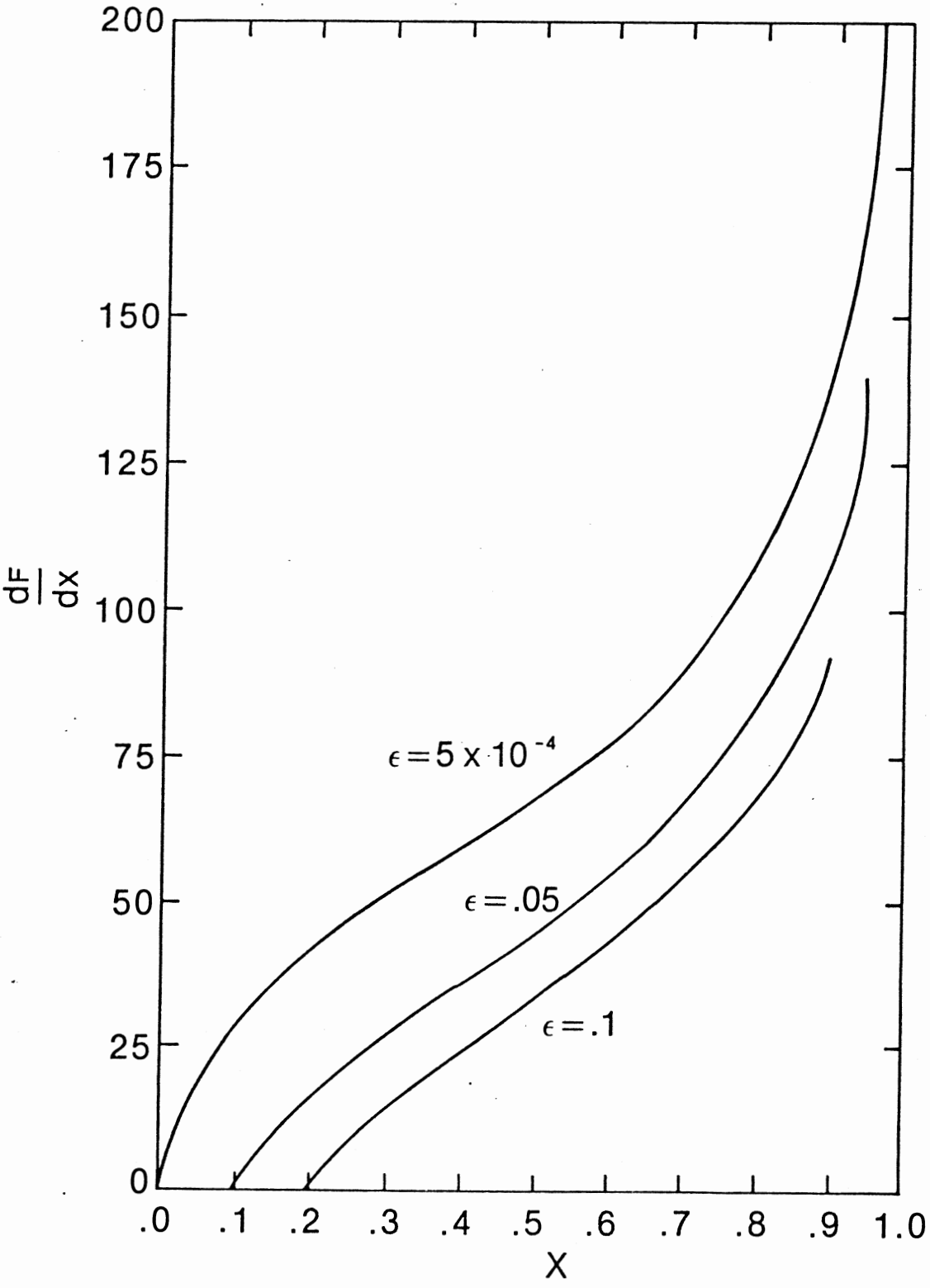

Figure 25. The Single Differential Decay Spectrum dF/dx, as a Function of x, for the Three Values of the Cut-off Parameter ε

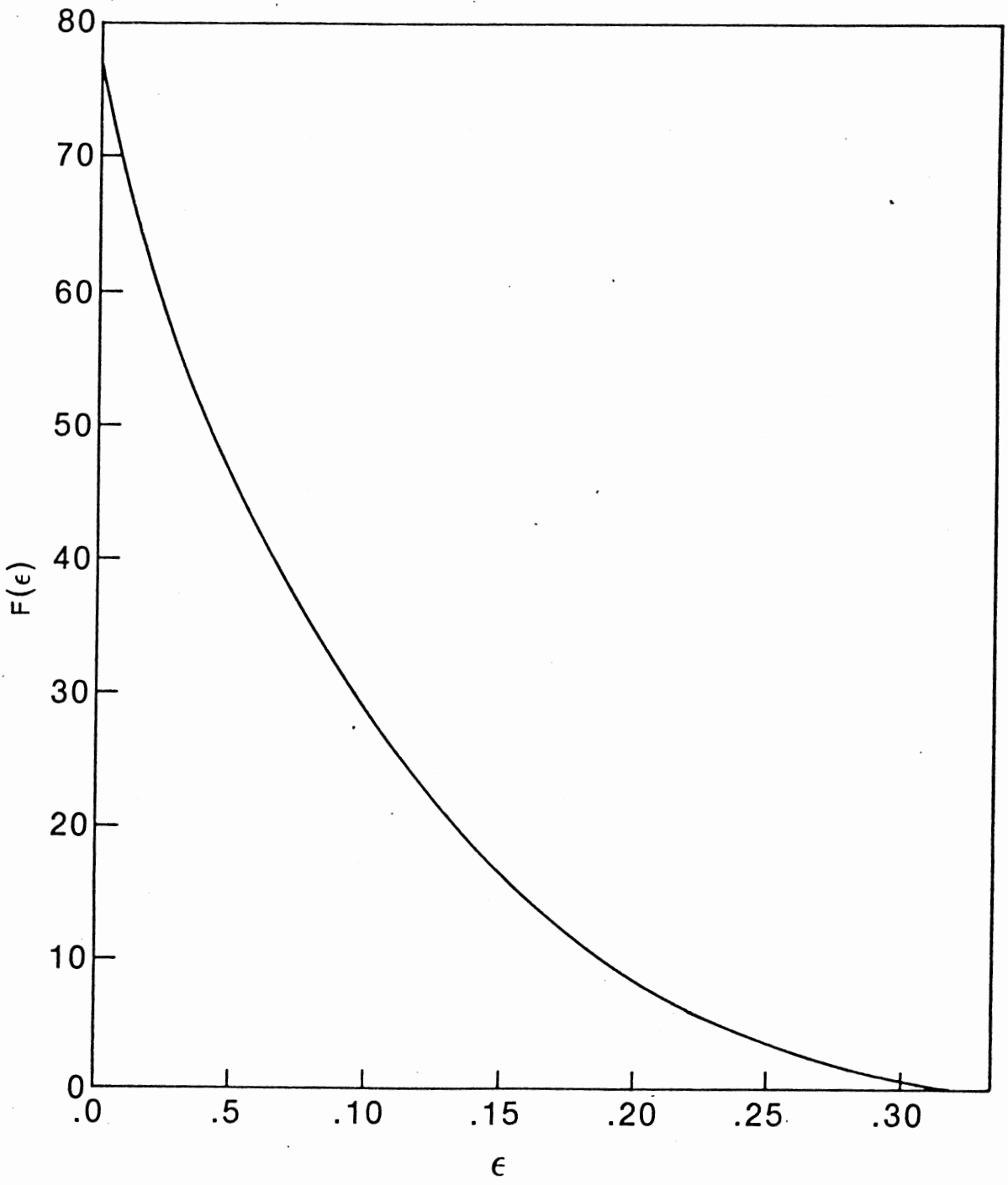

Figure 26. The Function $F(\varepsilon) = \int_{2\varepsilon}^{1-\varepsilon} dx \int_{1-x+\varepsilon}^{1-\varepsilon} dy\, d^2F/dxdy$. $F(\frac{1}{3})=0$ and $F(0) \simeq 80$

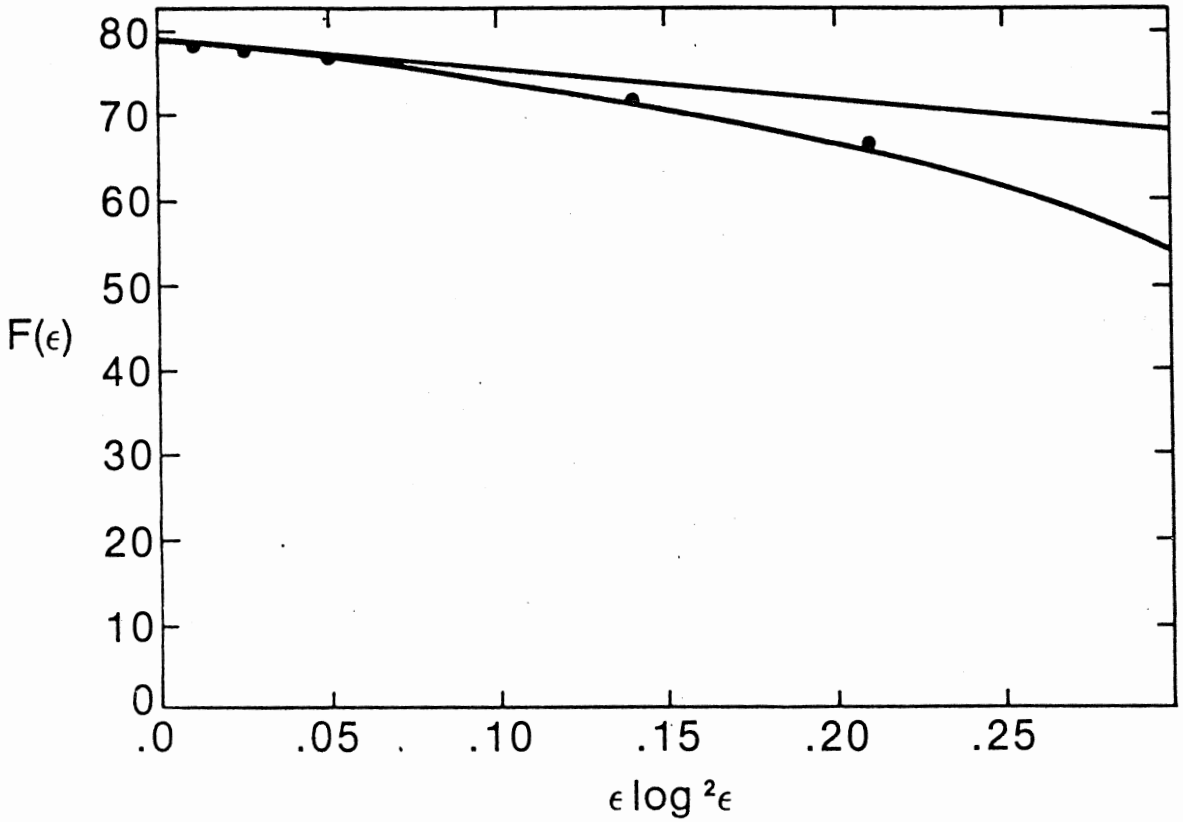

Figure 27. The Function $F(\varepsilon)$ Vs. $\varepsilon\log^2\varepsilon$ From $\varepsilon = 10^{-2}$ to $\varepsilon = 5\times10^{-4}$. It Approaches a Straight Line With Slope $dF/d\varepsilon \simeq -30$ and Intercept $F(o) \simeq 80$

For the $Z^o \to gg\gamma$ decay, we need only change the value of the constant multiplying $d^2F/dxdy$ in Eqn. (7-26). It becomes

$$\frac{1}{256}\left(\frac{\alpha_s}{\pi}\right)^2\left(\frac{\alpha}{\pi}\right)C^{gg\gamma}\ \frac{\left(\sum_i a_i q_i\right)^2}{\sum_i (a_i^2 + b_i^2)} \simeq 6.1 \times 10^{-8}$$

where q_i is the electric charge of quark i and the color factor $C^{gg\gamma} = \frac{1}{4}\sum_{a,b}\delta_{ab}\delta_{ab} = N^2-1 = 8$. We obtain a relatively large branching ratio $\Gamma(Z^o \to gg\gamma)/\Gamma_o = 4.9 \times 10^{-6}$, corresponding to one event per day. This is an interesting process because all three interactions, weak, strong and electromagnetic, are involved.

This process may be easier to handle experimentally, since we can detect the photon directly and accurately measure its energy, and the process is then only a quasi-two-jet event.

The $Z^o \to \gamma\gamma\gamma$ decay channel has a very small branching ratio as expected. The constant factor in Eqn. (8-26) becomes (N=3)

$$\frac{1}{256}\left(\frac{\alpha}{\pi}\right)^3\frac{4\left(3\sum_i a_i q_i^3 + \sum_{\text{leptons}} a_\ell q_\ell^3\right)^2}{\sum_i (a_i^2 + b_i^2)} \simeq 5.8 \times 10^{-11}$$

where we have included both quark loops and lepton loops. In addition, a third class of diagrams should be added in this case, namely W-loop diagrams which contribute coherently to the $Z^o \to \gamma\gamma\gamma$ amplitude. We have not calculated these diagrams, but we see no reason to suspect that W-loop contributions are much larger than fermion-loop contributions. They should be smaller. Our estimate, based on fermion-loops and including the statistical factor 1/3! is $\Gamma(Z^o \to \gamma\gamma\gamma)/\Gamma_o \simeq 7.7 \times 10^{-10}$.

Remarks

(a) With the flourishing of jet-physics, particularly in e^+e^- collisions, it is hoped that it will be possible to distinguish gluon jets from quark or antiquark jets.[17] Clearly, such distinction will be very helpful in separating the ggg from the more common $q\bar{q}g$ final state.

(b) We found earlier, that the decay $Z^o \to ggg$ is an infrared finite process, since $d^2F/dxdy$ behaves like $\log^2 z$ for $z \to 0$. Usually, infrared divergences come from terms like $1/z$, and they are related to the fact that the gluon is massless. In addition, the collinear divergences arise when $m_q \to 0$.

Let us first comment on the box diagrams. That these give an infrared finite answer follows from a general result proven by Yennie, Frautschi and Suura[18] for QED, that infrared logarithms come from external bremsstrahlung only, and not from inner bremsstrahlung. In particularly for four or more photons (gluons) attached to a closed fermion loop, we have a finite answer. This last statement follows, if we notice in the limit $k_4 \to 0$, the expressions for the box diagrams can be obtained by differentiating the lower order expressions (triangle) with respect to the loop momentum ℓ_ρ. We then have an integral of a perfect derivative, and the result is zero.

Explicitly, consider the derivative $\frac{\partial}{\partial \ell^\rho}$ of the two photon (gluon) expression:

$$\frac{\partial}{\partial \ell^\rho} \mathrm{Tr}[\gamma_\lambda (\not{\ell} - \not{k}_2 - m)^{-1} \gamma_\mu (\not{\ell} - m)^{-1} \gamma_\nu (\not{\ell} + \not{k}_3 - m)^{-1}] \ , \qquad (7\text{-}32)$$

Using

$$\frac{\partial}{\partial \ell^\rho} (\not{\ell}-m)^{-1} = -(\not{\ell}-m)^{-1}\gamma_\rho(\not{\ell}-m)^{-1} \tag{7-33}$$

we find three terms, one of which is

$$-\mathrm{Tr}[\gamma_\lambda(\not{\ell}-\not{k}_2-m)^{-1}\gamma_\mu(\not{\ell}-m)^{-1}\gamma_\nu(\not{\ell}+\not{k}_3-m)^{-1}\gamma_\rho(\not{\ell}+\not{k}_3-m)^{-1}] . \tag{7-34}$$

But this term is simply the corresponding expression for one of the box diagrams (VVVV) in the limit $k_4 \to 0$:

$$\mathrm{Tr}[\gamma_\lambda(\not{\ell}-\not{k}_2-m)^{-1}\gamma_\mu(\not{\ell}-m)^{-1}\gamma_\nu(\not{\ell}+\not{k}_3-m)^{-1}\gamma_\rho(\not{\ell}+\not{k}_3+\not{k}_4-m)^{-1}] . \tag{7-35}$$

The other two terms correspond to the remaining two box diagrams, and we obtain the statement above. Similarly this also applies to the AVVV box diagrams.

For the triangle diagrams, we also explicitly found an infrared finite answer (see Appendix B for details). However, in this case, we have external bremsstrahlung. We can use the Bloch-Nordsieck[19] formalism or, more generally, the Kinoshita-Lee-Nauenberg theorem,[20] which states that if we also include virtual corrections to the two-gluon process, the answer must be finite. Since this last process vanishes, the triangle diagrams are finite.

This is contrary to the $q\bar{q}g$ decay (Figure 28b), where we find an infrared divergence (the gluon attached to an external leg). However, by adding the contribution from the interference between the $q\bar{q}$ state (Figure 28a) and its virtual corrections (Figure 28c), a finite answer is obtained.

(c) It is interesting that the imaginary part of the amplitude for $Z^o \to ggg$ vanishes, but we can offer no physical explanation. However, we feel that it is connected with the absence of mass singularities in

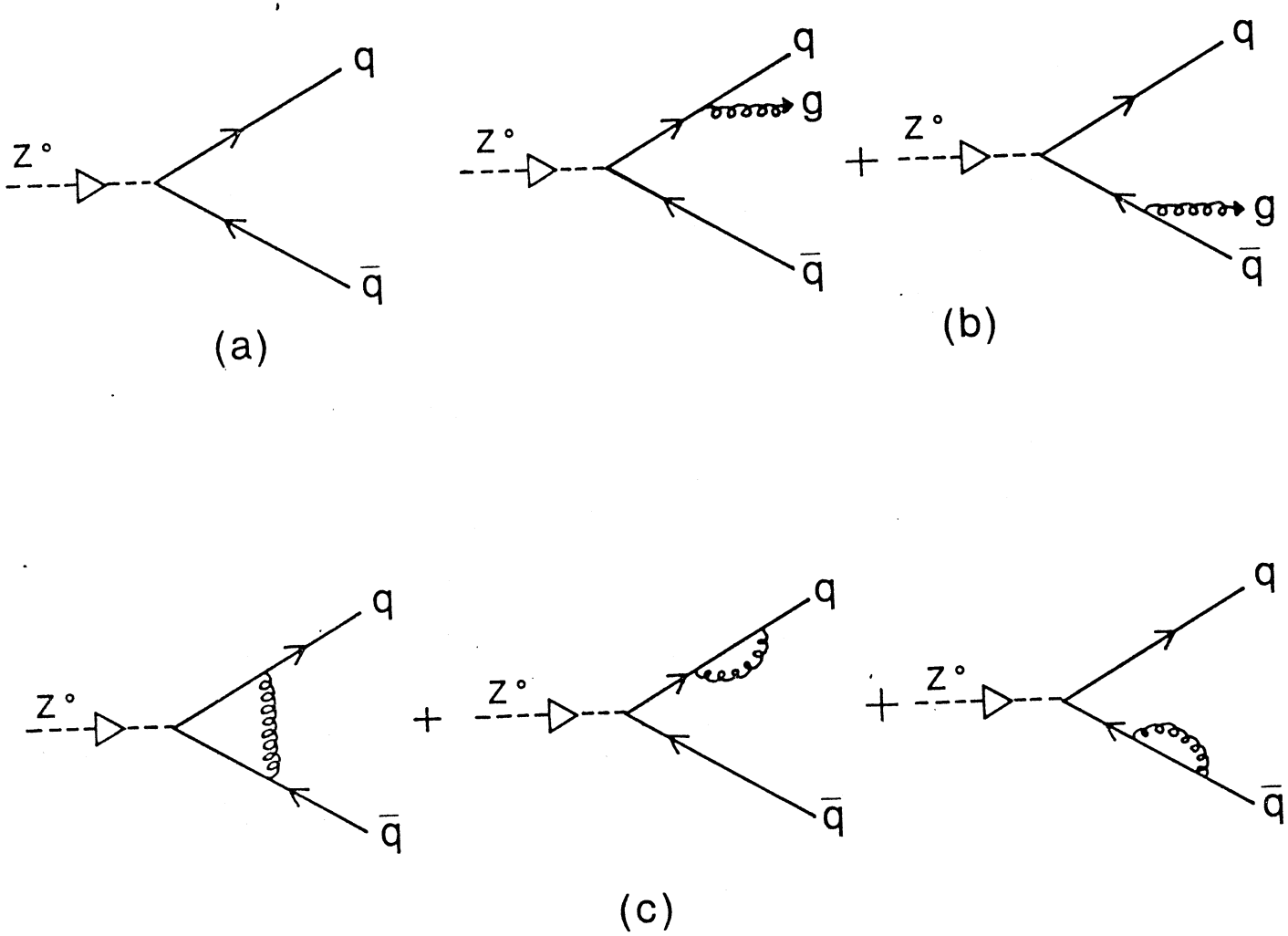

Figure 28. Feynman Diagrams for: (a) Lowest Order Decay $Z^{o} \rightarrow q\bar{q}$, (b) $Z^{o} \rightarrow q\bar{q}$ + Gluon Bremsstrahlung and (c) $Z^{o} \rightarrow q\bar{q}$ + Virtual Corrections

each amplitude. This conjecture is based on the relationship between mass divergences and imaginary parts of certain diagrams, as pointed out by Fabricius and Schmitt.[22]

Consider first the box-diagram with scalar particles. One finds, that in $n = 4-\varepsilon$ dimensions and with $m_q \to 0$, the amplitude $M(\varepsilon)$ is of the form:

$$M(\varepsilon) = \frac{\alpha}{\varepsilon^2} + \frac{\beta}{\varepsilon} + \gamma \tag{7-36}$$

and that the imaginary part

$$\text{Im } M(\varepsilon) = \frac{\pi}{2} \lim_{\varepsilon \to 0} \text{Re } M(\varepsilon) = \frac{\pi}{2} \{\frac{\text{Re}\alpha}{\varepsilon} + \text{Re}\beta\} \tag{7-37}$$

with Im $\alpha = 0$, Im $\beta = \frac{\pi}{2}$ Reα and Im$\gamma = \frac{\pi}{2}$ Reβ. The important point is that we are considering a decay process. Here the $1/\varepsilon^2$ term corresponds to a linear divergence, the $1/m_q$ and the $1/\varepsilon$ terms to a logarithmic divergence $\log m_q$. In our case, we also have a tensor structure, so that α, β and γ become tensors, however the form must still hold.

Since we have no mass singularities, we must have $\alpha=\beta=0$ and therefore Im $M(\varepsilon) = 0$ according to Eqn. (7-37).

(d) Finally, we point out that the pure 3-gluon state can also be produced in e^+e^- collisions through the decay of a virtual photon, even before the Z^o resonance is reached, and is, therefore, accessible in the energy region presently covered by PEP and PETRA.

Calculations on $e^+e^- \to ggg$ will be given in Chapter VIII.

REFERENCES

1. M. L. Perl, "e^+e^- Physics today and tomorrow", SLAC-PUB-2615, September 1980 (unpublished); C. H. Llewellyn Smith, "e^+e^- Physics beyond PETRA energies", LEP Summer Study/1-2, October, 1978.

2. B. Guberina, et al., Nucl. Phys. B174, 317 (1980).

3. H. P. Nilles, Phys. Rev. Lett. 45, 319 (1980); T. Rizzo, Phys. Rev. D22, 2213 (1980).

4. R. Cahn, M. S. Chanowitz and N. Fleishon, Phys. Lett. 82B, 113 (1979).

5. T. R. Grose and K. O. Mikaelian, Phys. Rev. D23, 123 (1981).

6. C. N. Yang, Phys. Rev. 77, 242 (1950).

7. V. Costantini, B. De Tollis and G. Pistoni, Nuovo Cim. 2A, 733 (1971); B. De Tollis Nuovo Cim. 32, 757 (1964); 35, 1182 (1965); R. Karplus and M. Neuman, Phys. Rev. 83, 776 (1951).

8. K. Fabricius et al., "Order α_s^2 Corrections to Jet Cross Sections in e^+e^- annihilation, DESY 80/91, September 1980 (unpublished); J. G. Körner, G. Schier holz and J. Willrodt, "QCD predictions for Four-jet Final states in e^+e^- annihilation," DESY 80/119, December, 1980; G. Schierholz, "Higher order QCD Corrections in e^+e^- annihilation into Hadrons", DESY 80/120, December, 1980.

9. F. E. Close, "An introduction to quarks and partons" (Academic Press, N.Y., 1979).

10. S. L. Adler,Phys. Rev. 177, 2426 (1969); J. S. Bell and R. Jackiw, Nuovo Cim. 60A, 47 (1969); L. Rosenberg, Phys. Rev. 129, 2786 (1963).

11. In going from the Pauli metric (ict) to the covariant metric, one uses the substitution rule $k_\mu \rightarrow ik_\mu$.

12. E. Byckling and K. Kajantie, "Particle Kinematics" (Wiley-Interscience, London, 1973).

13. C. Chlouber and M. A. Samuel, Comp. Phys. Comm. 15, 513 (1978).

14. J. Ellis, M. K. Gaillard and G. G. Ross, Nucl. Phys. B111, 253 (1976).

15. G. P. Lepage, "VEGAS", Jour. of Comp. Phys. 27, 192 (1978).

16. We use $\alpha_s = 4\pi/7 \log(M_Z^2/\Lambda^2) \simeq 17$ and $\sin^2\theta_w \simeq .23$.

17. E. G. Floratos, F. Hayot and A. Morel, Phys. Lett. 90B, 297 (1980); H. P. Nilles and K. H. Streng, Phys. Rev. D23 1944 (1981); S. J. Brodsky and J. F. Gunion, Phys. Rev. Letters 37, 402 (1976).

18. D. R. Yennie, S. C. Frautschi and H. Suura, Annals of Physics 13, 379 (1961).

19. F. Bloch and A. Nordsieck, Phys. Rev. 52, 54 (1937).

20. T. D. Lee and M. Nauenberg, Phys. Rev. 133, B1549 (1964); T. Kinoshita, J. Math. Phys. 3, 650 (1962).

21. R. D. Field, "Perturbative Quantum Chromodynamics and Applications to Large Momentum-Transfer Processes", NATO Advanced Study Institute on Quantum Flavordynamics, Quantum Chromodynamics, and Unified Theories, Boulder, Colorado 1979 (Plenum Press, N.Y. 1980).

22. K. Fabricius and I. Schmitt, Zeit. für Phys. C3, 51 (1979). J. G. Körner, et al., Phys. Lett. 94B, 207 (1980).

23. L. Lewin, "Dilogariths and Associated Functions", (MacDonald, London, 1958).

CHAPTER VIII

ELECTRON-POSITRON ANNIHILATION INTO THREE GLUONS

Introduction

The study of three-jet final states in electron-positron collisions has flourished both in experiment and in theory over the past several years.[1,2] Experiments[1] at PETRA reveal that three jets constitute a substantial fraction of hadronic events, which can be analyzed in terms of thrust, spherocity, etc. This is in accordance with theory[2] based on Quantum Chromodynamics, thus providing a firm basis for the existence of the gluon and, indeed, for QCD as a whole. To lowest order in QCD, the experimental results are interpreted to be electron-positron annihilation into a quark, an antiquark, and a gluon, all three particles then materializing as jets of hadrons. Energy and angular distributions have been examined in detail, and the above interpretation seems to be amply justified.

The only other three-jet final state accessible in e^+e^- annihilations is a state of three gluons. We have studied the reaction (in the continuum).

$$e^+ + e^- \rightarrow g + g + g$$

and present the results here. As a corollary, we also discuss

$$e^+ + e^- \rightarrow g + g + \gamma \ .$$

We study three gluon states as a test of higher-order perturbative QCD. The reaction proceeds via virtual quark loops, in particular, via the box diagram shown in Figure 29a. The triangle diagram, Figure 29b,

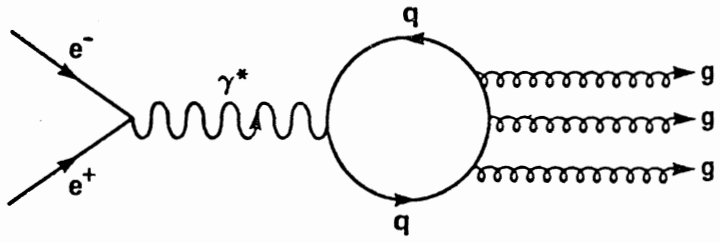

(a)

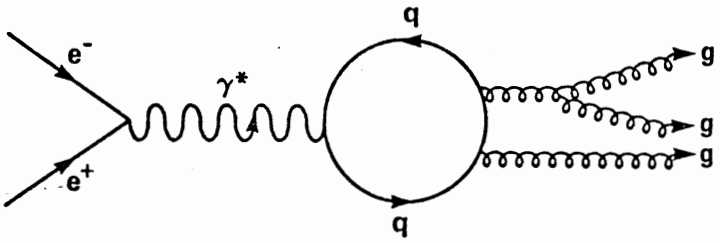

(b)

Figure 29. Feynman Diagrams for $e^+e^- \rightarrow ggg$. Permutations Must be Added. Only Box Diagrams (a) Contribute. Triangle Diagrams (b) Vanish by Charge Conjugation

vanishes, essentially because of charge conjugation symmetry. For the same reason, e^+e^- annihilation into two gluons is forbidden to lowest order, $e^+e^- \to \gamma^* \to gg$, but allowed in higher order, $e^+e^- \to \gamma^*\gamma^* \to gg$.

We should mention, of course, that the three gluon state ggg can also be produced, from the Quarkonia states J/ψ and Υ (Figure 30). However, even at the Υ resonance, the energy of the proposed gluon jets is still very low (about 3GeV/jet).

It is natural to compare ggg to $q\bar{q}g$, and we do so consistently throughout this chapter. Since $\sigma(ggg)/\sigma(q\bar{q}g) \sim (\frac{\alpha_s}{\pi})^2$, we expect very few ggg events at PEP and PETRA, though they are energetically accessible. We hope that the results presented here will encourage hunting for such events, which will require reliable identification of gluon jets[3,4] (for example by the fatness of the jets or their charge multiplicity). One might have to wait for a higher energy machine like LEP, not because of some intrinsic scale (there are no thresholds to be crossed), but because of the identification problem.

Here we consider the limit of massless quarks only. We use the work of Costantini et al.[5] on photon splitting, and the calculation is very similar to the decay $Z^o \to ggg$ (see Chapter VII).

Kinematics and $e^+e^- \to \gamma^* \to ggg$

The kinematics for $e^+e^- \to ggg$ and $q\bar{q}g$ being identical, we follow the conventions of Ellis et al.[6] The three final state gluons will lie in a plane, as indicated in Figure 31.

Let the $e^\mp$ momenta be denoted q_1 an q_2 respectively. In the "CM" frame we have $q_{10}=q_{20}=E = 1/2Q$ and $\bar{q}_1 = -\bar{q}_2$, E being the beam energy. It is convenient here to let the virtual photon γ^* have momentum $k_4 = (Q,\bar{o}) = (2\sqrt{|\mu_1|},\bar{o})$, while the three outgoing gluons have momenta k_i (i=1,2,3).

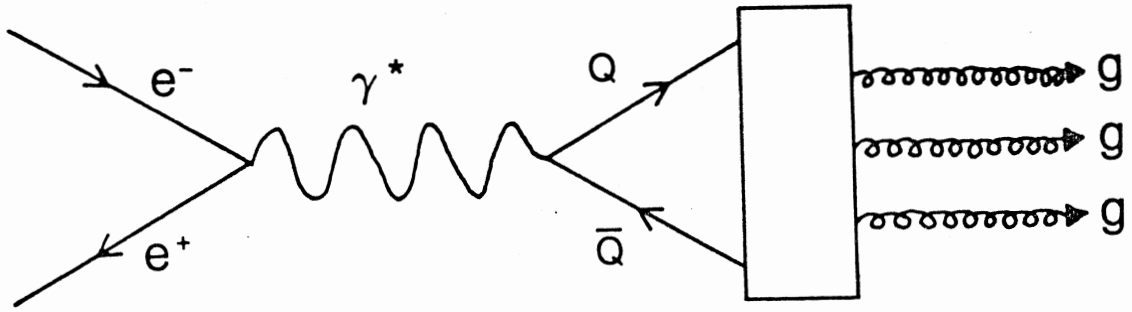

Figure 30. Formation of Quarkonia States in e^+e^- Annihilation and Its Decay Into Three Gluons

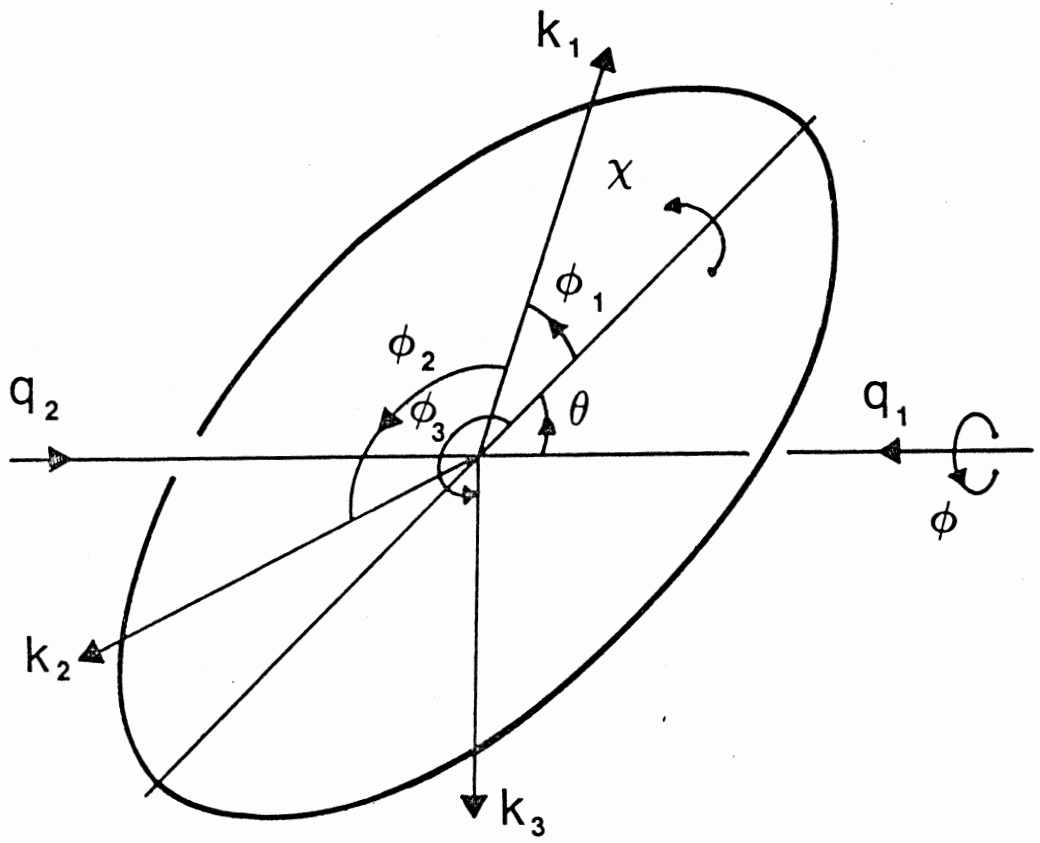

Figure 31. Kinematical Variables for Three-Jet Final States

This corresponds to the permutation (1234) → (4123) in the expression for G_μ (see Eqn. (7-9)).

Introducing scaling variables $x_i = \frac{E_i}{E} = \frac{2E_i}{Q}$ (i = 1,2,3), energy conservation is expressed as $x_1 + x_2 + x_3 = 2$, and the three scalar quanties $(r,s,t) = \frac{Q^2}{4}(1-x_1, 1-x_2, 1-x_3)$ (see Eqn. (8-7)).

Let θ denote the angle between the positron momentum q_2 and its projection in the plane containing the three final jets. In this plane ϕ_1, ϕ_2 and ϕ_3 are the angles between jets 1, 2 and 3 respectively and this projection axis, measured counterclockwise when seen along the direction of the positron, with $\phi_1 > \phi_2 > \phi_3$. The ϕ_i range between 0 and 2π, and θ between $-\pi/2$ and $+\pi/2$. The Euler angle χ denotes the angle between the projection axis and an arbitrary axis in the three-jet plane. Finally ϕ denotes the azimuth angle around the beam axis.

With these definitions we have (i = 1,2,3):

$$\bar{q}_1\cdot\bar{k}_i = -EE_i\cos\phi_i\cos\theta = -\frac{Q^2}{4}x_i\cos\phi_i\cos\theta$$

and

$$\bar{q}_2\cdot\bar{k}_i = -\bar{q}_1\cdot\bar{k}_i = \frac{Q^2}{4}x_i\cos\phi_i\cos\theta \qquad (8\text{-}1)$$

and for the angle $\phi_{ij} = \phi_i - \phi_j$ between any two of the three ϕ_i's:

$$\cos\phi_{ij} = \frac{\bar{k}_i\cdot\bar{k}_j}{|\bar{k}_i||\bar{k}_j|} = 1 - 2\frac{1-x_k}{x_i x_j}$$

and (8-2)

$$\sin\phi_{ij} = \frac{2e_{ij}}{x_i x_j}\{(1-x_i)(1-x_j)(1-x_k)\}^{1/2}$$

where $e_{ij} = \pm 1$ if $i \gtrless j$. We have assumed, of course, $m_q = 0$.

The differential cross section is

$$d\sigma = \frac{1}{2Q^2} \prod_{i=1}^{3} \frac{d^3\bar{k}_i}{(2\pi)^3 2E_i} (2\pi)^4 \delta(q_1+q_2 - k_1-k_2-k_3) |T|^2, \tag{8-3}$$

where the invariant matrix element squared

$$|T|^2 = 4\pi \alpha^2 \alpha_s^3 (\Sigma_i q_i)^2 C^{ggg} \sum_{\lambda_1\lambda_2\lambda_3} |M_{\lambda_1\lambda_2\lambda_3}|^2 \tag{8-4}$$

and

$$M_{\lambda_1\lambda_2\lambda_3} = \frac{1}{Q^2} \bar{V}(q_2)\gamma^\mu U(q_1) G_\mu^{(\lambda_1\lambda_2\lambda_3)}(4123) . \tag{8-5}$$

The hadronic tensor G_μ was described in the previous chapter. Here q_i is the electric charge of quark i in units of e. We have summed over colors as well as helicity states $(\lambda_1\lambda_2\lambda_3)$.

Averaging over $e^\pm$ polarizations we find for a given helicity state $(\lambda_1\lambda_2\lambda_3)$ (in the limit m_e=0):

$$\overline{|M_{\lambda_1\lambda_2\lambda_3}|^2} \equiv \frac{1}{4} \cdot \sum_{\text{spin}} |M_{\lambda_1\lambda_2\lambda_3}|^2 = \frac{1}{4Q^4} \mathrm{Tr}[\not{q}_1\gamma^{\mu_1}\not{q}_2\gamma^{\mu_2}] G_{\mu_1}^{(\lambda_1\lambda_2\lambda_3)} G_{\mu_2}^{(\lambda_1\lambda_2\lambda_3)}$$

$$= \frac{1}{Q^4} \{\frac{1}{2} Q^2 (\bar{G}^{(\lambda_1\lambda_2\lambda_3)})2 - 2(\bar{q}_1\cdot\bar{G}^{(\lambda_1\lambda_2\lambda_3)})2\}, \tag{8-6}$$

where we have used $G_o = 0$ (since $0 = (q_1+q_2)\cdot G = QG_o$ implies $G_o = 0$).

If we write

$$G_\mu^{(\lambda_1\lambda_2\lambda_3)}(4123) = G_{1\mu}^{(\lambda_1\lambda_2\lambda_3)}(4123) + G_{2\mu}^{(\lambda_1\lambda_2\lambda_3)}(4123), \tag{8-7}$$

with

$$G_{1\mu}^{(\lambda_1\lambda_2\lambda_3)}(4123) = \frac{-1}{\sqrt{32\Delta}}\,\xi_\mu^{(\lambda_1\lambda_2\lambda_3)}(4123)$$

and (8-8)

$$G_{2\mu}^{(\lambda_1\lambda_2\lambda_3)}(4123) = \frac{-1}{\sqrt{32\Delta}}\,E^{(2)}_{\lambda_1\lambda_2\lambda_3}(4123)\chi_\mu(4123)$$

we find using Eqn. (9-6)

$$\overline{|M_{\lambda_1\lambda_2\lambda_3}|^2} + \overline{|M_{-\lambda_1-\lambda_2-\lambda_3}|^2} =$$

$$\frac{1}{Q^4}\{Q^2[(\bar{G}_1^{(\lambda_1\lambda_2\lambda_3)})2 + (\bar{G}_2^{(\lambda_1\lambda_2\lambda_3)})2] - 4(\bar{q}_1\cdot\bar{G}_1^{(\lambda_1\lambda_2\lambda_3)})2$$

$$- 4(\bar{q}_2\cdot\bar{G}_2^{(\lambda_1\lambda_2\lambda_3)})^2\}\,. \qquad (8\text{-}9)$$

As expected, the cross-terms cancel out (no asymmetries). From Chapter VII, we know that only the helicitystates $(\lambda_1\lambda_2\lambda_3) = (\pm{+}{+})$ are independent, so let us concentrate on these in the following.

The $\bar{G}_1^2$, and $\bar{G}_2^2$ parts are known from the decay $Z^o \to ggg$: (see Eqns. (7-17) through (7-19):

$$A_{+++}(x_1,x_2,x_3) \equiv \frac{1}{8}(\bar{G}_1^{(+++)})^2 = \{x_2(1-x_2)(\hat{E}^{(1)}_{+++}(x_1,x_2,x_3))^2 + x_3(1-x_3)$$

$$\cdot(\hat{E}^{(1)}_{+++}(x_1,x_3,x_2))^2 - 2(1-x_2)(1-x_3)\hat{E}^{(1)}_{+++}(x_1,x_2,x_3)\hat{E}^{(1)}_{+++}(x_1,x_3,x_2)\}/x_1(1-x_1),$$

and (8-10)

$$B_{+++}(x_1,x_2,x_3) \equiv \frac{1}{8}(\bar{G}_2^{(+++)})^2 = [\hat{E}^{(2)}_{+++}(x_1,x_2,x_3)]^2, \qquad (8\text{-}11)$$

while for the corresponding (-++) state $A_{-++} = 0$ and $B_{-++} = 4$. Here (see Eqns. (7-28a) and (7-28b)):

$$\hat{E}^{(1)}_{+++}(x_1,x_2,x_3) = 2(1-x_3)/x_2 + [3 - 1/x_2 + 2(1-x_2)/(1-x_1) - 2(1-x_1)/x_2^2]\ell n(1-x_2) + (1-x_3)[1/x_3 + 2/(1-x_1)]\ell n(1-x_3) + \frac{1}{(1-x_1)}[x_2 - x_3 + 2(1-x_2)(1-x_3)/(1-x_1)]G(x_2,x_3) \tag{8-12a}$$

and

$$\hat{E}^{2}_{+++}(x_1,x_2,x_3) = [1 - 1/x_2 + 2(1-x_2)/(1-x_1)]\ell n(1-x_2) + [1-1/x_3 + 2(1-x_3)/(1-x_1)]\ell n(1-x_3) + \frac{1}{(1-x_1)}[x_1 + 2(1-x_2)(1-x_3)/(1-x_1)]G(x_2,x_3) \; . \tag{8-12b}$$

The function G is (Eqn. (7-29)):

$$G(x,y) = \ell n(1-x)\ \ell n(1-y) + Li_2(x) + Li_2(y) - \pi^2/6 \tag{8-13}$$

where $Li_2(x) = -\int_o^x \frac{dt}{t}\ell n(1-t)$.

Using Eqns. (7-10) and (7-11)

$$\bar{q}_1\cdot\bar{N}(4123) = \bar{q}_1\cdot\bar{k}_2 - \frac{(k_4\cdot k_2)}{(k_4\cdot k_1)}\bar{q}_1\cdot\bar{k}_1$$

$$= \frac{Q^2}{4}x_2[\cos\phi_2 - \cos\phi_1]\cos\theta \tag{8-14}$$

and

$$\bar{q}_1\cdot\bar{\chi}(4123) = q_{1i}\,\varepsilon_{i\nu\rho\sigma}\,k_4^{\nu}k_1^{\rho}k_2^{\sigma}$$

$$= -Q\,\bar{q}_1\cdot(\bar{k}_1 x \bar{k}_2) = \frac{Q^4}{8}\,x_1x_2\,\sin\phi_{21}\,\sin\theta \qquad (8\text{-}15)$$

we obtain

$$(\bar{q}_1\cdot\bar{G}_1^{(+++)})^2 = \frac{Q^2}{2}\,\frac{1}{(1-x_1)(1-x_2)(1-x_3)}\,\{[\cos\phi_2-\cos\phi_1]C_{+++}(x_1,x_2,x_3)$$

$$-\,[\cos\phi_3-\cos\phi_1]C_{+++}(x_1,x_3,x_2)\}^2\cos^2\theta \qquad (8\text{-}16)$$

with

$$C_{+++}(x_1,x_2,x_3) = x_2(1-x_2)\,\hat{E}^{(1)}_{+++}(x_1,x_2,x_3)\ . \qquad (8\text{-}17)$$

For the (-++) state $C_{-++} = 0$.

Finally

$$(\bar{q}_1\cdot\bar{G}_2^{(+++)})^2 = 2Q^2\,B_{+++}(x_1,x_2,x_3)\,\sin^2\theta \qquad (8\text{-}18)$$

Using Eqns. (8-16) and (8-18) for the four-fold differential cross section, (after a trivial integration over ϕ) can be written

$$\frac{d^4\sigma(e^+e^-\to ggg)}{d\chi d\sin\theta dx_1dx_2} = \left(\frac{\alpha}{8\pi}\right)^2\frac{\alpha_s^3}{Q^2}\,C^{ggg}\,\left(\sum_i q_i\right)^2\frac{d^4F}{d\chi d\sin\theta dx_1dx_2} \qquad (8\text{-}19)$$

where

$$\frac{d^4F}{d\chi d\sin\theta dx_1dx_2} \equiv \frac{Q^2}{4\pi}\,\sum_{\lambda_1\lambda_2\lambda_3}\overline{|M_{\lambda_1\lambda_2\lambda_3}|^2}$$

$$= \frac{2}{\pi}\,\{A_{+++}(x_1,x_2,x_3) + B_{+++}(x_1,x_2,x_3)\cos^2\theta$$

$$- \frac{1}{4(1-x_1)(1-x_2)(1-x_3)} \left[\cos\theta(\cos\phi_2 - \cos\phi_1)C_{+++}(x_1,x_2,x_3)\right.$$

$$- \cos\theta(\cos\phi_3 - \cos\phi_1)\, C_{+++}(x_1,x_3,x_2)\Big]^2$$

$$\left. + (1\leftrightarrow 2) + (1\leftrightarrow 3)\right\} + \frac{8}{\pi}\cos^2\theta. \qquad (8\text{-}20)$$

The function $d^4F/d\chi d\sin\theta\, dx_1 dx_2$ is defined, in such a way, that after integration over the angles χ and θ it becomes equal to the one used in the $Z^o \to ggg$ decay.

For the $q\bar{q}g$ result one has[2]:

$$\frac{d^4\sigma(e^+e^- \to q\bar{q}g)}{d\chi d\sin\theta dx_1 dx_2} = \frac{\alpha^2}{2\pi}\frac{\alpha_s}{Q^2}(\Sigma q_i)^2\left[x_1^2+x_2^2+\cos^2\theta(x_1^2\cos^2\phi_1+x_2^2\cos^2\phi_2)\right]$$

$$\times \quad (1-x_1)(1-x_2) \qquad (8\text{-}21)$$

The complete differential cross section in Eqn. (8-20), contains too many variables to be useful. We will integrate it step by step, beginning with the variable χ, until we get to the total cross section.

Using the integral

$$\int_o^{2\pi} \cos\phi_i \cos\phi_j \, d\chi = \pi \cos\phi_{ij}, \qquad (8\text{-}22)$$

and Eqn. (8-2) we obtain easily

$$\int_o^{2\pi}[\cos\phi_2-\cos\phi_1]^2 d\chi = 2\pi[1-\cos\phi_{21}] = 4\pi\frac{1-x_3}{x_1x_2}, \qquad (8\text{-}23a)$$

$$\int_o^{2\pi}[\cos\phi_3-\cos\phi_1]^2 d\chi = 2\pi[1-\cos\phi_{31}] = 4\pi\frac{1-x_2}{x_1x_3} \qquad (8\text{-}23b)$$

and

$$\int_o^{2\pi}[\cos\phi_2-\cos\phi_1][\cos\phi_3-\cos\phi_1]d\chi = \pi[\cos\phi_{32}-\cos\phi_{31}-\cos\phi_{21}+1]$$

$$= 2\pi\left[\frac{1-x_2}{x_1x_3} + \frac{1-x_3}{x_1x_2} - \frac{1-x_1}{x_2x_3}\right] . \qquad (8\text{-}23c)$$

Using Eqn. (8-20) and Eqns. (8-23a) through (8-23c), several simplifications take place, and the result can be written in the compact form:

$$\frac{d^3\sigma(e^+e^- \to ggg)}{d\sin\theta dx_1 ds_2} = \frac{\alpha^2\alpha_s^3}{(8\pi)^2Q^2} C^{ggg} (\Sigma q_i)^2 \frac{d^3F}{d\sin\theta dx_1 dx_2} \qquad (8\text{-}24)$$

with

$$\frac{d^3F}{d\sin\theta dx_1 dx_2} = 2\{(1+\sin^2\theta)A_{+++}(s_1,x_2,x_3) + 2\cos^2\theta\, B_{+++}(x_1,x_2,x_3)$$

$$+ (1\leftrightarrow 2) + (1\leftrightarrow 3)\} + 16\cos^2\theta \qquad (8\text{-}25)$$

For the $q\bar{q}g$ result we have[2]

$$\frac{d^3\sigma(e^+e^- \to q\bar{q}g}{d\sin\theta dx_1 dx_2} = \frac{\alpha^2\alpha_s}{2Q^2} (\Sigma q_i^2) \frac{(x_1^2 + x_2^2)}{(1-x_1)(1-x_2)} (2 + \cos^2\theta) \qquad (8\text{-}26)$$

In Figure 32, we plot the triple-differential cross section:

$$\frac{1}{\sigma_T(ggg)} \frac{d^3\sigma(e^+e^- \to ggg)}{d\sin\theta dx_1 dx_2} = \frac{1}{F(0)} \frac{d^3F}{d\sin\theta dx_1 dx_2}$$

as a function of $\sin\theta$ for $x_1 = x_2 = 0.9$.

We have normalized against the total cross section $\sigma_T(ggg)$, which we find below to be finite ($F(0) \simeq 80$).

The magnitude of the curve is different for other values of x_i, but the shape does not change much.

Integrating over θ we obtain the energy distributions of the final jets.

$$\frac{d^2\sigma(e^+e^- \to ggg)}{dx_1 dx_2} = \frac{\alpha^2\alpha_s^3}{(8\pi)^2Q^2} C^{ggg} (\Sigma q_i)^2 \frac{d^2F}{dx_1 dx_2} \qquad (8\text{-}27)$$

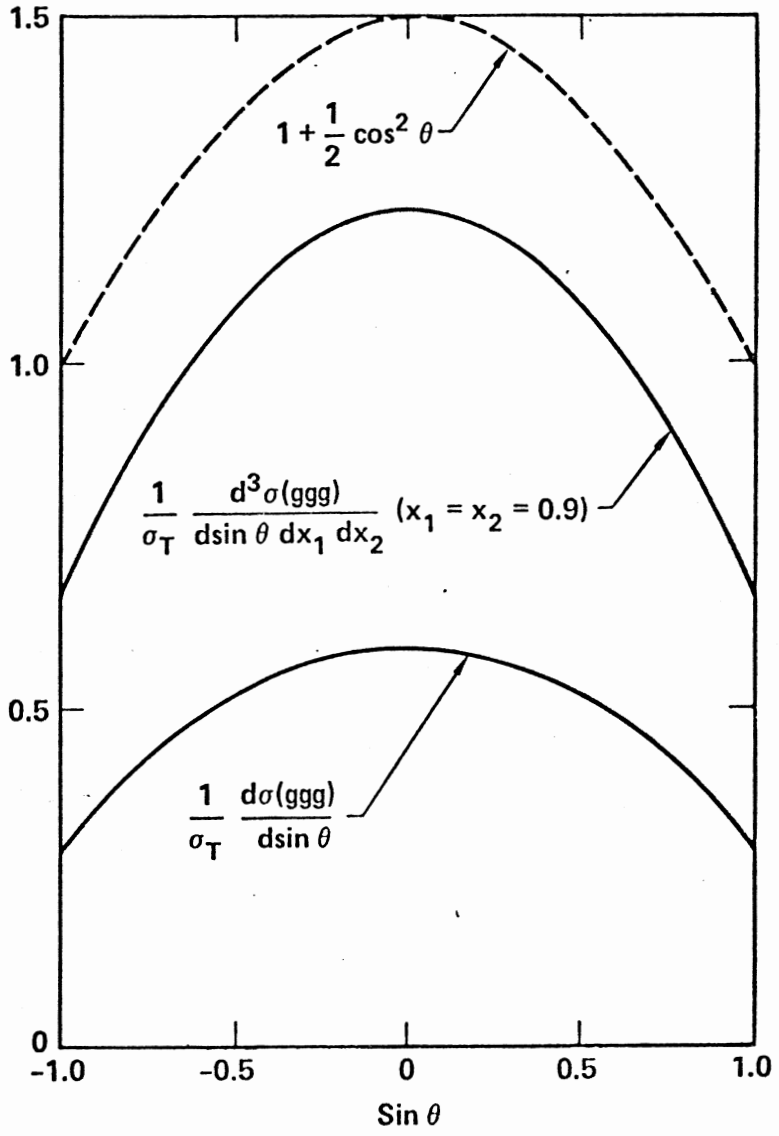

Figure 32. The Triple and Single Differential Angular Distributions for the Process $e^+e^- \rightarrow ggg$. The Dashed Curve is Included for Comparison With $e^+e^- \rightarrow qqg$

with

$$\frac{d^2F}{dx_1dx_2} = \frac{16}{3}\{A_{+++}(x_1,x_2,x_3) + B_{+++}(x_1,x_2,x_3) + (1\leftrightarrow 2) + (1\leftrightarrow 3)\} + \frac{64}{3} \tag{8-28}$$

and

$$\frac{d^2\sigma(e^+e^- \to q\bar{q}g)}{dx_1dx_2} = \frac{8\alpha^2}{3}\frac{\alpha_s}{Q^2}(\Sigma q_i^2)(x_1^2 + x_2^2)/(1-x_1)(1-x_2), \tag{8-29}$$

Comparing Eqns. (7-27), (8-10), (8-11) and (8-28), we see that d^2F/dx_1dx_2 is indeed equal to the corresponding one used in the $Z^o \to ggg$ decay.

In Figure 33, we show these energy distributions,

$$\frac{1}{\sigma_T}\frac{d^2\sigma(ggg)}{dx_1dx_2} \quad \text{and} \quad \frac{1}{10}\frac{x_1^2 + x_2^2}{(1-x_1)(1-x_2)}$$

as functions of x_1 for two values of x_2. Comparing the ggg distributions with those for $q\bar{q}g$, we see that they are substantially different, particularly around the region $x_1 + x_2 \simeq 1$, i.e., $x_3 \simeq 1$. In ggg we find an integrable $\log^2(1-x_i)$ divergence (for details see Appendix E) as any one of the $x_i \to 1$, while $q\bar{q}g$ diverges only when $x_1 \to 1$ and/or $x_2 \to 1$, and is non-integrable unless one introduces a cut-off, as discussed below. The same comments apply also to infrared divergences $x_i \to 0$: the ggg is integrable while $q\bar{q}g$ is not.[7] The absence of the $1/x_i$ infrared divergence in the reaction $e^+e^- \to ggg$ can be understood because there is no "bremsstrahlung" from external legs.

To obtain the angular distributions, as well as the total cross sections, we go back to Eqn. (8-20) and integrate over x_1 and x_2 after introducing a cut-off parameter ε, as was done by Ellis et al.[2]

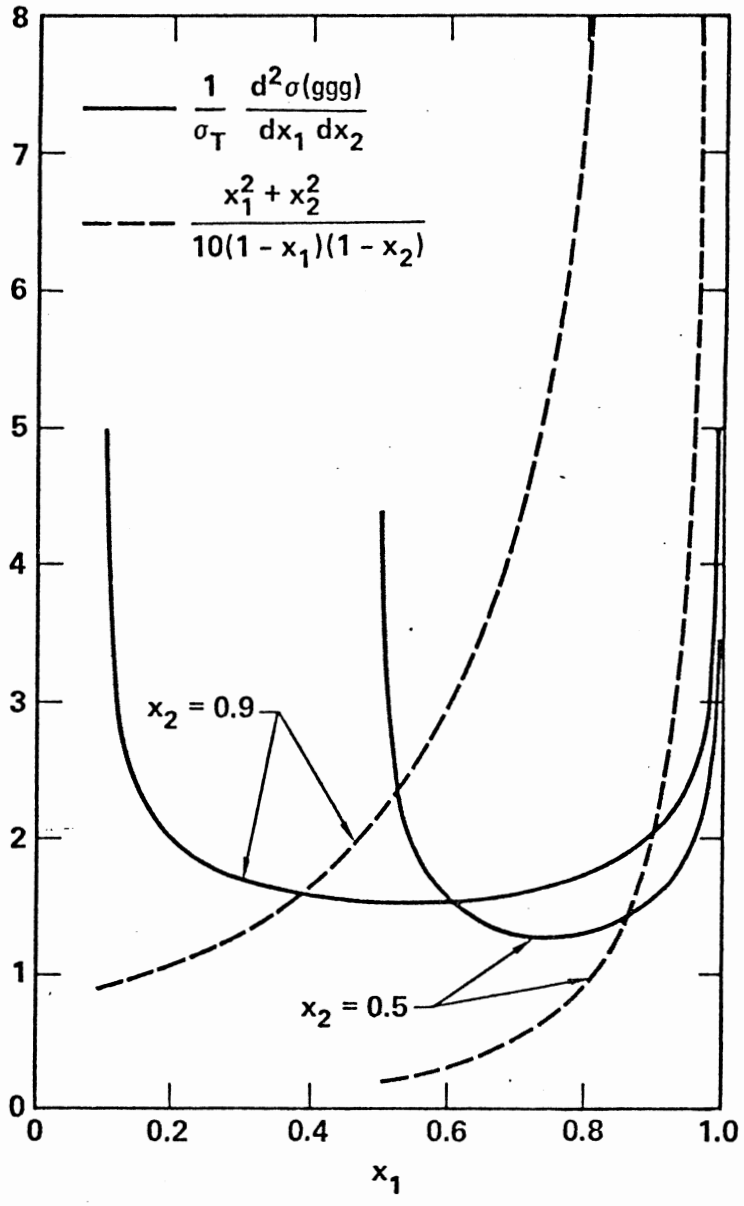

Figure 33. The Energy Distribution $\frac{1}{\sigma_T}\frac{d^2\sigma(ggg)}{dx_1 dx_2}$ as a Function of x_1 for $x_2 = 0.5$ and $x_2 = 0.9$ (Continuous Curves). The Dashed Curves are Included for Comparison With $e^+e^- \to q\bar{q}g$

$$\frac{1}{\sigma_T(\varepsilon)} \frac{d\sigma(ggg)}{d\sin\theta} = \frac{1}{F(\varepsilon)} \frac{dF(\varepsilon)}{d\sin\theta}$$

$$= \frac{3}{8}\left[\frac{F_1(\varepsilon) + 2F_2(\varepsilon)}{F(\varepsilon)}\right]\left[1 - \frac{2F_2(\varepsilon) - F_1(\varepsilon)}{2F_2(\varepsilon) + F_1(\varepsilon)} \sin^2\theta\right] \qquad (8\text{-}27)$$

where $F(\varepsilon) = F_1(\varepsilon) + F_2(\varepsilon)$,

$$F_1(\varepsilon) = \frac{16}{3} \int_{2\varepsilon}^{1-\varepsilon} dx_1 \int_{1-x_1+\varepsilon}^{1-\varepsilon} dx_2' \{A_{+++}(x_1,x_2,x_3) + (1\leftrightarrow 2)+(1\leftrightarrow 3)\} \qquad (8\text{-}28a)$$

and

$$F_2(\varepsilon) = \frac{16}{3} \int_{2\varepsilon}^{1-\varepsilon} dx_1 \int_{1-x_1+\varepsilon}^{1-\varepsilon} dx_2' \{B_{+++}(x_1,x_2,x_3) + (1\leftrightarrow 2)+(1\leftrightarrow 3)$$

$$+ B_{-++}(x_1,x_2,x_3)\} \qquad (8\text{-}28b)$$

We perform a two-dimensional numerical integration[8] and in Figure 34 we show $F_1(\varepsilon)$, $F_2(\varepsilon)$ as functions of ε. For $\varepsilon = 0$ we find $F_1(0) \simeq 33$, $F_2(0) \simeq 47$ and $F(0) \simeq 80$. Notice if $F_1 = F_2$ we would obtain an angular dependence $1 - \frac{1}{3}\sin^2\theta$, as in the $q\bar{q}g$ case or the decay $Q\bar{Q} \to ggg$. For $\varepsilon = 0$, we find an angular distribution $\frac{1}{\sigma_T} \frac{d\sigma(ggg)}{d\sin\theta} = 0.6\ \{1 - 0.48 \sin^2\theta\}$ which is shown in Figure 32. For $\varepsilon = 0.1$ and $\varepsilon = 0.05$, the angular dependences are $1 - 0.55 \sin^2\theta$ and $1 - 0.52 \sin^2\theta$, respectively. In the same Figure 32, we have shown the angular distribution $1 + \frac{1}{2}\cos^2\theta$ (equivalent to $1 - \frac{1}{3}\sin^2\theta$) for $q\bar{q}g$.

For the total cross sections, we find

$$\sigma_T(e^+e^- \to ggg) = \left(\frac{\alpha}{8\pi}\right)^2 \frac{\alpha_s^3}{Q^2} C^{ggg} \left(\sum_i q_i\right)^2 F(\varepsilon) \qquad (8\text{-}29)$$

and[9]

$$\sigma_T(e^+e^- \to q\bar{q}g) = \frac{16\alpha^2}{3} \frac{\alpha_s}{Q^2} \left(\sum_i q_i^2\right)\{\ell n^2\left(\frac{\varepsilon}{1-\varepsilon}\right)$$

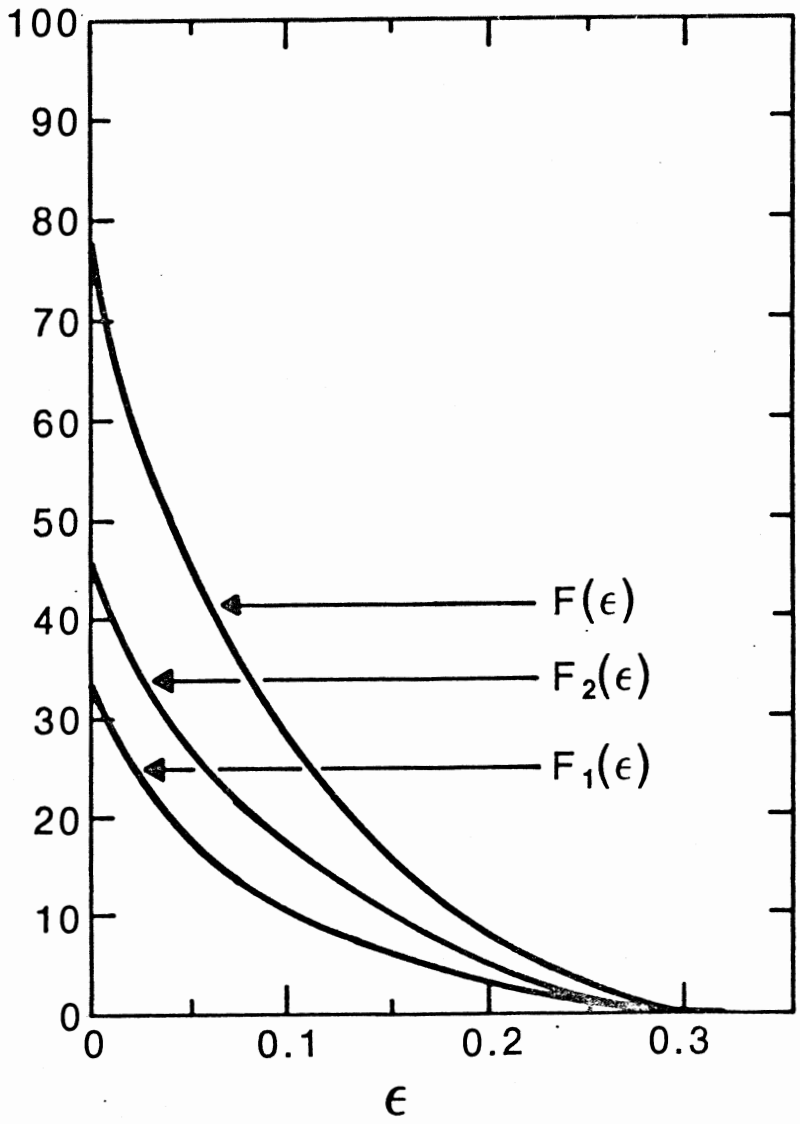

Figure 34. The Functions $F_1(\varepsilon)$, $F_2(\varepsilon)$ and $F(\varepsilon)$ Vs. ε. For $\varepsilon=0$, $F_1(0) \simeq 33$, $F_2(0) \simeq 47$ and $F(0) \simeq 80$

$$+ \frac{3}{2}(1-2\varepsilon)\ \ell n\left(\frac{\varepsilon}{1-2\varepsilon}\right) - \pi^2/6$$

and (8-30)

$$+ 1/4\ (5+3\varepsilon)(1-3\varepsilon) + 2Li_2\left(\frac{\varepsilon}{1-\varepsilon}\right)\}$$

which diverges like $\log^2\varepsilon$ for small ε.

Numerically $F(0) \simeq 80$, which, using $^{10}\alpha_s = 0.21$ at $Q^2 = 1600\ GeV^2$, gives $\sigma_T(e^+e^- \to ggg) \simeq 4.8 \times 10^{-38}\ cm^2$. In Figure 35, we plot the total cross sections for $e^+e^- \to ggg$ and $e^+e^- \to q\bar{q}g$, as functions of ε. From this figure we expect one ggg event for roughly every one or two thousand $q\bar{q}g$ events.

For the process $e^+e^- \to gg\gamma$, we need only replace the factor occurring in Eqn (9-29) by

$$\left(\frac{\alpha}{8\pi}\right)^2 \frac{\alpha\,\alpha_s^2}{Q^2} C^{gg\gamma} \left(\sum_i q_i^2\right)^2$$

where the color factor $C^{gg\gamma} = 8$. Hence the branching ratio $\sigma(gg\gamma)/\sigma(ggg) = 20\alpha/3\alpha_s \simeq 23\%$.

Note that the Feynman diagrams for this process, with the external photon radiated off the $e^{\pm}$, vanishes identically.

Remarks

(i) We find that all of our helicity amplitudes are real, even though we are above the $q\bar{q}$ threshold. The vanishing of the imaginary parts, true only in the limit $m_q/Q \to 0$, is connected with the absence of mass singularities[11], but we have no physical explanation. Of course, the box diagram does have imaginary parts in other channels like $\gamma\gamma \to gg$.

(ii) Eqn. (8-19) averages/sums over all helicities. The result for polarized colliding e^+e^- beams can be derived using the recipe of Bjorken,[13]

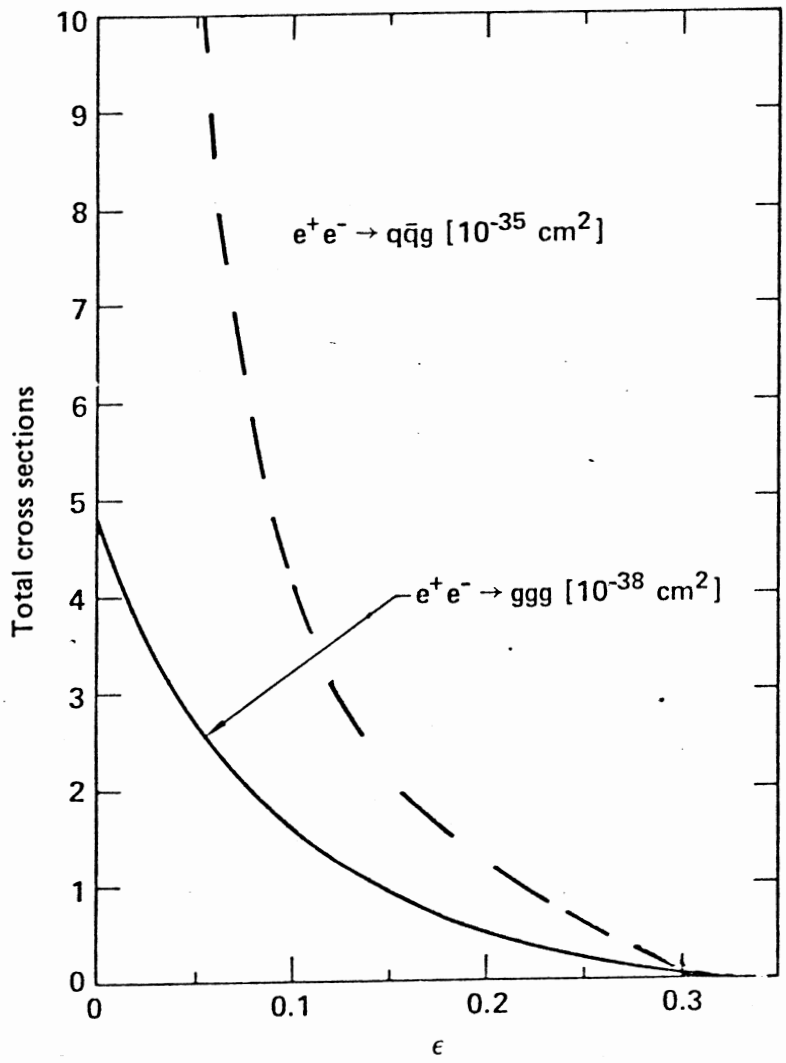

Figure 35. The Total Cross Sections for $e^+e^- \to ggg$ and $e^+e^- \to q\bar{q}g$ as Functions of the Cut-Off Parameter ε at $Q = 40$ GeV, Assuming Three Generations of "Massless" Quarks

as was done by Ellis et al.[2] for $q\bar{q}g$. Gluon helicities are a separate and non-trivial problem, to be studied elsewhere.[13]

(iii) Substantial enhancement in three-gluon final states is expected near $q\bar{q}$ resonances, since quarkonia, like ψ and Υ, decay predominantly into three gluons. The continuum contribution we have calculated is, of course, very interesting and important as a test of high-order QCD, but also very small. Identification of gluon jets will be necessary to separate the ggg state from the more common $q\bar{q}g$ events.

(iv) Other applications of the box diagram in QED like photon splitting or Delbrück scattering also have their analogs in QCD, when some of the photons are replaced by gluons: e.g., photon scattering and photon conversion into one or two gluons in the color field of a target. The calculations are fairly straightforward, but what is needed is a good experimental technique to separate them from the background.

REFERENCES

1. Reports by the MARK-J, PLUTO, TASSO and JADE collaborations in the "Proceedings of the International Symposium on Lepton and Photon Interactions at High Energies, T. B. W. Kirk and H. Abarbanel, Editors, 1979 (Batavia, Illinois). For a recent review see G. Wolf, DESY Preprint 80/85 (unpublished).

2. J. Ellis, M. K. Gaillard and G. G. Ross, Nucl. Phys. B111, 253 (1976); T. A. DeGrand, Y. J. Ng and S. H. H. Tye, Phys. Rev. D16, 3251 (1977); G. Sterman and S. Weinberg, Phys. Rev. Letters 39, 1436 (1977). For a recent review see T. F. Walsh, DESY Preprint 80/48 (unpublished).

3. H. P. Nilles and K. H. Streng, Phys. Rev. D23, 1944 (1981).

4. S. J. Brodsky and J. F. Gunion, Phys. Rev. Letters 37, 402 (1976); E. G. Floratos, F. Hayot and A. Morel, Phys. Lett. 90B, 297 (1980); H. P. Nilles, Phys. Rev. Letters 45, 319 (1980).

5. V. Costantini, B. De Tollis and G. Pistoni, Nuovo Cim. 2A, 733 (1971).

6. Ellis et al., Ref. 2 and erratum, Nuclear Physics B130, 516 (1977).

7. As $x_i \to 0$, $x_j \to 1$ and $x_k \to 1$, where i,j,k = 1,2 or 3.

8. It was necessary to calculate the Dilog functions very accurately because of delicate cancellations. We used the program "VAC4" developed by C. Chlouber and M. A. Samuel, Comp. Phys. Comm. 15, 513 (1978). For the two-dimensional integration over the phase space, we used the Monte Carlo program "VEGAS" developed by G. P. Lepage, Jour. of Comp. Phys. 27, 192 (1978).

9. The integrals are taken from the work of T. R. Grose and K. O. Mikaelian, Phys. Rev. D23, 123 (1981). Eqn. (9-30) is valid for arbitrary ε, $0 < \varepsilon \lesssim 1/3$. For small $\varepsilon \lesssim 0.01$ this result agrees with the expansion given by Ellis et al. in Ref. 2.

10. We have included the t quark in $\alpha_s = \dfrac{12\pi}{(33-2n_f)\log(\frac{Q^2}{\Lambda^2})}$ and set $n_f=6$, $\sum_i q_i = 1$, though our approximation $m_q \ll Q$ may fail for t quarks at $Q = 40$ GeV. $\Lambda = 0.5$ GeV.

11. K. Fabricius and I. Schmitt, Zeit. für Physik C3, 51 (1979).

12. J. D. Bjorken, Memo to SP-17 experimenters (1975); see also J. Ellis et al. in Ref. 2.

13. M. L. Laursen and M. A. Samuel, work in progress.

CHAPTER IX

SUMMARY AND CONCLUSIONS

In this work, we have analytically determined several higher-order corrections to the anomalous magnetic moment of the muon. We have also studied, within the framework of the standard Weinberg-Salam model and Quantum Chromodynamics three-gluon jets from the Z^{o} decay, as well as in $e^{+}e^{-}$ annihilation.

Chapter II was devoted to a review of lepton anomalous magnetic moments.

In Chapter III, we determined the $O(m_e/m_\mu)$ contribution to the sixth-order muon anomaly from proper fourth-order electron vacuum polarization insertion into the lowest-order muon vertex. Including the diagrams with improper fourth-order electron vac-pol. insertion we obtained:

$$\{-\frac{13}{18}\pi^3 - \frac{16}{9}\pi^2 \log 2 + \frac{383}{135}\pi^2\} \frac{m_e}{m_\mu}\left(\frac{\alpha}{\pi}\right)^3 = -6.56 \frac{m_e}{m_\mu}\left(\frac{\alpha}{\pi}\right)^3 .$$

We mentioned that this contribution could also be obtained for the order $\alpha^2(Z\alpha)$ vacuum polarization potential in muonic atoms. Interestingly, the result above contains a π^3 term. This is the first, and so far, the only place in QED where an odd power of π occurs.

In Chapter IV, we continued to determine the $O(\frac{m_e}{m_\mu})$ corrections from the second-order electron vacuum polarization insertion into the fourth-order muon vertex. This required knowledge of the full fourth-order muon anomaly with one heavy photon $K_\mu^{(4)}(b)$. From this, we extracted its

asymptotic expression in the limit where $b \to 0$. We also checked this numerically by constructing an integration subroutine for accurate evaluation of the trilog function. We found a contribution

$$\frac{\pi^2}{8} \left(\frac{m_e}{m_\mu}\right) \left(\frac{\alpha}{\pi}\right)^3 = 1.23 \frac{m_e}{m_\mu} \left(\frac{\alpha}{\pi}\right)^3 .$$

To summarize: the $O(\frac{m_e}{m_\mu})$ contribution from 18 of the 24 mass-dependent diagrams in sixth-order is:

$$-5.33 \frac{m_e}{m_\mu} \left(\frac{\alpha}{\pi}\right)^3 = -0.026 \left(\frac{\alpha}{\pi}\right)^3 = -0.29 \times 10^{-9}.$$

This corresponds to a 1.5% correction to the sum of the logarithmic and O(1) terms, which is $1.944 \left(\frac{\alpha}{\pi}\right)^3$.

To see if the $O(\frac{m_e}{m_\mu})$ terms and lower are really negligible in higher order, we calculated, analytically to O(1), the muon anomaly from the mass-dependent n-bubble diagram. Using the Borel transform technique, a recursion relation was establsihed to give the coefficients $b_{n,m}$ in

$$b_n = \sum_{m=o}^{n} b_{n,m} \log^m \left(\frac{m_e}{m_\mu}\right)$$

for arbitrary n. The exact anomaly a_n was evaluated numerically by Gaussian quadrature. Using the method of steepest descents, we found asymptotically for large n:

$$b_n \simeq \left(-\frac{2}{3}\right)^n n! e^{5/6} \left(\frac{m_e}{m_\mu}\right)$$

clearly leading to a breakdown in the "false expansion" since a_n is positive, while the true asymptotic limit c_n of a_n is

$$c_n \simeq \left(\frac{1}{6}\right)^n n!\, e^{-10/3} \left(\frac{m_\mu}{m_e}\right)^4 .$$

We compared a_n, b_n and c_n for two different mass ratios $\frac{m_\mu}{m_e} = 207$ (physical) and $\frac{m_\mu}{m_e} = 10$. Based on this, we found that, in the former case, the b_n would approximate a_n very well up to $n \lesssim 10$, while in the latter case this approximation would fail even for $n = 1$. Therefore even for moderately high mass ratios the calculation requires knowledge of $O(\frac{m_e}{m_\mu})$ and lower terms. We conclude, therefore, that the neglected terms are indeed large.

Chapter VI contained some topics in Gauge theories, such as gauge invariance of QED and QCD, the Weinberg-Salam model, the running coupling constant and the Renormalization Group equation.

In Chapter VII, we studied three-gluon jets from the Z^o decay. We argued and showed, by an explicit calculation of the VVA-triangle diagram, that the two-gluon decay of Z^o is forbidden. Next, we showed that the axial part (in the three-gluon case) cancels totally, within each doublet, in the limit $m_q/M_Z \to 0$, thus leaving us with only the pure vector part. It also eliminates the diagrams with triple-gluon couplings.

Starting from the exact expressions for photon splitting, we found, after performing an analytical continuation of the amplitudes, the double differential decay rate $d^2\Gamma/dxdy$. We extracted the analytical behavior $d^2\Gamma/dxdy \sim \log^2(1-x)$ and $\log^2 x$ for $x \to 1$ and $x \to 0$ respectively, leading to an infrared finite process, in accordance with the Kinoshita-Lee-Nauenberg theorem. This was also checked numerically using the "VAC4" subroutine to evaluate G(x,y) very accurately. The numerical integration was done using the program "VEGAS", and we found a branching-ratio

$$\frac{\Gamma(Z^o \to ggg)}{\sum_i \Gamma(Z^o \to q_i \bar{q}_i)} = 1.8 \times 10^{-5} .$$

Although the rate is small, with the proposed LEP machine, we expect approximately 3 events per day.

We found, surprisingly, that the imaginary part of the full amplitude vanishes in the limit $m_q/M_Z \to 0$.

This is related to the infrared finiteness of the process, but we are unable to give a physical explanation. A similar result was later obtained by Schierholtz et al. for the $O(\alpha_s)$ radiative corrections to $q\bar{q}g$ jets, and it would be very interesting to know if this result is also valid in higher order.

In Chapter VIII, we continued the jet analysis by considering $e^+e^- \to \gamma^* \to ggg$ in the continuum. We presented the four-fold differential cross section and integrated it step by step until we got to the total cross section $\sigma_T(ggg) = 4.8 \times 10^{-38}$ cm^2. This is very small indeed, and we expect only one event per one or two thousand $q\bar{q}g$ events. We found that the angular distribution $\frac{d\sigma}{d\sin\theta}$ has the form $1-0.48\sin^2\theta$ for $\varepsilon=0$, which should be compared with $1 - \frac{1}{3}\sin^2\theta$ for both the Υ-decay and $e^+e^- \to q\bar{q}g$.

Since the $q\bar{q}g$ rate is much higher than the ggg rate it is, of course, very important that we can distinguish between gluon and quark jets. Several papers in the literature are concerned with this question, and it is our hope that the experimentalist, with more statistics will be able to identify gluon and quark jets.

APPENDIXES

APPENDIX A

ASYMPTOTIC EXPANSION OF $K_\mu^{(4)}(b)$ AND $M_\mu^{(4)}(b)$ FOR $b \to 0$

Below we give some of the detailed steps leading to Eqn. (4-7). First we perform an analytical continuation of $K_\mu^{(4)}(b)$ and $M_\mu^{(4)}(b)$ for $b \leq 4$. If we write $\tau = \frac{b}{4}$, we can define $y = e^{i\phi}$, $-\pi < \phi < 0$ with

$$\phi = -2 \operatorname{Arccos} \sqrt{\tau} \ . \tag{A-1}$$

From Eqn. (A-1) follows

$$\log(1-y) = \log 2 + \frac{1}{2} \log(1-\tau) + \frac{i}{2} (\phi+\pi)$$

and (A-2)

$$\log(1+y) = \log 2 + \frac{1}{2} \log \tau + \frac{i}{2} \phi \ .$$

Using[6]

$$Li_2(e^{i\theta}) = GL_2(\theta) + iCL_2(\theta)$$

with

$$GL_2(\theta) = \frac{\pi^2}{6} - \frac{\pi}{2} |\theta| + \frac{1}{4} \theta^2$$

and (A-3)

$$CL_2(\theta) = \sum_{n=1}^{\infty} \frac{\sin(n\theta)}{n^2}$$

we find easily:

$$Li_2(y) = \frac{\pi^2}{6} - \frac{\pi}{2}|\phi| + \frac{1}{4}\phi^2 + iCL_2(\phi)$$

and (A-4)

$$Li_2(-y) = -\frac{\pi^2}{12} + \frac{\phi^2}{4} + iCL_2(\phi+\pi) \ .$$

Similarly, using

$$Li_3(e^{i\theta}) = iGL_3(\theta) + CL_3(\theta)$$

with

$$GL_3(\theta) = \frac{\pi^2}{6}\theta - \frac{\pi}{4}\theta|\theta| + \frac{\theta^3}{12}$$

and (A-5)

$$CL_3(\theta) = CL_3(O) - \int_o^{\theta} CL_2(\theta)\,d\theta$$

$$= \sum_{n=1}^{\infty} \frac{\cos(n\theta)}{n^3} \ ,$$

we find:

$$Li_3(y) = i\left[\frac{\pi^2}{6}\phi - \frac{\pi}{4}\phi|\phi| + \frac{\phi^3}{12}\right] + CL_3(\phi)$$

and (A-6)

$$Li_3(-y) = i\left[-\frac{\pi^2}{12}\ \phi + \frac{\phi^3}{12}\right] + CL_3(\phi+\pi)\ .$$

Using Eqns. (4-5), (A-1), (A-2), (A-4) and (A-6) we arrive at

$$D_p(\tau) = i\left[\phi \log 2 + \frac{\phi}{2}\ \log(1-\tau) + CL_2(\phi)\right]\ ,$$

$$D_m(\tau) = iCL_2(\phi+\pi)$$

and (A-7)

$$T(\tau) = -6CL_3(\phi) - 3CL_3(\phi+\pi) - 2\phi\ CL_2(\phi+\pi) - 4\phi\ CL_2(\phi)$$
$$+ \left(\frac{\pi^2}{2} - \frac{3\phi^2}{2}\right)\ \log 2 - \frac{\phi^2}{2}\ \log(1-\tau) + \frac{1}{4}(\pi^2-\phi^2)\ \log\tau\ .$$

Notice now, that D_m and D_p are purely imaginary while T is purely real. Eqn. (4-3) now reads ($b \leq 4$):

$$K_\mu^{(4)}(\tau) = -\frac{139}{144} + \frac{115}{18}\tau + \left[\frac{19}{12} - \frac{7}{9}\tau + \frac{23}{9}\tau^2 - \frac{1}{4}\ \frac{1}{1-\tau}\right]\log 4\tau$$

$$+ \left[\frac{2}{3} - \frac{127}{18}\tau + \frac{115}{9}\tau^2 - \frac{46}{9}\tau^3\right]\frac{\text{Arccos}\sqrt{\tau}}{\sqrt{\tau(1-\tau)}}$$

$$+ \left[\frac{9}{4} + \frac{5}{6}\tau - 8\tau^2 - \frac{1}{2\tau}\right]\ \zeta(2)$$

$$+ \frac{5}{6}\tau^2 \log^2 4\tau + \left[\tau - \frac{17}{3}\tau^2 + \frac{14\tau^3}{3}\right]\frac{\text{Arccos}\sqrt{\tau}}{\sqrt{\tau(1-\tau)}}\ \log 4\tau$$

$$- \left[\frac{19}{6} + \frac{53}{3}\tau - \frac{58}{3}\tau^2 - \frac{1}{3\tau} - \frac{2}{1-\tau}\right](\text{Arccos}\sqrt{\tau})^2 \qquad \text{(A-8)}$$

$$+ \left[-2\tau + \frac{34}{3}\tau^2 - \frac{28}{3}\tau^3\right]\ \frac{\text{Im } D_p(\tau)}{\sqrt{\tau(1-\tau)}}$$

$$+ \left[\frac{13}{12} - \frac{7}{6}\tau + \tau^2 - \frac{8}{3}\tau^3 + \frac{1}{4}\ \ \frac{1}{1-\tau}\right]\ \frac{\text{Im } D_m(\tau)}{\sqrt{\tau(1-\tau)}}$$

$$+ \left[\frac{1}{2} - \frac{14}{3}\tau + 8\tau^2\right] \quad \mathrm{Re}\ T(\tau), \tag{A-8}$$

while Eqn. (4-4) reads:

$$\begin{aligned} M_\mu^{(4)}(\tau) &= \frac{35}{36} + \frac{32}{9}\tau + \left[\frac{4}{3} - \frac{4}{9}\tau - \frac{40}{9}\tau^2\right] \log 4\tau \\ &+ \left[\frac{2}{3} - \frac{38}{9}\tau - \frac{32}{9}\tau^2 + \frac{20}{9}\tau^3\right] \frac{\mathrm{Arccos}\sqrt{\tau}}{\sqrt{\tau(1-\tau)}} \\ &+ \left[1 + \frac{4}{3}\tau - \frac{8}{3}\tau^2 - \frac{1}{2\tau}\right] \zeta(2) \\ &+ \left[-2 - \frac{8}{3}\tau + \frac{16}{3}\tau^2 + \frac{1}{3\tau}\right]\left[\mathrm{Arccos}\sqrt{\tau}\right]^2 \\ &+ \left[\frac{4}{3} - \frac{4}{3}\tau - \frac{16}{3}\tau^2 + \frac{16}{3}\tau^3\right] \frac{\mathrm{Im}\ D_m(b)}{\sqrt{\tau(1-\tau)}} \ . \end{aligned} \tag{A-9}$$

We now go to the limit $\tau \to 0$. We have

$$\phi = -\pi + 2\tau^{1/2} + \frac{\tau^{3/2}}{3} + O(\tau^{5/2}) \ . \tag{A-10}$$

By Taylor-series expansion of $CL_2(\phi)$ around $\phi = -\pi$, together with $\left.\frac{dCL_2(\phi)}{d\phi}\right|_{\phi=-\pi} = -\log 2$, we find

$$CL_2(\phi) = -2(\log 2)\tau^{1/2} + O(\tau) \ . \tag{A-11}$$

For $\theta \to 0$ we use the expansion[6]

$$CL_2(\theta) = \theta\left[1 - \log|\theta| + \frac{B_1 \cdot \theta^2}{2\cdot 3\cdot 2!} + \frac{B_2 \cdot \theta^4}{4\cdot 5\cdot 4!} + \cdots\right] \tag{A-12}$$

where $B_1 = 1/6$ and $B_2 = 1/32$ are the first and second Bernoulli Numbers.

From Eqns. (A-10) and (A-12) follows

$$CL_2(\phi+\pi) = 2\tau^{1/2} - \tau^{1/2} \log 4\tau - \frac{\tau^{3/2}}{6} \log 4\tau + \frac{\tau^{3/2}}{9} + O(\tau^2) \quad . \quad \text{(A-13)}$$

Finally using Eqns. (A-5), (A-11) and (A-12) we find

$$CL_3(\phi) = CL_3(-\pi) + O(\tau)$$

and (A-14)

$$CL_3(\phi+\pi) = CL_3(O) + \tau \log \tau + O(\tau) \quad .$$

From Eqns. (A-7) and (A-10) through (A-14) we arrive at

$$\text{Im } D_p(\tau) = -\pi \log 2 + O(\tau) \quad ,$$

$$\text{Im } D_m(\tau) = 2\tau^{1/2} - \tau^{1/2} \log 4\tau - \frac{\tau^{3/2}}{6} \log 4\tau + \frac{\tau^{3/2}}{9} + O(\tau^2) \quad \text{(A-15)}$$

$$\text{Re } T(\tau) = \frac{3}{2}\zeta(3) - \pi^2 \log 2 + \pi \left[4 - 6 \log 2 - \log \tau\right]\tau^{1/2} + O(\tau) \quad .$$

Use of Eqns. (A-7), (A-8), (A-10) and (A-15) now easily leads to

$$K_\mu^{(4)}(\tau) = K_\mu^{(4)}(o) - \frac{\pi}{4} \tau^{1/2} - 2\tau \log \tau + o(\tau)$$

and

$$M_\mu^{(4)}(\tau) = M_\mu^{(4)}(o) + \left[\frac{115}{27} - \frac{4\pi^2}{9}\right] \tau + O(\tau^{3/2}) \quad , \quad \text{(A-16)}$$

with $K_\mu^{(4)}(o)$ and $M_\mu^{(4)}(o)$ as in Eqns. (4-7) and (4-8), respectively.

APPENDIX B

CALCULATION OF THE VVA AMPLITUDE $S_{\lambda\mu\nu}(k_1,k_2)$

Using the well-known Feynman rules, one finds for the triangular fermion loop with two vector vertices and one axial vector vertex (VVA):

$$S_{\lambda\mu\nu}(k_1,k_2) = 2\int \frac{d^4\ell}{(2\pi)^4} \frac{\mathrm{Tr}[\gamma_5\gamma_\lambda(\not{\ell}-\not{k}_1+m)\gamma_\mu(\not{\ell}+m)\gamma_\nu(\not{\ell}+\not{k}_2+m)]}{[(\ell-k_1)^2-m^2][\ell^2-m^2][(\ell+k_2)^2-m^2]} \cdot \quad \text{(B-1)}$$

The factor two, in front of the Feynman integral, comes from the fact that both diagrams (Figure 21) contribute equally. Needless to say, the VVV-part vanishes due to charge conjugation conservation.

To do the integral, we shall use the standard technique of Feynman parametrization. The three terms in the denominator are combined via the following triple integral:

$$\frac{1}{a_1a_2a_3} = 2!\int d\alpha_1 d\alpha_2 d\alpha_3\ \delta(1-\alpha_1-\alpha_2-\alpha_3)[a_1\alpha_1+a_2\alpha_2+a_3\alpha_3]^{-3}. \quad \text{(B-2)}$$

The integration is over the 3-dimensional hypercube.

We obtain easily:

$$a_1\alpha_1 + a_2\alpha_2 + a_3\alpha_3 = \alpha_1[(\ell-k_1)^2-m^2] + \alpha_2[(\ell+k_2)^2-m^2] + \alpha_3[\ell^2-m^2]$$

$$= (\ell-\ell_o)^2 + D(k_1,k_2)\ .$$

with

$$\ell_o = \alpha_1 k_1 - \alpha_2 k_2 \tag{B-3}$$

and

$$D(k_1,k_2) = \alpha_1\alpha_2(k_1+k_2)^2 + \alpha_1\alpha_3 k_1^2 + \alpha_2\alpha_3 k_2^2 - m^2 .$$

Next we would like to shift the variable $\ell \to \ell+\ell_o$, but simple power counting, reveals that the integral contains a linearly divergent part, so that shifting this variable is in fact illegal. However, it is sufficient here to know only the "leading" terms, i.e. terms of the form:

$$\varepsilon_{\lambda\mu\alpha\beta}\, k_1^{\alpha} k_2^{\beta}\, k_{2\nu} . \tag{B-4}$$

They are all finite and the only ones unambiguously defined. For these terms, the shift $\ell \to \ell+\ell_o$ is permitted.

The correct tensor is then determined by the requirement of gauge invaraince (vector current conservation):

$$k_1^{\mu}\, S_{\lambda\mu\nu}(k_1,k_2) = k_2^{\nu}\, S_{\lambda\mu\nu}(k_1,k_2) = 0 . \tag{B-5}$$

This method, equivalent to any regularization scheme, determines the finite "subleading" terms uniquely. It was introduced by Karplus and Neumann[7] in their first calculation of light by light-scattering.

Performing the trace in Eqn. (B-1) and integrating over ℓ, we obtain for the "leading" part of the tensor:

$$\hat{S}_{\lambda\mu\nu}(k_1,k_2) = -\frac{1}{\pi^2}\int d\alpha_1 d\alpha_2 d\alpha_3\ \delta(1-\alpha_1-\alpha_2-\alpha_3)\ \frac{\hat{N}_{\lambda\mu\nu}}{D(k_1,k_2)}$$

with

$$\hat{N}_{\lambda\mu\nu} = \alpha_1(1-\alpha_1)\ \varepsilon_{\lambda\nu\alpha\beta}\ k_1^{\alpha}k_2^{\beta}k_{1\mu} - \alpha_2(1-\alpha_2)\varepsilon_{\lambda\mu\alpha\beta}k_1^{\alpha}k_2^{\beta}k_{2\nu}$$

$$- \alpha_1\alpha_2\{\varepsilon_{\lambda\mu\alpha\beta}\ k_{1\nu} - \varepsilon_{\lambda\nu\alpha\beta}\ k_{2\mu}\}k_1^{\alpha}k_2^{\beta} \qquad \text{(B-6)}$$

Now writing the correct tensor (C_1 and C_2 constants):

$$N_{\lambda\mu\nu} = \hat{N}_{\lambda\mu\nu} + C_1\ \varepsilon_{\lambda\mu\nu\alpha}\ k_1^{\alpha} + C_2\ \varepsilon_{\lambda\mu\nu\alpha}\ k_2^{\alpha} \qquad \text{(B-7)}$$

and imposing gauge invariance we obtain:

$$N_{\lambda\mu\nu} = \{\alpha_1(1-\alpha_1)k_1^2+\alpha_1\alpha_2k_1\cdot k_2\}\varepsilon_{\eta\mu\nu\alpha}k_2^{\alpha} - \{\alpha_2(1-\alpha_2)k_2^2+\alpha_1\alpha_2k_1\cdot k_2\}\varepsilon_{\lambda\mu\nu\alpha}k_1^{\alpha}$$

$$+ \alpha_1(1-\alpha_1)\varepsilon_{\lambda\nu\alpha\beta}k_1^{\alpha}k_2^{\beta}\ k_{1\mu} - \alpha_2(1-\alpha_2)\varepsilon_{\lambda\mu\alpha\beta}\ k_1^{\alpha}k_2^{\beta}\ k_{2\nu}$$

$$- \alpha_1\alpha_2\{\varepsilon_{\lambda\mu\alpha\beta}\ k_{1\nu} - \varepsilon_{\lambda\nu\alpha\beta}\ k_{2\mu}\}k_1^{\alpha}k_2^{\beta}. \qquad \text{(B-8)}$$

Finally, using the identity:

$$g_{af}\ \varepsilon_{bcde} + g_{bf}\ \varepsilon_{cdea} + g_{cf}\ \varepsilon_{deab} + g_{df}\ \varepsilon_{eabc} + g_{ef}\ \varepsilon_{abcd} = 0, \qquad \text{(B-9)}$$

and, also defining the integrals $J_{rst}(k_1,k_2)$:

$$J_{rst}(k_1,k_2) = -\frac{1}{\pi^2}\int d\alpha_1 d\alpha_2 d\alpha_3\ \delta(1-\alpha_1-\alpha_2-\alpha_3)$$

$$\times\ \frac{\alpha_1^r\ \alpha_2^s\ \alpha_3^t}{[\alpha_1\alpha_2(k_1+k_2)^2 + \alpha_1\alpha_3 R_1^2 + \alpha_2\alpha_3 k_2^2 - m_q^2]} \qquad \text{(B-10)}$$

we arrive at:

$$S_{\lambda\mu\nu}(k_1,k_2) = J_{110}(k_1,k_2)\varepsilon_{\mu\nu\alpha\beta}\, k_1^{\alpha}k_2^{\beta}(k_1+k_2)_{\lambda}$$

$$+ J_{101}(k_1,k_2)\{{}^{3}_{\lambda\nu\alpha\beta}k_1^{\alpha}k_2^{\beta}k_{1\mu} + k_1^2\,\varepsilon_{\lambda\mu\nu\alpha}\,k_2^{\alpha}\}$$

$$- J_{011}(k_1,k_2)\{\varepsilon_{\lambda\mu\alpha\beta}k_1^{\alpha}k_2^{\beta}k_{2\nu} + k_2^2\,\varepsilon_{\lambda\mu\nu\alpha}\,k_1^{\alpha}\}. \quad \text{(B-11)}$$

We notice, that even for real gluons ($k_1^2 = k_2^2 = 0$), the axial current is not conserved

$$(k_1+k_2)^{\lambda}\, S_{\lambda\mu\nu}(k_1,k_2) = J_{110}(k_1,k_2)\;\varepsilon_{\mu\nu\alpha\beta}\,k_1^{\alpha}k_2^{\beta}(k_1+k_2)^2 \neq 0, \quad \text{(B-12)}$$

which is the famous result on triangle anomalies.[10]

As a consequence of Eqn. (B-11), we show that the triangle diagrams (Figure 22b) are infrared finite, and free of mass singularities.

The amplitude is proportional to the two-gluon amplitude $S_{\lambda\mu\nu}(k_1,k_2)$ with one real gluon (say $k_1^2 = 0$) and one virtual gluon, and the triple gluon coupling $\Gamma_{p\sigma}{}^{\nu}(k_3,k_4)$:

$$M \;\alpha\; \frac{1}{k_2^2}\, S_{\lambda\mu\nu}(k_1,k_2)\Gamma_{p\sigma}{}^{\nu}(k_3,k_4)\;\varepsilon^{\lambda}\varepsilon_1^{\mu}\varepsilon_3^{p}\varepsilon_4^{\sigma}\,. \quad \text{(B-13)}$$

Here $k_2 = k_3 + k_4$ is the momentum of the virtual gluon, which splits into two real gluons with momenta k_3 and k_4 respectively. The triple gluon coupling is:

$$\Gamma^{\nu}_{p\sigma}(k_3,k_4) = -\,(2k_3+k_4)_{\sigma}\,g_p^{\nu} + (k_3-k_4)^{\nu}g_{p\sigma} + (k_3+2k_4)_p\,g_{\sigma}{}^{\nu}. \quad \text{(B-14)}$$

Now using $k_1^2 = 0$, $k_1\cdot\varepsilon_1 = 0$, $(k_1+k_2)\cdot\varepsilon = 0$, and also current con-

servation $k_{2\nu}\Gamma_{p\sigma}{}^{\nu}(k_3,k_4) = 0$, we obtain

$$M\ \alpha\ - J_{011}(k_1,k_2)\varepsilon_{\lambda\mu\nu\alpha}k_1^{\alpha}\ \Gamma_{p\sigma}{}^{\nu}(k_3,k_4)\ . \tag{B-15}$$

Notice that the term $1/k_2^2$ has cancelled away, suggesting infrared finiteness.

Consider now the limit where $k_4 \to 0$, and using $k_3\cdot\varepsilon_3 = k_4\cdot\varepsilon_4 = 0$ we arrive at

$$M\ \alpha\ J_{011}(k_1,k_4)\varepsilon_{\lambda\mu\nu\alpha}k_1^{\alpha}\ \{2k_{3\sigma}\ g_p^{\nu} + k_3^{\nu}g_{p\sigma}\} \tag{B-16}$$

with

$$J_{011}(k_1,k_4) = -\frac{1}{\pi^2}\int d\alpha_1 d\alpha_2 d\alpha_3\ \delta(1-\alpha_1-\alpha_2-\alpha_3)$$

$$x\ \frac{\alpha_2\alpha_3}{[\alpha_1\alpha_2 M_z^2 + 2k_3\cdot k_4\ \alpha_2\alpha_3 - m_q^2]}\ . \tag{B-17}$$

Let $m_q \to 0$, and change variables $(\alpha_1,\alpha_2,\alpha_3) \to (xy,x(1-y),1-x)$. J_{011} then reduces to

$$-\frac{2}{\pi^2}\int_o^1 xdx\int_o^1 dy\ \frac{1-x}{xy\ M_z^2 + 2k_3\cdot k_4(1-x)}\ . \tag{B-18}$$

This integral is now trivial, and we obtain easily, using $r \equiv \frac{1}{2}k_3\cdot k_4$ and $M_z^2 = |\mu_1|$,

$$J_{011} = \frac{2}{M_z^2\pi^2}\cdot\log\left|\frac{r}{\mu_1}\right|, \tag{B-19}$$

which is indeed free of any mass singularity. The other diagrams, of

course, have a similar form ($\log|\frac{s}{\mu_1}|$ and $\log|\frac{t}{\mu_1}|$).

APPENDIX C

THE EXACT EXPRESSIONS FOR $E^{(1)}_{\pm++}$, $E^{(2)}_{\pm++}$ AND THEIR ASYMPTOTIC VALUES FOR $m_q/M_z \to 0$

We begin by giving the exact expressions for the four basic amplitudes $E^{(i)}_{\pm++}(1234)\,(i=1,2)$.

These are as follows:

$$\begin{aligned}\frac{1}{8}E^{(1)}_{+++}(1234) = &-\frac{2st}{s_1}+\{-\frac{4s^2t}{rs_1}-\frac{4\mu_1 st}{s_1^2}+\frac{2s^2}{s_1}\}B(s)+\{\frac{4st}{r}-\frac{2st}{t_1}\}B(t)\\
&+\{-\frac{4\mu_1 st}{rs_1}+\frac{4\mu_1 st}{s_1^2}+\frac{2\mu_1 s}{s_1}-\frac{2\mu_1 s}{t_1}\}B(-\mu_1)+\{\frac{s}{r}-\frac{s}{t}\}T(r)\\
&+\{\frac{2s(s-t)}{r}-\frac{4s^2t}{r^2}-\frac{3s}{s_1}-\frac{2st}{s_1^2}-\frac{s}{r}-1\}T(s)\\
&+\{\frac{2s(s-t)}{r}-\frac{4s^2t}{r^2}+\frac{s}{t_1}-\frac{s}{r}\}T(t)\\
&+\{-\frac{2s(s-t)}{r}+\frac{4s^2t}{r^2}+\frac{3s}{s_1}-\frac{s}{t_1}+\frac{2st}{s_1^2}+\frac{s}{r}+\frac{s}{t}\}T(-\mu_1)\\
&-\frac{r_1(r-t)}{rt}I_o(r,s,\mu_1)+\frac{r_1 s}{rt}I_o(r,t,\mu_1)\\
&+\{-\frac{2s(s-t)}{r}+\frac{4s^2t}{r^2}-\frac{s}{t}+\frac{3s}{r}+2\}I_o(s,t,\mu_1)\ ,\end{aligned}\tag{C-1a}$$

$$\frac{1}{8}E^{(1)}_{-++}(1234) = \{\frac{s}{t}-\frac{s}{r}\}[T(r)+T(s)+T(t)-T(-\mu_1)]+\frac{r_1}{t}I_o(r,s,\mu_1)\tag{C-1b}$$

$$- \frac{t_1}{r} I_o(s,t,\mu_1), \qquad \text{(C-1b)}$$

$$\frac{1}{4} E^{(2)}_{+++}(1234) = \{\frac{4s}{r} + \frac{2s}{s_1}\}B(s) + \{\frac{4t}{r} + \frac{2t}{t_1}\}B(t) + \{\frac{4\mu_1}{r} + \frac{2\mu_1}{s_1} + \frac{2\mu_1}{t_1}\}B(-\mu_1)$$

$$+ \{- \frac{1}{r} - \frac{1}{s} - \frac{1}{t}\}T(r) + \{- \frac{4st}{r^2} + \frac{2r_1}{r} + \frac{r}{s_1 t} - \frac{3}{r}\}T(s)$$

$$+ \{- \frac{4st}{r^2} + \frac{2r_1}{r} + \frac{r}{st_1} - \frac{3}{r}\}T(t) + \{\frac{4st}{r^2} - \frac{2r_1}{r} - \frac{r_1}{st}$$

$$+ \frac{1}{s_1} + \frac{1}{t_1} + \frac{3}{r}\}T(-\mu_1)$$

$$+ \{\frac{t}{rs} - \frac{s_1}{rt} + \frac{1}{rs}\}I_o(r,s,\mu_1) + \{\frac{s}{rt} - \frac{t_1}{rs} + \frac{1}{rt}\}I_o(r,t,\mu_1)$$

$$+ \{\frac{4st}{r^2} - \frac{2r_1}{r} - \frac{r_1}{st} + \frac{5}{r} + \frac{1}{st}\}I_o(s,t,\mu_1), \qquad \text{(C-1c)}$$

and

$$\frac{1}{4} E^{(2)}_{-++}(1234) = - 2 + \{- \frac{1}{r} - \frac{1}{s} - \frac{1}{t}\}[T(r) + T(s) + T(t) - T(-\mu_1)]$$

$$+ \{\frac{1}{t} + \frac{1}{rs}\}I_o(r,s,\mu_1) + \{\frac{1}{s} + \frac{1}{rt}\}I_o(r,t,\mu_1)$$

$$+ \{\frac{1}{r} + \frac{1}{st}\}I_o(s,t,\mu_1) \; . \qquad \text{(C-1d)}$$

The functions $B(r)$, $T(r)$ and $I_o(r,s,\mu_1)$ appearing in Eqns. (C-1a) through (C-1d) read:

$$\mathrm{Re}\{B(r)\} = \mathrm{Re}\{- 1 + \frac{b(r)}{2} \ln(\frac{b(r)+1}{b(r)-1})\} \; ,$$

$$\mathrm{Im}\{B(r)\} = - \frac{\pi}{2} b(r)\theta(r-1) \qquad \text{(C-2a)}$$

$$\mathrm{Re}\{T(r)\} = \mathrm{Re}\left[\frac{1}{2}\ln\left(\frac{b(r)+1}{b(r)-1}\right)\right]^2,$$

$$\mathrm{Im}\{T(r)\} = -\pi\ \mathrm{arcosh}\ \sqrt{r}\ \theta(r-1), \qquad \text{(C-2b)}$$

and

$$I_o(r,s,\mu_1) \equiv F(r,a) + F(s,a) - F(-\mu_1,a)$$

with

$$\mathrm{Re}\{F(r,a)\} = \mathrm{Re}\left\{\frac{1}{2a}\left[\ln\{r(a^2-b^2(r))\}\ln\left(\frac{a+1}{a-1}\right) - \mathrm{Li}_2\left(\frac{a+1}{a+b(r)}\right)\right.\right.$$

$$\left.\left. + \mathrm{Li}_2\left(\frac{a-1}{a+b(r)}\right) - \mathrm{Li}_2\left(\frac{a+1}{a-b(r)}\right) + \mathrm{Li}_2\left(\frac{a-1}{a-b(r)}\right)\right]\right\},$$

$$\mathrm{Im}\{F(r,a)\} = \frac{\pi}{2a}\ln\left(\frac{a-b(r)}{a+b(r)}\right)\theta(r-1) \qquad \text{(C-2c)}$$

Finally,

$$a = \left(1 + \frac{t}{rs}\right)^{1/2}, \qquad \text{(C-2d)}$$

$$b(r) = \left(1 - \frac{1}{r}\right)^{1/2}.$$

and the dilog-function is defined as

$$\mathrm{Li}_2(x) = -\int_o^x dt\ \frac{\log(1-t)}{t}.$$

The above expressions are all exact for any value of r,s,t and μ_1. From now on, we will only consider the limit where $r,s,t,-\mu_1 \to \infty$, which is equivalent to letting the quarkmass go to zero. It turns out then, to be convenient to write:

$$\hat{E}^{(1)}_{\pm++}(1234) \equiv \frac{1}{8S} E^{(1)}_{\pm++}(1234)$$

and (C-3)

$$\hat{E}^{(2)}_{\pm++}(1234) \equiv \frac{1}{4} E^{(2)}_{\pm++}(1234) \ .$$

Keeping only terms of $O(\frac{r}{s})$ several simplifications occur.

From Eqns. (C-1a) and (C-3) we obtain:

$$\hat{E}^{(1)}_{+++}(1234) = -\frac{2t}{s_1} + \{-\frac{4st}{rs_1} - \frac{4\mu_1 t}{s_1^2} + \frac{2s}{s_1}\}B(s) + \{\frac{4t}{r} - \frac{2t}{t_1}\}B(t)$$

$$+ \{-\frac{4\mu_1 t}{rs_1} + \frac{4\mu_1 t}{s_1^2} + \frac{2\mu_1}{s_1} - \frac{2\mu_1}{t_1}\}B(-\mu_1)$$

$$+ \{\frac{2st}{r^2} - \frac{s-t}{r}\}G(s,t,\mu_1) \qquad \text{(C-4)}$$

with

$$G(s,t,\mu_1) \equiv 2\{I_o(s,t,\mu_1) - T(s) - T(t) + T(-\mu_1)\} \ .$$

Using the old trick of writing:

$$B(s) = [B(s) - B(-\mu_1)] + B(-\mu_1) \qquad \text{(C-5)}$$

and similarly for B(t) Eqn. (C-4) can be written as:

$$\hat{E}^{(1)}_{+++}(1234) = -\frac{2t}{s_1} + \{-\frac{rst}{rs_1} - \frac{4\mu_1 t}{s_1^2} + \frac{2s}{s_1}\}[B(s) - B(-\mu_1)]$$

$$+ \{\frac{4t}{r} - \frac{2t}{t_1}\}[B(t) - B(-\mu_1)] + \{\frac{2st}{r^2} - \frac{s-t}{r}\}G(s,t,\mu_1). \qquad \text{(C-6)}$$

Finally, introducing scaling variables x, y and z and using the following asymptotic expressions (see Eqns. (D-1a) and (D-9))

$$B(s) = B(-\mu_1) = \frac{1}{2}\log\left|\frac{s}{\mu_1}\right| = \frac{1}{2}\log(1-y),$$

$$B(t) - B(-\mu_1) = \frac{1}{2}\log\left|\frac{t}{\mu_1}\right| = \frac{1}{2}\log(1-z) \qquad \text{(C-7)}$$

and

$$F(s,t,\mu_1) \equiv G(y,z) = \lg o(1-y)\log(1-z) + Li_2(y) + Li_2(z) - \frac{\pi^2}{6}$$

we arrive at:

$$\hat{E}^{(1)}_{+++}(x,y,z) = 2\left(\frac{1-z}{y}\right) + \left[3 - \frac{1}{y} + 2\left(\frac{1-y}{1-x}\right) - 2\left(\frac{1-x}{y^2}\right)\right]\log(1-y)$$

$$+ \left[-1 + \frac{1}{z} + 2\left(\frac{1-z}{1-x}\right)\right]\log(1-z)$$

$$+ \left[\frac{y-z}{1-x} + 2\,\frac{(1-y)(1-z)}{(1-x)^2}\right]G(y,z)\ . \qquad \text{(C-8)}$$

The $\hat{E}^{(1)}_{-++}(1234)$ is trivial and gives zero:

$$\hat{E}^{(1)}_{-++}(x,y,z) = 0\ . \qquad \text{(C-9)}$$

A similar analysis can be performed for $\hat{E}^{(2)}_{+++}(1234)$ for which we find:

$$\hat{E}^{(2)}_{+++}(1234) = \left\{\frac{4s}{r} + \frac{2s}{s_1}\right\}\left(B(s) - B(-\mu_1)\right] + \left\{\frac{4t}{r} + \frac{2t}{t_1}\right\}\left[B(t) - B(-\mu_1)\right]$$

$$+ \left\{2\,\frac{st}{r^2} - \frac{r_1}{r}\right\}G(s,t,\mu_1) \qquad \text{(C-10)}$$

or, in terms of scaling variables:

$$\hat{E}^{(2)}_{+++}(x,y,z) = [1 - 1/y + 2(1-y)/(1-x)]\ell n(1-y)$$

$$+ [1 - 1/z + 2(1-z)/(1-x)]\ell n(1-z)$$

$$+ [x/(1-x) + 2(1-y)(1-z)/(1-x)^2]G(y,z) \ . \qquad (C\text{-}11)$$

Finally:

$$\hat{E}^{(2)}_{-++}(x,y,z) = -2 \ . \qquad (C\text{-}12)$$

As can be easily seen from Eqns. (C-9) and (C-11), the $\hat{E}^{(2)}_{+++}$-function is symmetric in interchanging $y \leftrightarrow z$, while $\hat{E}^{(1)}_{+++}$ does not have this property.

APPENDIX D

DERIVATION OF THE FUNCTION G(x,y)

Here we will give the asymptotic expressions for B(r), T(r) and $G(r,s,\mu_1)$ in the limits $r,s,t,-\mu_1 \to \infty$.

For the B and T functions one has $(r \to \infty)$[7]:

$$\mathrm{Re}\{B(r)\} \simeq -1 + \frac{1}{2}\log(4r),$$

$$\mathrm{Im}\{B(r)\} \simeq -\frac{\pi}{2} \qquad \text{(D-1a)}$$

and

$$\mathrm{Re}\{T(r)\} \simeq \frac{1}{4}\log^2(4r) - \frac{\pi^2}{4},$$

$$\mathrm{Im}\{T(r)\} \simeq -\frac{\pi}{2}\log(4r)\ . \qquad \text{(D-1b)}$$

So the only function left to study is $G(r,s,\mu_1)$. We recall from Eqns. (C-2c) and (C-5):

$$\begin{aligned} G(r,s,\mu_1) &= 2\{I_o(r,s,\mu_1) - T(r) - T(s) - T(-\mu_1)\} \\ &= 2\{[F(r,a) - T(r)] + [F(s,a) - T(s)] \\ &\quad - [F(-\mu_1)a) - T(-\mu_1)]\} \end{aligned} \qquad \text{(D-2a)}$$

where the exact expression for F(r,a) is:

$$\mathrm{Re}\{F(r,a)\} = \frac{1}{2}\,\mathrm{Re}\{\frac{1}{a}\log[r(a^2-b^2(r))]\log(\frac{a+1}{a-1}) - \mathrm{Li}_2(\frac{a+1}{b(r)+1}) + \mathrm{Li}_2(\frac{a-1}{a+b(r)}) - \mathrm{Li}_2(\frac{a+1}{a-b(r)}) + \mathrm{Li}_2(\frac{a-1}{a-b(r)})\} \qquad \text{(D-2b)}$$

and

$$\mathrm{Im}\{F(r,a)\} = \frac{\pi}{2a}\log(\frac{a-b(r)}{a+b(r)}) \ .$$

Also

$$a = [1 + \frac{t}{rs}]^{1/2}$$

and (D-2c)

$$b(r) = [1 - \frac{1}{r}]^{1/2} \ .$$

Let u collectively stand for r,s,t or $-\mu_1$. Expanding a and b(r) to lowest nontrivial order, Eqn. (D-2b) with r=u reduces to:

$$\mathrm{Re}\{F(u,a)\} = \frac{1}{2}\,\mathrm{Re}\{\log(\frac{ut+rs}{rs})\log(\frac{4rs}{t}) - \mathrm{Li}_2(\frac{4urs}{ut+rs}) + \mathrm{Li}_2(\frac{ut}{ut+rs}) - \frac{\pi^2}{6}\}$$

and (D-3)

$$\mathrm{Im}\{F(u,a)\} = \frac{\pi}{2}\log(\frac{ut+rs}{4urs}) \ .$$

The following three equations from Lewins book[23] prove to be useful

in the further reduction of F(u,a):

$$Li_2(v) + Li_2(\frac{1}{v}) = -\frac{1}{2}\log^2 v + \frac{\pi^2}{3} - i\pi\log v, \quad v > 1 \qquad \text{(D-4a)}$$

$$Li_2(v) + Li_2(1-v) = -\log v \cdot \log(1-v) + \frac{\pi^2}{6}, \quad 0<v<1 \qquad \text{(D-4b)}$$

and Abel's relation:

$$Li_2(\frac{1-v}{w} \cdot \frac{1-w}{v}) - Li_2(\frac{1-v}{w}) - Li_2(\frac{1-w}{v})$$

$$= -Li_2(1-v) - Li_2(1-w) - \log v \cdot \log w \; . \qquad \text{(D-4c)}$$

Now using Eqn. (D-4a) with

$$v = \frac{4urs}{ut+rs} >> 1$$

and Eqn. (D-4b) with:

$$v = \frac{ut}{ut+rs}$$

Eqn. (D-3) reduces to

$$\text{Re}\{F(u,a)\} = \frac{1}{4}\log^2(4u) - \frac{\pi^2}{6} - \frac{1}{4}\log^2(\frac{rs}{ut+rs}) - \frac{1}{2}Li_2(\frac{rs}{ut+rs}) \; . \qquad \text{(D-5)}$$

Finally, using the asymptotic expression for T(r), Eqn. (D-6), with r=u, can be written as:

$$\text{Re}\{F(u,a) - T(u)\} = -\frac{1}{4}\log^2(\frac{rs}{ut+rs}) - \frac{1}{2}Li_2(\frac{rs}{ut+rs}) + \frac{\pi^2}{12}$$

and (D-6)

$$\text{Im}\{F(u,a) - T(u)\} = \frac{\pi}{2}\log(\frac{ut+rs}{rs}) \; .$$

Notice that all the arguments in the above equation are dimensionless. We have therefore proven that there are no quark mass singularities, which otherwise would show up in terms such as log r.

We are now ready to attack the function $G(r,s,\mu_1)$ itself. Using the fact that: $(t+r)(t+s) = -\mu_1 t + rs$ one finds for the imaginary part:

$$\mathrm{Im}\{G(r,s,\mu_1)\} = \pi\{\log(\frac{t+r}{r}) + \log(\frac{t+s}{s}) - \log(-\frac{\mu_1 t+rs}{rs})\} = 0 \ . \qquad \text{(D-7)}$$

That is, the amplitude $G(r,s,\mu_1)$ is purely real in the limit of vanishing quark mass!

Using Eqns. (D-2a) and (D-6), the real part reads:

$$\mathrm{Re}\{G(r,s,\mu_1)\} = \log(\frac{r}{t+r})\log(\frac{s}{t+s}) + \frac{\pi^2}{6}$$

$$+ \mathrm{Li}_2(\frac{rs}{-\mu_1 t+rs}) - \mathrm{Li}_2(\frac{r}{t+r}) - \mathrm{Li}_2(\frac{s}{t+s})$$

$$= \log(\frac{1-x}{y})\log(\frac{1-y}{x}) + \frac{\pi^2}{6} + \mathrm{Li}_2(\frac{1-x}{y}\,\frac{1-y}{x})$$

$$- \mathrm{Li}_2(\frac{1-x}{y}) - \mathrm{Li}_2(\frac{1-y}{x}) \ . \qquad \text{(D-8)}$$

The last equation has been re-expressed in the convenient scaling variables x and y, defined in the main text.

Using Abel's relation Eqn. (D-4c) and Eqn. (D-4b) once more, we obtain G(x,y) in its final form:

$$\mathrm{Re}\{G(x,y)\} = \log(1-x)\cdot\log(1-y) + \mathrm{Li}_2(x) + \mathrm{Li}_2(y) - \frac{\pi^2}{6}$$

and $\qquad \text{(D-9)}$

$$\mathrm{Im}\{G(x,y)\} = 0 \ .$$

This is really a remarkably simple function. Notice that all the divergences at, say x = 0 or x = 1, have now been transformed into the log function.

An interesting property of G(x,y), is that it vanishes identically for y = 1-x, according to Eqn. (D-4b):

$$G(x,1-x) = \log x \log(1-x) + Li_2(x) + Li_2(1-x) - \frac{\pi^2}{6} = 0. \quad \text{(D-10)}$$

This identity proves important to show that the decay process is finite, that is, no infrared singularities are present.

APPENDIX E

ANALYTICAL EXPRESSIONS FOR $d^2F/dxdy$ ALONG THE THREE EDGES (I, II AND III) OF THE PHASE SPACE

In this appendix, we will first determine the asymptotic expression for $|M_{+++}(x,y,z)|^2$ close to the three edges I, II and III in the phase-space (see Figure 23 in main text). Then $d^2F/dxdy$ follows automatically. Since the $y \leftrightarrow z$ symmetry is satisfied, it is sufficient to find $|M|^2$ in the region $y \to 1$ (denoted II) and also in the region $x \to 1$ (denoted I).

First let $y = 1-\varepsilon$ and therefore $z = 1+\varepsilon-x$. We shall determine:

$$\hat{E}^{(1)}_{+++}(x,y,z),$$

$$\hat{E}^{(1)}_{+++}(x,z,y)$$

and (E-1)

$$\hat{E}^{(2)}_{+++}(x,y,z)$$

in the limit where $\varepsilon \to o$.

Using the fact that the leading expression for $G(y,z)$ (see Eqn. (C-8)) is

$$G(1-\varepsilon,\ 1+\varepsilon-x) \simeq \log \varepsilon \cdot \log x \qquad \text{(E-2)}$$

it now follows easily from Eqns. (C-9) and (C-11) that

$$\hat{E}^{(1)}_{+++}(x,1-\varepsilon,1+\varepsilon x) \simeq \left[2x + \frac{x}{1-x}\log x\right]\log\varepsilon$$

and (E-3)

$$\hat{E}^{(1)}_{+++}(x,1+\varepsilon-x,1-\varepsilon) = -\hat{E}^{(2)}_{+++}(x,1-\varepsilon,1+\varepsilon-x) = -\frac{x}{1-x}\log x \cdot \log\varepsilon \ .$$

Inserting Eqn. (E-3) into Eqn. (8-20) yields

$$\left|M_{+++}(x,1-\varepsilon,1+\varepsilon-x)\right|^2 \simeq 8\{[\hat{E}^{(1)}_{+++}(x_1) + \varepsilon-x,1-\varepsilon)]^2 + [\hat{E}^{(2)}_{+++}(x_1 1-\varepsilon,1+\varepsilon-x)]^2\}$$

$$= 16\left(\frac{x}{1-x}\right)^2 \log^2 x \log^2\varepsilon \ . \qquad \text{(E-4)}$$

From Eqn. (E-4), we see that $|M|^2$ vanishes for $x \to o$, and for $x \to 1$ it diverges only as $\log^2\varepsilon$. Therefore, in region II and III $|M|^2$ is integrable. We show below that this statement holds also for the region I.

Next let $x = 1-\varepsilon$ and $z = 1+\varepsilon-y$. This time we must be more careful with the expansion of $G(y,z)$, simply because $|M|^2$ contains terms like $\frac{1}{(1-x)^2}$.

Using

$$G(y,1+\varepsilon-y) = \log(1-y)\log(y-\varepsilon) + Li_2(y) + Li_2(1+y-\varepsilon) - \frac{\pi^2}{6} \qquad \text{(E-5)}$$

with the asymptotic expansions for $\varepsilon \to o$:

$$\log(y-\varepsilon) \simeq \log y - \frac{\varepsilon}{y} - \frac{1}{2}\frac{\varepsilon^2}{y^2}$$

and

$$Li_2(1+\varepsilon-y) \simeq Li_2(1-y) - \frac{\log y}{1-y}\varepsilon + \frac{1}{2}\left[\frac{1}{y(1-y)} + \frac{\log y}{(1-y)^2}\right]\varepsilon^2 \qquad \text{(E-6)}$$

and also Eqn. (D-46), we obtain:

$$G(y,1+\varepsilon-y) \simeq -\left[\frac{\log y}{1-y} + \frac{\log(1-y)}{y}\right]\varepsilon + \frac{1}{2}\left[\frac{1}{y(1-y)} + \frac{\log y}{(1-y)^2} - \frac{\log(1-y)}{y^2}\right]\varepsilon^2. \tag{E-7}$$

Substituting Eqn. (E-7) into Eqns. (C-9) and (C-11) gives after a trivial, but tedious calculation, the simple answer:

$$\hat{E}^{(1)}_{+++}(1-\varepsilon,y,1+\varepsilon-y) = \hat{E}_{+++}(1-\varepsilon,1+\varepsilon-y,y) =$$

$$\hat{E}^{(2)}_{+++}(1-\varepsilon,y,1+\varepsilon-y) = 1 + \frac{\log y}{1-y} + \frac{\log(1-y)}{y} \tag{E-8}$$

Inserting Eqn. (E-8) into Eqn. (8-20) yields

$$\left|M_{+++}(1-\varepsilon,y,1+\varepsilon-y)\right|^2 = 8\left\{\left[\hat{E}^{(1)}_{+++}(1-\varepsilon,y,1+\varepsilon-y)\right]^2 + \left[\hat{E}^{(2)}_{+++}(1-\varepsilon,y,1+\varepsilon-y)\right]^2\right\}$$

$$= 16\left\{1 + \frac{\log y}{1-y} + \frac{\log(1-y)}{y}\right\}^2 \tag{E-9}$$

The above expression, at first glance, does not look symmetric in $y\leftrightarrow z$, however, since $x\to 1$ we have $y\to 1-z$, so that $\log(1-y)/y \to \log z/(1-z)$. Therefore, let us use the symmetrical form:

$$\left|M_{+++}(x,y,z)\right|^2 = 16\left\{1 + \frac{\log y}{1-y} + \frac{\log z}{1-z}\right\}^2 \tag{E-10}$$

for $x\to 1$. If also $q\to o$, then $|M|^2 \simeq 16 \log^2 q$. This is the infrared divergence.

We are now ready to give the asymptotic expressions for $d^2F/dxdy$ in the three regions. Using the fact that the asymptotic expression for $|M|(y,x,z)|^2$ in region II is the same as $|M(x,y,z)|^2$ in region I and similarly for $|M(z,y,x)|^2$, we obtain in region I:

$$\frac{d^2F}{dxdy} = \frac{32}{3}\left\{1 + \frac{\log y}{1-y} + \frac{\log z}{1-z}\right\}^2 + \frac{32}{3}\left\{\left(\frac{y}{1-y}\right)^2 \log^2 y + \left(\frac{z}{1-z}\right)^2 \log^2 z\right\}\log^2(1-x) \tag{E-11}$$

The expressions for the other two regions are easily obtained by the interchanges $x \leftrightarrow y$ and $x \leftrightarrow z$.

In the infrared limit, $z \to o$ and therefore $x = g \to 1$, we obtain from Eqn. (E-11)

$$\frac{d^2F}{dxdy} \simeq \frac{64}{3} \log^2 y \ . \tag{E-12}$$

To summarize, we have shown that in the infrared region $z \to o$ $d^2F/dxdy$ behaves like $\log^2 z$, while in the case of collinear gluons, $z \to 1$, $d^2F/dxdy$ behaves like $\log^2(1-z)$. We conclude that this process is infrared finite and is free of any mass singularities.

APPENDIX F

EVALUATION OF THE SLOPE $dF/d\varepsilon$

Here we shall give an expression for $F(\varepsilon)-F(o)$ in the limit $\varepsilon\to o$. Assuming $F(\varepsilon)$ is a well-behaved function, we can expand it around $\varepsilon=o$:

$$F(\varepsilon) = F(o) + \left(\frac{dF(\varepsilon)}{d\varepsilon}\right)_{\varepsilon\to o} \varepsilon + \cdots \qquad \text{(F-1)}$$

The leading term $dF/d\varepsilon$ is the only part which we will be concerned about.

Now, for any function $f(x,y)$, let us define the following double integral:

$$F(\varepsilon) = \int_{2\varepsilon}^{1-\varepsilon} dx\, F_1(x,\varepsilon) \qquad \text{(F-2)}$$

where

$$F_1(x,\varepsilon) = \int_{1+\varepsilon-x}^{1-\varepsilon} dy\, f(x,y)$$

Using the well-known differentiation rule:

$$\frac{d}{d\varepsilon}\int_{a(\varepsilon)}^{b(\varepsilon)} dx\, g(x,\varepsilon) = \int_{a(\varepsilon)}^{b(\varepsilon)} dx\, \frac{\partial g(x,\varepsilon)}{\partial \varepsilon}$$

$$+ g(b(\varepsilon),\varepsilon)\,\frac{\partial b(\varepsilon)}{\partial \varepsilon} - g(a(\varepsilon),\varepsilon)\,\frac{\partial a(\varepsilon)}{\partial \varepsilon} \qquad \text{(F-3)}$$

we easily obtain:

$$\frac{dF(\varepsilon)}{d\varepsilon} = -\int_{2\varepsilon}^{1-\varepsilon} dy\ f(1-\varepsilon,y) + \int_{2\varepsilon}^{1-\varepsilon} dx\ \frac{\partial F_1(x,\varepsilon)}{\partial \varepsilon}$$

$$= -\int_{2\varepsilon}^{1-\varepsilon} dy\ f(1-\varepsilon,y) - \int_{2\varepsilon}^{1-\varepsilon} dx\ f(x,1-\varepsilon) - \int_{2\varepsilon}^{1-\varepsilon} dx\ f(x,1+\varepsilon-x)\ . \qquad \text{(F-4)}$$

These three integrals represent precisely integrations in the regions I, II and III, respectively. In particular, if f(x,y) is the double-differential function $d^2F/dxdy$, we can use the asymptotic expressions in Eqn. (E-11). Each of the integrals then give the same contribution, and changing $y \to x$ in the first integral, we obtain from Eqn. (E-11)

$$\frac{dF(\varepsilon)}{d\varepsilon} = -3 \cdot \frac{64}{3} \int_0^1 dx \left(\frac{x}{1-x}\right)^2 \log^2 x \cdot \log^2 \varepsilon$$

$$= -128\{\zeta(2) + 1 - 2\zeta(3)\}\log^2 \varepsilon \qquad \text{(F-5)}$$

To summarize, the function $F(\varepsilon)$ behaves like $\varepsilon \log^2 \varepsilon$ around $\varepsilon = o$ with a coefficient: $-128\{\zeta(2) + 1 - 2\zeta(3)\} \simeq -30$.

VITA

Morten Laurits Laursen

Candidate for the Degree of

Doctor of Philosophy

Thesis: HIGHER-ORDER CORRECTIONS IN QUANTUM ELECTRODYNAMICS AND QUANTUM CHROMODYNAMICS

Major Field: Physics

Biographical:

Personal Data: Born in Copenhagen, Denmark, March 6, 1951, the son of Laurits Christian and Ruth Martine (Hansen) Laursen.

Education: Graduated from Efterslaegtselskabets High School, Copenhagen, Denmark, in June 1970; received Cand. Scient. degree in Physics with a minor in Mathematics from Niels Bohr Institute, University of Copenhagen, Copenhagen, Denmark in January 1980; completed the requirements for the Doctor of Philosophy degree at Oklahoma State University in July, 1981.

Professional Experience: Graduate Teaching Assistant, Physics Laboratory II, University of Copenhagen, Copenhagen, Denmark 1976-1978; Graduate Research Assistant, Department of Physics, Oklahoma State University, 1978-1981.

Professional Organizations: American Physical Society, European Physical Society and Danish Physical Society.